JPRS L/10119

17 November 1981

USSR Report

METEOROLOGY AND HYDROLOGY

No. 7, July 1981

FBIS FOREIGN BROADCAST INFORMATION SERVICE

NOTE

JPRS publications contain information primarily from foreign newspapers, periodicals and books, but also from news agency transmissions and broadcasts. Materials from foreign-language sources are translated; those from English-language sources are transcribed or reprinted, with the original phrasing and other characteristics retained.

Headlines, editorial reports, and material enclosed in brackets [] are supplied by JPRS. Processing indicators such as [Text] or [Excerpt] in the first line of each item, or following the last line of a brief, indicate how the original information was processed. Where no processing indicator is given, the information was summarized or extracted.

Unfamiliar names rendered phonetically or transliterated are enclosed in parentheses. Words or names preceded by a question mark and enclosed in parentheses were not clear in the original but have been supplied as appropriate in context. Other unattributed parenthetical notes within the body of an item originate with the source. Times within items are as given by source.

The contents of this publication in no way represent the policies, views or attitudes of the U.S. Government.

APPROVED FOR RELEASE: 2007/02/09: CIA-RDP82-00850R000400070034-3

JPRS L/10119

17 November 1981

USSR REPORT

METEOROLOGY AND HYDROLOGY

No. 7, July 1981

Translations or abstracts of all articles of the Russian-language monthly journal METEOROLOGIYA I GIDROLOGIYA published in Moscow by Gidrometeoizdat.

CONTENTS

* Denotes items which have been abstracted.

* Denotes items which have been abstracted.

UDC 551.509.324

SHORT-RANGE PRECIPITATION FORECASTING

Moscow METEOROLOGIYA I GIDROLOGIYA in Russian No 7, Jul 81 (manuscript received 15 Dec 80) pp 5-17

[Article by A. I. Snitkovskiy, candidate of geographical sciences, USSR Hydrometeorological Scientific Research Center]

[Text]

Abstract: A method is proposed for predicting the fact and quantity of steady precipitation for 24 and 36 hours by application of the MOS concept. The possibilities for predicting summer precipitation are considered.

The theoretical principles for predicting steady precipitation, developed by A. F. Dyubyuk, have been set forth in the MANUAL [6]. The computation formula for the quantity of steady precipitation has the form

$$Q = \frac{1}{g}\int_0^t \int_{P_0}^{P} \frac{dq}{dt}\, dP\, dt, \qquad (1)$$

where Q is the quantity of moisture concentrated in a column of the atmosphere between the levels P_0 and P during the time Δ t: q is specific humidity at maximum saturation; t is time; g is the acceleration of free falling.

It follows from formula (1) that the quantity of precipitation is determined by the product of the baric thickness of air and the individual change of specific humidity in it. The individual change in specific humidity is associated first of all with the sign and intensity of vertical air movements. Since in a column of air with a section 1 cm^2 with a thickness of 100 mb the condensation of 1 g of moisture in 1 kg of air is equivalent to the falling of precipitation in a quantity of 1 mm, the working formula for predicting the quantity of steady precipitation during some time interval will be as follows:

$$Q' = 1{,}5\ \Delta q_{850} + 1{,}8\ \Delta q_{700} + \Delta q_{500}, \qquad (2)$$

where Δq_{850}, Δq_{700} and Δq_{500} are the individual changes of specific humidity in the case of ascent from the levels 850, 700 and 500 mb.

Accordingly, knowing the actual distribution of specific humidity with altitude and in this same time interval the vertical movements, it is possible to use (2) to compute the quantity of steady precipitation and compare it with the actual

quantity, thereby in a diagnostic plan evaluating the reliability of the working formula. However, when we proceed to a forecast, it is necessary to have information on the prognostic values of specific humidity and vertical air movements. The prediction of tropospheric humidity is accomplished in the usual way: on the basis of a model of air particle trajectories and the advective humidity values, with transformation taken into account. However, due to imperfection of objective analysis of the humidity field and errors in computations of air particle trajectories, the prediction of humidity also contains errors. Nevertheless, the fundamental error in the prediction of steady precipitation arises due to a failure to know the real distribution of ordered vertical air movements, which are computed from the equations of thermohydrodynamics, and naturally, the impossibility of comparing them with the prognostic vertical movements. However, it is not for these reasons alone that synoptic forecasts of precipitation are better than the forecasts prepared by numerical and computation methods. It is most important that weathermen in forecasts use information on weather phenomena and elements for the region from which the transport of air masses occurs, whereas in numerical and computation methods information on weather phenomena and elements are not used at all. Such phenomena as steady rain, showers, thunderstorms, squalls and a number of others are computed in numerical models on the basis of physico-theoretical concepts or empirical dependences.

With these circumstances taken into account, in this article, in addition to known atmospheric parameters, determining the formation of steady precipitation, as the predictors, the same as in done by weathermen in the case of a real forecast, extensive use is made of information on advective precipitation quantities.

In this article, which is a natural continuation of [8], we propose a method for predicting the fact and quantity of steady precipitation in the cold half-year for 24 and 36 hours on the basis of a synoptic-statistical approach; the possibilities of predicting summer precipitation are also examined. The forecasting method is developed in the example of Moscow. In contrast to [8], where use was made of two forecasting concepts -- PP (perfect prognosis) and MOS (model output statistics) -- here we examine only the MOS concept as indicating, in accordance with [8, 9, 10, 13, 14], the best results in operational forecasting.

Initial Data and Processing Method

Data on steady precipitation were taken for the period from October through March 1974-1978. The predictant was the quantity of precipitation, averaged for all meteorological stations of Moscow and Moscow Oblast during the period of day from 2100 to 0900 hours (for a 24-hour period) and from 0900 to 2100 hours (for a 36-hour forecast).

The predictors were selected on the basis of general concepts concerning the physics of formation of steady precipitation and taking into account the latest results of investigations in this field [5, 6, 8, 10-14]. The list of potential predictors, selected for the prediction of precipitation, is given below.

***

LIST OF POTENTIAL PREDICTORS FOR PREDICTION OF FACT AND QUANTITY OF STEADY PRECIPITATION IN MOSCOW AND MOSCOW OBLAST FOR 24 AND 36 HOURS

P_0 is the pressure at sea level, mb;
H_{1000} is the geopotential at the 1000-mb level, dam;
H_{850}, H_{700}, H_{500} is the geopotential at the levels 850, 700 and 500 mb, dam;
D_{700}, D_{500} is wind direction at the levels 700 and 500 mb, degrees;
ff_{700}, ff_{500} is wind velocity at the levels 700 and 500 mb, m/sec;
W_{850}, W_{700}, W_{500} are the vertical air movements at the levels 850, 700 and 500 mb, mb/12 hours;
K is the instability index, $K = (H_{1000}+H_{500})-2H_{850}$, dam; $\sum_{850}^{700}(T-T_d)$ is the total dew point spread at the levels 850 and 700 mb, °C; $\sum_{850}^{700} q$ is the total specific humidity at the levels 850 and 700 mb, g/kg; $\sum_{\text{земля}}^{850} f$ (ground) is the total relative humidity at the ground level and at the surface 850 mb, %;
T, T_d, $T - T_d$ are temperature, dew point and dew point spread at the earth's surface, °C;
PW^{500}_{gr} is the precipitated water in the layer between the ground and the level 500 mb, mm; $PW^{500}_{gr} = 5\ q_{gr} + q_{500}/2$, where q_{gr} and q_{500} is specific humidity in g/kg at the surface and at the level 500 mb;
Q_{in} and Q_{adv} are the fact and quantity of initial and advective precipitation. Coding for the fact of precipitation: presence 3, absence 1. Quantity of precipitation, mm;
Q^{syn}_{M}, $Q^{syn}_{M_0}$ are the fact and quantity of precipitation in synoptic predictions of precipitation. Coding the same;
Q_M, Q_{M_0} is the actual precipitation (predictants). Coding the same.

The archives of predictors for predicting precipitation for 24 and 36 hours in accordance with the MOS concept were obtained on the basis of prognostic charts of pressure, geopotential and ordered vertical air movements, at whose initial points data were read on temperature, humidity and other atmospheric parameters using a model of air particle trajectories. The fact and quantity of advective precipitation in the corresponding time intervals were determined from the prognostic trajectory at the 700-mb level. If precipitation was noted at the ground along the corresponding segment of the trajectory path at the 700-mb level, it was assumed that the fact of precipitation is established and the mean quantity of precipitation was determined along this very same trajectory on the basis of data for stations falling in its zone. For the fact and quantity of initial precipitation we took its mean value during the past night for all stations of Moscow or Moscow Oblast in dependence on the territory for which the investigation was made.

The statistical processing of data included the forming of paired correlation matrices, the "sifting" of predictors for the purpose of finding among them those which are most closely related to the predictant, and at the same time,

independent of one another, the writing of multiple regression equations and their evaluation. The evaluations of real forecasts were made using the correlation coefficient (r), reliability test (H) and accuracy test (Q) [3]; the total guaranteed probability, guaranteed probability of the presence and absence of precipitation were determined.

The same as in [9], the "sifting" of predictors was carried out using the algorithm in [2], in accordance with which in the first interval there is selection of the paired correlation coefficient of maximum value between the predictant and predictor and then the correlation coefficients between the selected predictor and the others are found. Then, by means of a definite procedure, the orthogonalization of the values of the predictors is carried out. Among the orthogonalized predictors the predictor most closely related to the predictant is again selected, etc. Thus, such a number of predictors is selected that the difference in the accumulated dispersions of the predictant in two adjacent intervals would not be less than 0.03.

After ranking of the predictors a regression was formed using the algorithm in [1], in which the number of predictors ensuring the best quality of writing of the regression equation is determined. An evaluation of the regression is made on the basis of the mean risk ($I_{(k)}$). Such a number of predictors k is selected as to guarantee a minimum value of the mean risk in the examination. A comparison of the $I_{(k)}$ values for different groups of predictors was the basis for selecting the working regression equations for the purpose of forecasting precipitation.

The prediction of steady precipitation by statistical methods is an extremely complex problem because the distribution of precipitation does not conform to a normal law. An attempt to normalize precipitation by means of $\sqrt{x}$ and lg x did not lead to positive results. An attempt at simultaneous prediction of the fact and quantity of steady precipitation by means of regression equations also was without success.

Bearing these circumstances in mind, it was decided to predict precipitation in two successive steps: first prediction of the fact of precipitation and in the case of its presence -- prediction of the quantity of steady precipitation.

An analysis indicated that the "pure" absence of precipitation in Moscow is observed in only 20-30% of the cases. Accordingly, it was decided to regard as a fact of absence also such cases when its mean quantity is 0.0 mm (we note that in climatology a quantity of 0.1 mm or more is regarded as a day with precipitation). With such an approach the newly formed class of absence of precipitation has a probability on the average of 63-45%, whereas the class of presence of precipitation (quantity of precipitation $\geqslant$ 0.1 mm) is 37-54% respectively, that is, the classes of presence and absence of precipitation have approximately identical probabilities.

As a result, two approximately equiprobable classes were formed:

-- presence of precipitation -- cases when the averaged quantity of precipitation for all the stations of Moscow or Moscow Oblast was 0.1 mm and more;

-- absence of precipitation -- cases when precipitation in Moscow and Moscow Oblast was absent or its mean quantity was 0.0 mm.

It is possible to separate these two classes by means of a regression evaluation of the probabilities of events, which, as was demonstrated in [7], is advantageous in comparison with linear discriminant analysis. In this case the predictants and predictors should have a binary character. Hence the following coding was adopted for the actual, initial and adequate precipitation: precipitation -- 3, absence of precipitation -- 1; for the ascending vertical movements -- 3, for ascending vertical movements -- 1. The remaining predictors could not be represented in binary form.

When the predicted value of the predictant in the regression equation, written in accordance with a regression evaluation of the probabilities of events, exceeds a definite threshold (in our case -- two), the fact of precipitation is predicted, and then using another regression equation the quantity of steady precipitation is computed.

With this approach to the prediction of precipitation it was necessary to prepare the eight data archives: four archives for predicting the fact of precipitation for 24 and 36 hours, four for the prediction of the quantity of precipitation for 24 and 36 hours in Moscow and Moscow Oblast.

Analysis of Results

For each of the indicated eight archives initially in all the potential predictors we obtained correlation matrices. Analysis of these matrices indicated that an entire series of predictors, including the surface pressure value, geopotential at the levels 850, 700 and 500 mb, temperature and dew point at the earth, have virtually no significant correlation with precipitation. As a result of many numerical experiments it was possible to select predictors which relatively better than the others were related to the fact and quantity of precipitation. We have

ff_{500}, W_{700}, K, $\sum_{850}^{700} (T - T_d)$, PW_{gr}^{500}, Q_{in} and Q_{adv}. The correlations of precipitation with these predictors for 24 and 36 hours are given in Table 1. Depending on the archives and the advance time of the forecast, the degree of closeness of the correlation changes and among the data in this table there are very small correlation coefficients. Naturally, the correlation coefficients for 24 hours are higher than for 36 hours; for an advance time of 36 hours the correlation coefficients are low, especially for predicting the quantity of precipitation. Two conclusions can therefore be drawn: first -- there are difficulties in predicting the fact and quantity of precipitation in general; second -- there is a low quality (in the sense of prediction of precipitation) of the prognostic fields of vertical movements and predicted trajectories of air particles obtained from numerical models, at the initial points of which the initial data were taken. It must be mentioned that the correlation coefficients between the fact of precipitation and the diagnostic values W_{700} do not exceed -0.47, although it appeared that the vertical movements in the middle troposphere virtually unambiguously determine the falling of precipitation. It is evident that here only the vertical movements of air are involved.

Table 1

Correlation Coefficients Between Precipitation and Predictors

Territory	Advance time hrs	ff_{500}	W_{700}	K	$\sum_{850}^{700}(T-T_d)$	pw_{gr}^{500}	Q_{1n}	Q_{adv}
Fact of precipitation								
Moscow	24	0,12	−0,32	−0,25	−0,27	0,01	0,43	0,51
	36	0,14	−0,21	−0,04	−0,17	0,02	0,40	0,44
Moscow Oblast	24	0,16	−0,32	−0,17	−0,30	0,13	0,48	0,44
	36	0,16	−0,32	−0,05	−0,17	0,09	0,45	0,40
Quantity of precipitation								
Moscow	24	0,08	−0,21	−0,17	−0,12	0,11	0,15	0,43
	36	0,01	−0,07	−0,03	−0,13	0,14	0,11	0,42
Moscow Oblast	24	0,12	−0,28	−0,19	−0,18	0,14	0,18	0,44
	36	0,04	−0,09	−0,08	−0,15	0,17	0,12	0,39

Table 2

Correlation Coefficients Between Actual (Q_{act}) and Advective Precipitation (Q_{adv}) and Quantity of Precipitation in Synoptic Forecasts (Q^{syn}) (219 Cases)

	$Q_{act M_{24}}$	$Q_{act Mo_{24}}$	$Q_{act M_{36}}$	$Q_{act Mo_{36}}$	$Q^{syn}_{M_{24}}$	$Q^{syn}_{Mo_{24}}$	$Q^{syn}_{M_{36}}$	$Q^{syn}_{Mo_{36}}$	$Q_{adv_{24}}$	$Q_{adv_{36}}$
	1	2	3	4	5	6	7	8	9	10
1	1									
2	0,82	1								
3	0,37	0,40	1							
4	0,41	0,44	0,97	1						
5	0,44	0,45	0,20	0,16	1					
6	0,43	0,44	0,20	0,16	0,99	1				
7	0,43	0,44	0,40	0,39	0,57	0,56	1			
8	0,43	0,43	0,40	0,38	0,56	0,56	0,99	1		
9	0,24	0,26	−0,01	−0,05	0,37	0,36	0,23	0,23	1	
10	0,22	0,19	0,42	0,45	0,13	0,12	0,25	0,25	0,03	1

We note that relatively high correlation coefficients (more than 0.4) are observed only between precipitation in Moscow and precipitation in the region from which it moves toward Moscow. This circumstance reflects the well-known fact of

an exceptional significance of advective values of the characteristics of state of the atmosphere in synoptic forecasts.

As a result of "sifting" of all the predictors, for predicting the fact of precipitation we selected W_{700}, Q_{in}, Q_{adv}, and for predicting the quantity of precipitation

$$W_{700},\ K,\ \sum_{850}^{700}(T - T_d),\ PW_{gr}^{500},\ Q_{in} \text{ and } Q_{adv}.$$

We note that the predictors for prediction of the fact of precipitation for 24 hours explain not more than 26-29% of the dispersion of the predictant (R^2); for Moscow Oblast, naturally, the explicable part of the dispersion of the predictant is greater than for Moscow. R^2 of the synoptic forecast of the fact of precipitation is 2-3% less. For 36 hours the R^2 values decreased and for the selected predictors are 22-25%; for a synoptic forecast they are 5-7% less. A similar relationship was maintained in the $I_{(k)}$ evaluations of the regression equations written in accordance with the selected predictors and on the basis of a synoptic forecast. For example, $I_{(k)}$ for the regression equation with the predictors for 24 and 36 hours were 0.94 and 0.88, but with allowance for a synoptic forecast -- 0.97 and 1.00.

As a result of the analysis of the $I_{(k)}$ evaluations for predicting the fact of precipitation in Moscow and Moscow Oblast we selected the following regression equations:

for 24 hours

$$Q_M = -0.005\ W_{700} + 0.112\ Q_{in} + 0.076\ Q_{adv} + 1.58,$$
$$Q_{M0} = -0.008\ W_{700} + 0.178\ Q_{in} + 0.120\ Q_{adv} + 1.37; \quad (3)$$

for 36 hours

$$Q_M = -0.003\ W_{700} + 0.060\ Q_{in} + 0.34\ Q_{adv} + 1.81,$$
$$Q_{M0} = -0.004\ W_{700} + 0.085\ Q_{in} + 0.47\ Q_{adv} + 1.86. \quad (4)$$

When the algebraic summation of the right-hand side of equations (3) and (4) $\geqslant$ 2.0, precipitation is expected; if it is less than 2.0, precipitation is not expected.

A prediction of the quantity of steady precipitation is a considerably more complex problem than a forecast of the fact of precipitation. This is indicated, in particular, by the small correlation coefficients cited in Table 1.

Before proceeding to an evaluation and analysis of the regression equations for predicting the quantity of steady precipitation we will examine the status of synoptic forecasting of the quantity of steady precipitation. These data are presented in Table 2. As the quantity of precipitation in synoptic forecasts we used the median quantity of precipitation in the anticipated gradation in accordance with the current Instructions on Evaluation of Forecasts [4].

An analysis of the data in Table 2 makes it possible to draw the following conclusions:
-- the correlation coefficients between the actual quantity of precipitation and the anticipated quantity are 0.43-0.45, which corresponds to the level of forecasting of precipitation in the United States [13];
-- approximately 80-85% of the information on the quantity of precipitation anticipated in the synoptic forecasts is contained in advective precipitation;
-- the anticipated quantity of steady precipitation in synoptic forecasts for Moscow and Moscow Oblast for 24 and 36 hours does not differ (r = 0.99).

For predicting the quantity of steady precipitation by means of regression equations the selected number of predictors was small

$(W_{700}, K, PW_{gr}^{500}, \sum_{850}^{700}(T - T_d), Q_{in}, Q_{adv})$, and by virtue of the small correlations between them and the actual precipitation they explained not more than 18-22% of the dispersion of the predictant. Regression equations were written on the basis of 2/3 of the sample and were checked using 1/3 of the sample. It was found that the correlation coefficients between the predicted precipitation for 24 hours and the actual precipitation for Moscow were 0.30, and for Moscow Oblast 0.4; for 36 hours the corresponding values were 0.36 and 0.34. Such evaluations enabled us to write equations on the basis of a full sample, evaluating them using the mean risk $I_{(k)}$. It was found that in comparison with the 2/3 sample in the full sample the $I_{(k)}$ values decrease by 10-15% and for 24 hours for Moscow constitute 2.47 and for Moscow Oblast 1.80; for 36 hours the corresponding values are 2.18 and 2.16. Accordingly, taking into account the decrease in $I_{(k)}$ with an increase in the sample, it is correct to assume that in the operational checking of the regression equations the correlation coefficients between the predicted and actual precipitation will at least be close to synoptic values.

The working regression equations for prediction of the quantity of steady precipitation for Moscow and Moscow Oblast for 24 and 36 hours in the case of the full sample were as follows:

for 24 hours

$$Q_M = -0.033\, W_{700} + 0.462K + 1.54\, PW_{gr}^{500} + 0.20\, Q_{in} + 0.23\, Q_{adv} - 37.3,$$
$$Q_{M_0} = -0.030\, W_{700} + 1.05\, PW_{gr}^{500} + 0.19\, Q_{in} + 0.20\, Q_{adv} + 62.9; \quad (5)$$

for 36 hours

$$Q_M = -0.134\, W_{700} - 0.53 \sum_{850}^{700} (T - T_d) + 0.21\, Q_{in} + 0.62\, Q_{adv} + 23.1,$$
$$Q_{M_0} = -0.110\, W_{700} - 0.47 \sum_{850}^{700} (T - T_d) + 0.13\, Q_{in} + 0.58\, Q_{adv} + 20.7. \quad (6)$$

In order to determine the quantity of precipitation in mm/12 hours the resulting sums of the right-hand sides of equations (5) and (6) must be divided by 100.

Operational Checking

In the course of October 1979 - March 1980 forecasts of the fact and quantity of steady precipitation for Moscow and Moscow Oblast for 24 and 36 hours were prepared almost daily on workdays in an operational regime on the basis of the derived regression equations. A total of 94 forecasts were prepared. It is important to note that in determining

$$W_{700},\ K,\ PW^{500}_{gr},\ \sum_{850}^{700}(T - T_d),\ Q_{adv}$$

at the initial points we used the air particle trajectories at the isobaric surfaces from a numerical operational model. In this case Q_{adv} was determined at the earth's surface along the trajectory at the 700-mb level.

In order to compare precipitation forecasts on the basis of the regression equations and synoptic forecasts we also evaluated the latter. As the fact of precipitation for the synoptic forecasts and on the basis of regression equations we used a case when the averaged quantity of precipitation for Moscow or Moscow Oblast was $\geqslant 0.1$ mm. The quantity of precipitation in the synoptic forecasts was determined as the median value of the anticipated gradation in accordance with the Instructions (little snow -- 1 mm, locally limited snow (30% of the territory) -- for Moscow 0.3 mm, for the oblast 0.2 mm, etc.).

Table 3

Results of Operational Checking of Forecasts of Fact and Quantity of Steady Precipitation and Synoptic Forecasts (October 1979-March 1980)

Advance time, hours	Evaluations	Regression		Synoptic	
		Moscow	Moscow Oblast	Moscow	Moscow Oblast
24	Total guaranteed probability, %	76.5	79.5	61.6	64.5
	Guaranteed probability of phenomenon	78.0	85.0	95.0	95.7
	Guaranteed probability of absence of phenomenon, %	75.0	74.0	28.0	33.3
	H	0.53	0.65	0.26	0.34
	Q	0.55	0.61	0.34	0.50
	r	0.51	0.41	0.53	0.35
36	Total guaranteed probability, %	75.4	77.8	62.3	59.8
	Guaranteed probability of phenomenon, %	74.3	72.7	92.3	88.6
	Guaranteed probability of absence of phenomenon, %	76.5	82.8	32.3	31.0
	H	0.50	0.50	0.26	0.23
	Q	0.56	0.49	0.31	0.38
	r	0.38	0.29	0.33	0.29

The results of routine checking of precipitation forecasts are given in Table 3, where all the lines of evaluations, other than r, relate to a forecast of the fact of precipitation, whereas r is the correlation coefficient between the quantities of predicted and actual precipitation. It can be seen that when precipitation is divided into two classes (precipitation with a quantity 0.0 mm and situations without precipitation are assigned to the class of absence of precipitation) the quality of the forecasts of the fact of precipitation on the basis of regression equations is better than the quality of synoptic forecasts. The principal reason for this is that in synoptic forecasts it is relatively rare to give a forecast of the absence of precipitation and therefore the guaranteed probability of the absence of the phenomenon is low in these forecasts. However, the guaranteed probability of the presence of precipitation in synoptic forecasts is high because in them precipitation is expected considerably more frequently than it actually occurs.

A comparison of the correlation coefficients between the predicted and actual quantities of precipitation indicates that in general the success of forecasts using regression equations is somewhat better than in synoptic forecasts. However, as a rule considerable precipitation is not detected by synoptic forecasts and regression equations.

Our checking of the forecast of the fact and quantity of steady precipitation, computed using a synoptic-hydrodynamic scheme [11, 12] for the period October-December 1979 (61 cases) for Moscow, indicated that the total probable success of the fact of precipitation ($\geqslant 0.1$ mm) is 57.4%, presence of precipitation 73%, absence of precipitation 41.7% with the test H = 0.13. In a forecast for 36 hours H = 0.04. The correlation coefficient between the quantity of predicted and actual precipitation for 24 hours is 0.29. It can be seen that the cited evaluations are considerably inferior to synoptic forecasts and forecasts based on regression equations.

In the forecasting of the quantity of precipitation using regression equations it is important to estimate advective precipitation, because on the average it makes the principal contribution to the quantity of falling precipitation. In this connection it appears that if in the determination of advective precipitation use is not made of trajectories at the 700-mb level, but precipitation in those parts of the pressure formations at the ground level which were expected in the prediction time period [9], the results of the prediction of the quantity of precipitation could be better.

Prediction of Summer Precipitation

The basis for the prediction of summer convective precipitation is information on the positive energy of atmospheric instability. In order to determine the rate of convective air movements use is made of the relationship between the vertical velocity of a moving particle and instability energy. It is assumed that all the instability energy goes into the kinetic energy of convective movement:

$$W_{con} = \sqrt{W^2_{con_0} + \frac{2}{\rho}(P - P_0)\left(\frac{T - T'}{T}\right)_{mean}}, \qquad (7)$$

where W_{kin} and W_{kin_0} are the velocities of convective vertical movement at the upper and lower boundaries of the layer P and P_0; ρ is air density; T is air temperature; T' is temperature of a rising particle.

As can be seen from (7), in the stipulated layer of the atmosphere $W^2_{con_0}$, ρ, $P - P_0$ are virtually constant values and W_{con} is determined for the most part by the difference $T' - T$. For this reason almost all methods for the diagnosis and prediction of convective phenomena, including shower precipitation, are based on the correlations between $T' - T$ and the weather phenomenon.

However, such an approach to a forecast of showers is applicable on a practical basis only in the case of thermal convection. In situations when there is development of considerable ordered vertical movements in many cases the role of convection may or may not be detected in ordinary thermodynamic computations. For this reason in [11] two approaches to a forecast were simultaneously correctly used in the forecast: the first, based on thermodynamic computations, and the second, based on allowance for ordered vertical air movements.

Taking these circumstances into account, we will examine the possibilities of forecasting the quantity of summer precipitation for the current day using statistical methods, employing the two mentioned approaches. For this purpose we analyzed more than 200 cases of summer (June-August) daytime (0900-2100 hours Moscow time) rains in Moscow during 1976-1979 when the quantity of precipitation as an average for all stations was $\geq$ 0.1 mm.

Proceeding on the basis of the physics of formation of summer precipitation [5, 6, 11, 12], for the investigation we selected a number of potential predictors, a list of which is given below. All the values of the predictors were taken prognostically, for 12 hours in advance (forecast for the current day), that is, in accordance with the MOS concept.

LIST OF POTENTIAL PREDICTORS FOR PREDICTING SUMMER PRECIPITATION IN MOSCOW

T_{max}, T_d are the maximum temperature and dew point at the earth, °C;
T_{700}, T_{d700}, T_{500}, T_{d500} are temperature and dew point at the levels 700 and 500 mb, °C;
PW^{700}_{gr} is the quantity of precipitated water in the layer ground-700 mb, mm;
$(T'^{gr} - T)_{500}$ is the deviation of the curve of state from the stratification curve at the level 500 mb, °C; K is the instability index, dam; u_{700}, v_{700} are the wind velocity components at the 700-mb level, m/sec; W^{700}_{850} is the averaged value of ordered vertical air movements, mb/12 hours; $H_{-10°C}$ is the altitude of the -10°C, isotherm, km; $T_{gr} - T_{500}$ is the temperature difference between the ground and at the level 500 mb, °C; type of front.

Table 4

Mean Errors (Δ) and Standard Deviations (σ) of Predictors and Correlation Coefficients (r) Between Quantity of Precipitation at Moscow and Predictors (1976-1979, 200 Cases)

Statistics	T_{max}	T_d	T_{700}	$T_{d_{700}}$	PW^{700}_{gr}	T_{500}	$T_{d_{500}}$
Δ	20,0	10,6	—2,5	—5,4	18,6	—18,0	—23,0
σ	4,7	3,5	3,6	4,0	4,3	4,2	5,2
r	0.17	0,27	0,22	0,13	0,23	0,19	0,21

Table 4 (continued)

$(T'-T)_{500}$	K	u_{700}	v_{700}	$\overline{W}^{700}_{850}$	$H_{-10°C}$	T_1-T_{500}	Type of front
0,15	279,4	4,0	3,1	—12,4	4,3	37,8	3,6
2,8	5,2	6,8	7,8	37,9	0,6	3,4	1,4
0,22	0,23	—0,35	0,11	—0,21	0,24	0,03	0,02

Table 4 gives some statistical characteristics of the predictors and their correlation coefficients with the quantity of daytime precipitation. We note the near-zero mean value $(T' - T)_{500}$, mean small ordered ascending air movements $\overline{W}^{700}_{850}$, and also the absence of a close correlation between the selected predictors and the quantity of precipitation in Moscow. Even with $(T' - T)_{500}$ and the atmospheric front type such a correlation is absent, which indicates a difficulty in predicting summer precipitaion in general and inadequate informativeness of the predictors used.

It can be postulated that the slight correlations between the quantity of precipitation and the predictors (Table 4) are attributable to the fact that the sample included cases of precipitation caused by different atmospheric processes. In order to check whether this is so the entire sample was divided into two approximately equal classes on the basis of the sign and intensity of ordered vertical movements (W^{700}_{850}). When $W^{700}_{850} < -30$ mb/12 hours the cases were assigned to the class of cyclonic regions; in the remaining cases it was postulated that the precipitation was caused for the most part by convection. An evaluation of the informativeness of the predictors of these classes was made on the basis of the Mahalanobis distance (Δ^2):

$$\Delta^2 = \left[\frac{m(A) - m(\overline{A})}{\overline{\sigma}}\right]^2$$

where $m(A)$ and $m(\overline{A})$ are the mathematical expectations of the considered predictor of two classes; $\overline{\sigma}$ is the averaged standard deviation of the predictor of both classes.

The checking indicated that these classes were virtually inseparable by the selected predictors, it goes without saying, except for $\overline{W}^{700}_{850}$, which indicates the correctness of the analysis made using the full sample.

Is it possible to increase the reliability of forecasting of summer precipitation (in the sense of an increase in the correlation coefficient between the quantities of predicted and actual precipitation)? We made such an attempt. A forecast of the quantity of summer precipitation was prepared only in a case when rain (brief, showers, etc.) was called for in the synoptic forecast of precipitation, since the guaranteed probability of synoptic forecasts of the fact of summer precipitation ($\geqslant 0.1$ mm) for the considered cases is 92%; the guaranteed probability of the absence of precipitation is about 40% (rain is predicted more frequently and the absence of precipitation is rarer than it occurs). We also note that the mean quantity of precipitation for Moscow in the particular sample is 4.2 mm with $\sigma =$ 6.5 mm. Accordingly, the term "brief rain" contains about 2σ of the precipitation. Therefore, in many cases a prediction of summer precipitation on a practical basis contains information about the fact of precipitation, not about its quantity.

Initially in the entire sample we "sifted" eight predictors: u_{700}, K, $(T' - T)_{500}$, type of front, T_{d700}, T_{d500}, $\overline{W}^{700}_{850}$, PW^{700}_{gr}, which explained about 18-20% of the dispersion of the predictant.

An evaluation of the regression equations written using the eight predictors revealed that with a decrease in the number of predictors to three the $I_{(k)}$ values virtually do not change, which indicates the difficulty of predicting summer precipitation and the inadequate informativeness of the selected predictors. An equation using three predictors for forecasting the quantity of summer precipitation is given below.

$$Q = 0.05\ PW^{700}_{gr} - 0.03\ T_{d500} + 0.282K - 76.4. \quad (8)$$

Here Q is in mm/12 hours. The variables entering into equation (8) reflect atmospheric instability and moisture content. In a teaching sample this equation ensured a correlation coefficient 0.4.

Under operational conditions the checking of equation (8) for predicting the quantity of summer precipitation for the current day was made from 19 June through 4 August 1980. As a comparison we simultaneously made evaluations of synoptic forecasts on the basis of a numerical synoptic-hydrodynamic model [11, 12] and carried out a comparison of the precipitation measured with the radar at the Central Aerological Observatory with the precipitation actually falling at Moscow stations. The correlation coefficients between the quantity of falling precipitation and the quantity of precipitation: according to regression equations 0.20, in synoptic forecasts (median value of the anticipated gradation according to the Instructions [4]) 0.10; in synoptic-hydrodynamic forecasts 0.05 and with measurements with the Central Aerological Observatory radar 0.86.

As indicated by these data, the results of a forecast of the quantity of precipitation by means of regression equations are somewhat better than for other forecasting methods, but remain rather low. Precipitation $>$ 15-20 mm is not detected by all forecasting methods. It is entirely probable that the forecast of the quantity of summer precipitation by means of regression equations could be better if the forecast makes use of information on advective precipitation, which, as demonstrated above, is of great importance in the prediction of steady precipitation.

Taking into account the poor results obtained in the prediction of summer precipitation, it seemed desirable to examine the problem of what atmospheric factors better explain the physics of precipitation formation in a diagnostic plan. For this purpose we analyzed 65 days with and without precipitation at Moscow during the period 1 June-23 September 1980. In addition to the predictors which were enumerated above, in the analysis we used: divergence of wind velocity at the ground and at 300 mb (D), sec^{-1}; $(T' - T)_{max}$, °C; altitude of the condensation level (H_{cond}), km; cloud thickness (ΔH), km; W_{500}, mb/12 hours; instability index (I), °C, taken from [4],

$$I = (T_{850} - T_{500}) + T_{d_{850}} - (T_{700} - T_{d_{700}}).$$

Data on atmospheric parameters were taken from actual and diagnostic weather maps; these were determined from a convection model by the particle method on the basis of data for 1500 hours. Information on wind divergence at the ground level and at

300 mb was computed using observational data on the wind in a radius of 500 km from Moscow. The number of stations with wind data was not less than 10-12 [6].

In the diagnosis, as in the forecast, the closeness of the correlation between the quantity of precipitation and most of the considered atmospheric factors in general is low: r = ±0.1-0.2. For example, the correlation coefficient between the quantity of precipitation and $(T' - T)_{500}$ is 0.09, with ΔH -- 0.18, with $H_{-10°C}$ -- 0.12, with D_{300} -- 0.28. However, there are atmospheric parameters which better than others are related to the quantity of precipitation. In particular, this includes wind velocity divergence at the ground D_{gr}, correlation coefficient r = -0.61; T_{d700}· r = 0.32; I, r = 0.31; H_{cond}, r = -0,36; W_{700} and W_{500}, r = -0.43. These atmospheric parameters explain 37-44% of the dispersion of precipitation. The regression equation written using these predictors has the form

$$Q = -0.16\ D_{gr} + 0.05\ T_{d700} + 0.01\ I - 0.69\ H_{cond} - 0.03\ W_{700} + 2.6 \qquad (9)$$

and in the teaching sample ensures a correlation coefficient 0.66 (here Q is in mm/12 hours).

Therefore, from an analysis of the diagnostic factors it can be concluded that precipitation is observed when there is wind convergence at the ground, there is adequate moisture in the middle troposphere, there are ordered ascending air movements and the condensation level lies below 1 km. If the wind divergence value at the ground is less than $-0.5 \cdot 10^{-6}$ sec^{-1}, it can be said with a probability 83% that the situation is favorable for the falling of precipitation, whereas with $D_{gr} < -4.2 \cdot 10^{-6}$ sec^{-1} with an almost 100% probability it is possible to expect precipitation and its quantity will exceed 1 mm.

Equation (9) was not checked on the basis of operational data because there is still no solution of the problem where wind divergence at the earth should be computed for the forecast: should it be the forecast region, or in the advection region, or should their mean values be taken? Bearing in mind that evaluations of the regression equation (8) give $I_{(k)} = 7.04$ and for equation (9) give $I_{(k)} = 4.6$, that is, differ considerably, it can be assumed that the results of the forecast of the quantity of precipitation by means of equation (9) should be better than on the basis of (8).

Thus, in the prediction of the quantity of summer precipitation it is important to take into account the divergence of wind velocity at the ground, ordered vertical movements in the troposphere, generalized characteristics of vertical atmospheric instability and also the quantity of advective precipitation.

BIBLIOGRAPHY

1. Vapnik, V. N., VOSSTANOVLENIYE ZAVISIMOSTEY PO EMPIRICHESKIM DANNYM (Reconstruction of Dependences on the Basis of Empirical Data), Moscow, Nauka, 1979.

2. Dobryshman, Ye. M. and Tagaymuradov, Yu. T., "Use of the 'Sifting' Method for Analysis and Prediction of the Geopotential Field Over Central Asia During Cold Intrusions," TRUDY GIDROMETTSENTRA SSSR (Transactions of the USSR Hydrometeorological Center), No 39, 1969.

3. METODICHESKIYE UKAZANIYA PO PROVEDENIYU OPERATIVNYKH ISPYTANIY NOVYKH METODOV GIDROMETEOROLOGICHESKIKH PROGNOZOV (Methodological Instructions on Carrying Out Operational Tests of New Methods for Hydrometeorological Forecasts), Leningrad, Gidrometeoizdat, 1977.

4. NASTAVLENIYE PO SLUZHBE PROGNOZOV. RAZDEL 2. SLUZHBA METEOROLOGICHESKIKH PROGNOZOV (Instructions for the Forecasting Service. Section 2. Meteorological Forecasting Service), Parts III, IV, V, Moscow, Gidrometeoizdat, 1978.

5. Orlova, Ye. M., KRATKOSROCHNYY PROGNOZ ATMOSFERNYKH OSADKOV (Short-Range Forecasting of Atmospheric Precipitation), Leningrad, Gidrometeoizdat, 1979.

6. RUKOVODSTVO PO KRATKOSROCHNYM PROGNOZAM POGODY (Manual on Short-Range Weather Forecasting), Parts I, II, Leningrad, Gidrometeoizdat, 1964, 1965.

7. Suzuki, E., "Equation for Regression Evaluation of the Probabilities of Events and Forecasting Using Minimum Risk," TEORIYA VEROYATNOSTEY I MATEMATICHESKAYA STATISTIKA V ATMOSFERNYKH NAUKAKH (Theory of Probabilities and Mathematical Statistics in the Atmospheric Sciences), Leningrad, Gidrometeoizdat, 1975.

8. Snitkovskiy, A. I., "Short-Range Forecasting of Air Temperature, Steady Precipitation and Wind on the Basis of Prognostic Pressure Charts," METEOROLOGIYA I GIDROLOGIYA (Meteorology and Hydrology), No 9, 1979.

9. Snitkovskiy, A. I., "Short-Range Forecasting of Air Temperature," METEOROLOGIYA I GIDROLOGIYA, No 12, 1980.

10. Snitkovskiy, A. I., et al., SISTEMA OB"YEKTIVNOGO KRATKOSROCHNOGO PROGNOZA YAVLENIY I ELEMENTOV POGODY V SShA (System for Objective Short-Range Prediction of Weather Phenomena and Elements in the United States)(Review), Obninsk, Informatsionnyy Tsentr, 1978.

11. Uspenskiy, B. D., Mertsalov, A. N., Orlova, Ye. M., Belousov, S. L., Petrichenko, I. A. and Veselova, G. K., "Synoptic-Hydrodynamic Scheme for the Quantitative Forecasting of Steady and Shower Precipitation," TRUDY GIDROMETTSENTRA SSSR (Transactions of the USSR Hydrometeorological Center), No 157, 1976.

12. Uspenskiy, V.D., Mertsalov, A. N., Orlova, Ye. M. and Petrichenko, I. A., "Features of Forecasting of Precipitation in Numerical Operational Synoptic-Hydrodynamic Schemes for Times Up to 36 Hours," TRUDY GIDROMETTSENTRA SSSR, No 176, 1977.

13. Bermowitz, R. J., "An Application of Model Output Statistics to Forecasting Quantitative Precipitation," MON. WEATHER REV., Vol 103, No 2, 1975.

14. Boccihieri, J. R., "A New Operational System for Forecasting Precipitation Type," MON. WEATHER REV., Vol 107, No 6, 1979.

UDC 551.509.313(4)

NONADIABATIC MODEL OF ATMOSPHERE IN PRIMITIVE EQUATIONS FOR PREDICTING METEOROLOGICAL ELEMENTS OVER EUROPE

Moscow METEOROLOGIYA I GIDROLOGIYA in Russian No 7, Jul 81 (manuscript received 28 Oct 80) pp 18-26

[Article by S. O. Krichak, USSR Hydrometeorological Scientific Research Center]

[Abstract] A six-level adiabatic model of the atmosphere (S. L. Belousov, et al., TRUDY GIDROMETTSENTRA SSSR, No 212, 1978) is being used at the present time in preparing routine hemispheric forecasts at the USSR Hydrometeorological Scientific Research Center. During 1977-1978 the author and his associates carried out work for modifying the program of this model in FORTRAN language and implementing a system of programs for ensuring one-sided interaction with a hemispheric model in the course of regional forecasting. This gave a regional variant of the six-level adiabatic prognostic model of the atmosphere whose use was approved in 1980. Thereafter the principal nonadiabatic processes (influence of orography, surface friction, heat flows from the underlying surface, radiation processes in the atmosphere with allowance for the diurnal variation of the influx of solar radiation, processes of macroscale and convective formation of precipitation, etc.) were included in the model. The article discusses the principal characteristics of this model. It is emphasized that except for the region of the forecast, resolution, boundary conditions employed, filtering procedures, allowance for nonadiabatic factors and inclusion of the humidity field as one of the predicted variables this variant of the model coincides with the hemispheric model. The success of such forecasts is evaluated. An example of prediction of precipitation is given. Figures 1, tables 2; references 9: 5 Russian, 4 Western.

UDC 551.(515.2:515.3)

INVESTIGATION OF PATTERNS OF MOVEMENT OF MACROSCALE VORTICES RELATIVE TO A PURELY ZONAL FLOW

Moscow METEOROLOGIYA I GIDROLOGIYA in Russian No 7, Jul 81 (manuscript received 28 Oct 80) pp 27-35

[Article by B. Ya. Shmerlin, Institute of Experimental Meteorology]

[Abstract] A model of the movement of macroscale vortices relative to a purely zonal steering flow is proposed. The movement of middle-latitude cyclones and anticyclones is examined. The velocities of movement of vortices in a meridional direction were determined. The movement of tropical cyclones is also considered. It is shown that there are three types of trajectories of tropical cyclones. The values of the parameters of the vortices and steering flow for which each of the types of trajectories is realized are determined. The conclusions drawn are compared with observations of macroscale vortices in the middle latitudes and tropical hurricanes. The analysis given here shows that all the parameters introduced into the problem, describing flow and vorticity, are of considerable importance in predicting the movement of a vortex. Near the values of the parameters at which there is a change in the type of trajectory small changes in the parameters lead to considerable changes in the type of vortex trajectory and this is very important to take into account in predicting the movement of tropical hurricanes. The results presented here are easily extended to any (not necessarily purely zonal) geostrophic steering current. The results can be applied in the parameterization of the meridional transfer of heat and moisture by macroscale vortices, in solving the problem of "self-consistent" formation of meridional and zonal circulation and in predicting the movement of tropical hurricanes. Figures 2; references 12: 9 Russian, 3 Western.

UDC 551.510.534

INFORMATIVENESS OF GLOBAL SYSTEMS FOR OBSERVING TOTAL OZONE CONTENT

Moscow METEOROLOGIYA I GIDROLOGIYA in Russian No 7, Jul 81 (manuscript received 2 Jul 80) pp 36-45

[Article by O. M. Pokrovskiy, candidate of physical and mathematical sciences, and A. Ye. Kaygorodtsev, Main Geophysical Observatory]

[Text]

Abstract: On the basis of a spectral scheme for the objective analysis of the field of total ozone content in the northern hemisphere the authors made computations of the characteristics of informativeness of the surface ozonometric network (SON) and two remote sensing systems based on methods making use of backscattering of solar UV radiation and characteristic atmospheric IR radiation. Combined observation systems are examined. Recommendations are presented on the preferable choice of solar UV radiation or atmospheric IR radiation for measurements in different latitude zones for each of the two seasons. The article gives an analysis of the informativeness for individual orbits. The optimum regions for the collection of information by means of the solar ultraviolet and atmospheric IR systems are defined with allowance for the layout of the surface observation network.

The timeliness of the problem of monitoring atmospheric ozone distribution is determined by the fact that according to existing concepts [4] the ozone concentration to a definite degree can be changed due to the influence of contaminants caused by man's economic activity (nitrogen oxides, chlorofluoromethanes, etc.). The influence of anthropogenic factors is not limited to photochemical processes in the stratosphere and lower mesosphere. It is of the greatest interest to study the influence of anthropogenic contaminants on the entire sequence of interrelated processes of photochemistry, radiation heating and cooling, and also the transport of air masses in the stratosphere and their resultant role in modern changes in climate. The inadequacy of actual data on physical mechanisms in the stratosphere, as well as the impossibility of reproducing the mentioned chain of processes with adequate accuracy and detail by means of numerical modeling, make it necessary to

create simplified models which must be refined on the basis of the results of actual observations of the fields of ozone and other gas components and the principal meteorological parameters (temperature, pressure, wind velocity).

Observational data must serve as additional information for adaptation of the developed numerical models and for clarification of the degree of their adequacy in predicting the possible consequences of anthropogenic modification.

The planning of new observation systems makes it necessary to study two parameters: the total content and vertical distribution of ozone within the limits of the middle and upper stratosphere.

The influence of photochemistry on the formation of the vertical profile of ozone is reflected in the atmospheric layer situated above the 35-km level. The ozone concentration at altitudes 50-60 km changes insignificantly with latitude and season, since here the ozone is in photochemical equilibrium. Accordingly, information on the variability of the ozone concentration in the layer 35-50 km gives some idea concerning the distribution of the "inputs" and "outputs" and is necessary for adjustment of the photochemical part of the stratospheric model. However, this atmospheric layer contains only about one-third of the ozonospheric mass. The remaining two-thirds are situated below 35 km and to a considerable degree are subject to the influence of dynamic factors. The spatial distribution of total content reflects the peculiarities of atmospheric circulation in the upper troposphere and lower stratosphere. Accordingly, information on the field of total ozone content is necessary for refining the dynamic block of three-dimensional stratospheric models.

Thus, the formulation of the problem of remote sensing of the ozone field involves measurements of the vertical distribution of total content of ozone in the middle and upper stratosphere characterizing quite independent physical processes.

At the present time extensive observational data relating to a period of two decades have made it possible to clarify the principal patterns of spatial and seasonal variability of the total ozone content [5]. The existing network, consisting of more than a hundred ozonometric stations, is very nonuniformly distributed even in the northern hemisphere. Nevertheless, the accumulated information must serve as a basis for the rational expansion of ground observations and the planning of new measurement systems. A satellite monitoring system can become an important addition to the existing ozonometric network. This study is devoted to an examination of the problems involved in evaluating the information content and planning remote systems for monitoring the variability of the field of total ozone content in the northern hemisphere, taking into account the existing network of stations.

Formulation of Problem

During recent years several experiments have been carried out for determining the total ozone content on the basis of two schemes for remote measurement of this parameter. The possibilities of a method using data on the spectrum of UV radiation in the Hartley-Huggins absorption band, reflected by the atmosphere, have been studied most intensively. Experience has shown [9] that the method of backscattering of solar UV radiation makes it possible to determine the total content with an accuracy of about 6% at all latitudes. As a comparison we note that

the relative error in surface measurements of total ozone content is 1-2%. However, the spatial resolution of such data is 150-200 km or less [9]. Other shortcomings include the fact that this method can be used only on the daytime side of our planet. In particular, the extensive polar zone of the winter hemisphere, where the ozone fluctuations are extremely significant, remains inaccessible for measurements.

Another approach is based on measurement of atmospheric IR radiation of the atmosphere-earth system at the nadir in the region of the ozone absorption band 9.6 μm [7]. The error in this method is about 7% in the low latitudes [7] and increases by a factor of approximately 3 in a poleward direction, attaining a maximum value of about 20% at 75°N [10], where ozone fluctuations are most significant. The relatively low accuracy of the IR method is compensated by a higher spatial resolution, attaining 30-40 km [7]. An important merit of the IR method is its applicability at any time of day. An extremely high spatial density of measurements can be attained by means of scanning with an IR spectrometer across the orbit.

The problem of planning observation systems is characterized by those temporal and spatial scales of disturbances of the ozone field, data on which are of interest for practical problems. At the present time the considerable interest in ozone is related to the problem of modern changes in climate [4]. Here the following characteristic scales are operative: time interval from a month to a season, zonal averaging from 20 to 360°. In addition to disturbances of a climatic scale there is a broad spectrum of aperiodic fluctuations caused by synoptic processes in the troposphere. In regions with a great (small) ozone content there is usually a pressure field trough (ridge) [10].

Fluctuations of different scales can be separated by spectral analysis. This approach is used below for discriminating and indicating disturbances of a climatic scale. The basis for determining the climatic modes of the ozone field in the northern hemisphere was obtained by computing the empirical orthogonal functions (EOF) on the basis of a 10-year series of mean monthly data from analysis in a regular grid cited in the atlas [6]. Despite the spatial nonuniformity, the ozonometric network of stations provides data on the most important regions of zonal nonuniformity of the ozone field in the northern hemisphere.

It is well known [4, 11] that the redistribution of ozone from the low into the middle and high latitudes is associated with the structure of baroclinic zones forming cyclones and anticyclones and also planetary waves in the upper troposphere and lower stratosphere. An analysis of the results of satellite observations [7] confirmed that the most important regions of zonal nonuniformity of the ozone field are located in Western Europe, in Eastern Siberia, in the middle-latitude zone of the Pacific Ocean coast of Asia and the Atlantic coast of North America. For the most part the regions mentioned here are situated on the continent-ocean boundary and are zones of active interaction between the atmosphere and ocean. These regions were defined earlier on the basis of surface observations.

It is therefore not surprising that on the EOF graphs [1], computed on the basis of statistical data [6], it is possible to detect the mentioned regions. The EOF base which we used for spectral analysis cannot be considered entirely adequate. The feasibility of its use for the planning of remote sensing systems (RSS) is determined by the fact that it contains all the information from surface measurements.

The principal practical purpose of this study was an examination of three problems related to the planning of RSS: in what way is there a relationship between the surface ozonometric network, on the one hand, and the planned RSS, on the other? Which of the two RSS -- IR or UV -- should be regarded as the more promising from the point of view of monitoring fluctuations of the ozone field? In what regions is it desirable, taking into account the currently existing surface ozonometric network, to accomplish collection of remote sensing data, bearing in mind the limitations on the storage capacity of on-board memory units?

In order to obtain answers to the formulated problems we will discuss the results of numerical modeling in accordance with the spectral analysis scheme presented below.

Method for Computing Informativeness Characteristics of Observation Systems

Now we will examine the method for evaluating the informativeness of global systems for observing fluctuations of the ozone field. In the case of surface observations the relationship between the measured and true values of the sought-for parameter has the form

$$\bar{x}(s)=x(s)+\varepsilon(s), \tag{1}$$

where $\varepsilon(s)$ is the random error in measurements at a station located at a point of intersection of a horizontal grid $s(s = 1,\ldots,N)$. The equation written in terms of deviations from the mean climatic values $x(s)$ has a similar form. It can be assumed that $\varepsilon = (\varepsilon(1),\ldots,\varepsilon(N))^T$ is the random vector of observation errors having mean components ($\varepsilon(s) = 0$) and a stipulated diagonal matrix of the covariations $K_\varepsilon = \sigma^2 I$ (I is a unit matrix, T is the transposition sign). The latter means that the errors in observations at different stations are statistically independent.

It is known [2] that the interpretation of remote sensing data is related to solution of the linearized algebraic system

$$\Delta L(s)=A\cdot\Delta q(s)+\delta(s). \tag{2}$$

Here ΔL and Δq are the vectors of deviations in the intensities of outgoing radiation and the ozone profiles from the corresponding means $\bar{L}(s)$ and $\bar{q}(s)$, $\delta(s)$ is the vector of measurement errors. We will assume that the δ components have zero means and a known covariation matrix K_δ and that remote measurements were made at M points ($s = N + 1,\ldots,N + M$). The deviation of the $\Delta x(s)$ value is a linear functional of the form $r^T\cdot\Delta q(s)$ (r is an arbitrary vector) from the vertical profile of deviations $\Delta q(s)$ at the s point of intersection. Here the vector is the row $x^T = (b_1,\ldots,b_n)$; b_i are quadrature coefficients used for an approximation of the integral in computing the parameter of total ozone content in a vertical column of the atmosphere. The evaluations $\Delta\tilde{x}(s)$, obtained in the form of a linear function of $\Delta\tilde{L}(s)$, are related to the true values of the $\Delta x(s)$ parameters by the expression

$$\Delta\tilde{x}(s)=\Delta x(s)+\varepsilon(s), \tag{3}$$

in which $\varepsilon(s) = p^T \cdot \delta(s) - r^T \cdot R \cdot \Delta q$, $p^T = r^T \cdot A^+$, A^+ is a matrix pseudoinverse of A, $R = I - A^+ \cdot A$. The dispersion $\varepsilon(s)$ in (3) is described by the equation $\sigma_\varepsilon^2 = p^T \cdot K_s \cdot p + r^T \cdot R \cdot K_q \cdot R \cdot r$, where K_q is the matrix of covariations for the Δq vector.

We will combine the observation equations (1) and (3) for the entire set of points of intersection (s = 1,..., N+M), using a spectral form of writing. The EOF base affords such a possibility. Assume that the matrix

$$Z = \left\{ z_{ij} \right\}_{i=1,\ j=1}^{t \qquad k}$$

was formed by the values of the first k EOF in a grid containing t points of intersection. We will assume that $k < N+M < t$. For the vector of deviations of the total ozone content at the grid points of intersection $\Delta X = (\Delta x(1),..., \Delta x(t))^T$ the following representation is correct

$$\Delta X = Z \cdot c + \gamma. \tag{4}$$

Here $c = (c_1,...,c_k)^T$ is a set of unknown coefficients of the expansion, γ is the vector of residues of the series. In the set of grid points of intersection we discriminate the set N+M of observation points and denote it ω. Then from (4) we can separate out the subsystem

$$\Delta X_\omega = Z_\omega \cdot c + \tilde{\varepsilon}_\omega, \tag{5}$$

where $\tilde{\varepsilon}_\omega = \gamma_\omega + \varepsilon_\omega$, ε_ω is a vector whose components represent a set of observation errors in (1) and (3). With the use of EOF as the system of base functions the components of the vector c are independent random values with zero mean and stipulated dispersions λ_i^2 (i = 1,...,k). The dispersion of the γ norm is determined by the "tail" of the series

$$\sum_{i=1}^{t} \lambda_i^2.$$

The covariation matrix of the vector c $\Lambda = \mathrm{diag}\,(\lambda_1^2,..., \lambda_k^2)$. We use $\tilde{K}_\omega$ to denote the covariation matrix $\tilde{\varepsilon}_\omega$. For the residual covariation matrix $\tilde{\Lambda}$ of evaluations of the c vector the following formula is correct

$$\tilde{\Lambda} = (Z_\omega^T \cdot \tilde{K}_\varepsilon^{-1} \cdot Z_\omega + \Lambda^{-1})^{-1}. \tag{6}$$

We note that here it is necessary to invert a matrix of the dimensionality k x k, which is virtually always applicable. Transformation to a regular grid makes it possible to obtain evaluations of accuracy on the basis of computations of the matrix of residual covariations

$$\tilde{\Sigma} = Z \cdot \tilde{\Lambda} \cdot Z^T. \tag{7}$$

It is desirable that the results be analyzed on the basis of absolute and relative accuracy characteristics. The values of the standard deviations $\tilde{\sigma}_{ii}$ (i = 1,...,t), representing the square roots of the diagonal elements $\tilde{\Sigma}$, characterize the accuracy in analysis of the ozone field. The values of the relative residual dispersions $d_i^2 = \tilde{\sigma}_{ii}^2 / \sigma_{ii}^2$ (i = 1,...,t). Here σ_{ii}^2 are the diagonal elements of the matrix for natural covariations in the regular grid $\Sigma = Z \cdot \Lambda \cdot Z^T$. It

is also desirable to examine the mean values in the grid.

$$\overline{\overline{\sigma^2}} = \frac{1}{t}\sum_{i=1}^{t}\tilde{\sigma}^2_{ii}, \quad \overline{d^2} = \frac{1}{t}\sum_{i=1}^{t} d_i^2.$$

Henceforth the

$$\sqrt{\overline{\overline{\sigma^2}}}, \quad \sqrt{\overline{d^2}}$$

values will be called the analytical error (AE) and the relative analytical error (RAE).

Mean Indices of Informativeness of Observation Systems

The spatial grid in which EOF computations were made had an interval of 2.5° in latitude and 10° in longitude. The EOF were computed for two seasons: I (winter-spring), II (summer-autumn). Stations in the surface observation network were modeled by the nearest grid points of intersection. It was assumed that the satellite observations are made in polar orbits, one displaced relative to the other by 20°. Three densities of satellite measurements were modeled along the orbit with a latitude interval $\Delta\theta_{1,2,3}$ = 2.5°, 5°, 10°. In accordance with the comments cited in the first section we modeled 2 RSS. The first was a solar UV system simulating the UV measurement system, having a constant relative error along the orbit equal to 6%. In the computations of the informants for the solar UV variant I (EOF for season I) we excluded the measurements in the polar zone (to the north of 70°N). The second -- atmospheric IR, modeling an IR sensing system, had a relative error variable with latitude along the orbit (as was indicated in the first section).

Now we will analyze the results of computations of the mean indices of informativeness of AE and RAE, presented in the table. During the period of season I the surface observation system is somewhat more informative than any RSS. In the course of season II the informativeness of the solar UV system appreciably exceeds the similar indices of the surface observation system. In this case the atmospheric IR system is close in its indices to the surface observation system. The dependence of the accuracy of analysis based on data on solar UV radiation on measurement density, as can be seen from the table, is of the order of magnitude 0 ($\sqrt{m}$), where m is the number of observations. Computations show that the role of the indicated factor is also important in an analysis of the troposphere, with the surface observation system taken into account. Thus, an increase in the density of spatial measurements is an important reserve for an increase in the effectiveness of the contribution of RSS data.

Due to the lack of data from UV measurements in the polar zone of the winter hemisphere the solar UV system is inferior in its informativeness to the atmospheric IR system in the period of season I. Computations show that the absence of measurements in the polar zone causes an increase in the AE according to solar UV radiation by a factor of approximately 1.5-1.7. Even taking into account data from the surface observation system, the AE increases by 20-25% as a result of the indicated factor. On the other hand, during the summer hemisphere the solar UV system has an appreciable advantage over atmospheric IR. This advantage almost disappears under the condition that atmospheric IR measurements are made in twice as dense a spatial measurement grid as solar UV measurements. Thus,

the relatively low accuracy of atmospheric IR can be compensated by the possibilities of using a higher spatial resolution of atmospheric IR for increasing the density of measurements.

Table 1

Characteristics of Informativeness of Different Systems for Observing Field of Total Ozone Content

Observation system	Season	Density of remote measurements, degrees	AE	RAE
SOS	I	--	3.95	0.14
SOS	II	--	3.72	0.18
SUV	I	2.5	4.9	0.15
SUV	I	5	6.3	0.19
SUV	I	10	8.9	0.26
SUV	II	2.5	2.9	0.14
SUV+SOS	I	2.5	2.7	0.09
SUV+SOS	II	2.5	2.2	0.11
AIR	II	2.5	3.84	0.18
AIR+SOS	II	2.5	2.61	0.13
SIR	I	2.5	4.09	0.14
SIR+SOS	I	2.5	2.69	0.09

The AE and RAE values, according to data from the combined observations systems -- atmospheric IR + surface observation system and solar ultraviolet + surface observation system -- virtually coincide in the winter hemisphere. The solar UV system, in combination with the SOS, is more informative in the period of season II than atmospheric IR. Changes in the AE according to data for the combined observation systems, in comparison with the AE for individual systems, occur in conformity to nonlinear relationships determined by the complex dependence of the matrix components $\tilde{\Lambda}$ in (6) on the dispersions of measurement errors entering into $\tilde{K}_{\xi}$.

In summarizing the results of this examination, we note the following conclusions. In the winter hemisphere the SOS has an advantage over the RSS; in the summer hemisphere the opposite picture is observed. Ultraviolet measurements must be made in the summer hemisphere and IR measurements are more effective in the winter hemisphere.

Latitudinal Distributions of RAE

The field of the total ozone content has a known latitudinal structure. The dispersion of natural ozone fluctuations decreases, although not monotonically, from the pole to the equator. The SOS is distributed nonuniformly in the latitude coordinate. Most of the stations are located in the middle latitudes; the tropical and polar zones are covered less well. Accordingly, taking into account the spectrum of natural fluctuations of the ozone field it is desirable to evaluate the possible information contribution of the RSS, to clarify in what latitude zones satellite measurements are especially necessary.

The zonally averaged RAE values d^2_θ (θ indicates a dependence on latitude), corresponding to different observation systems, are given in Fig. 1. The surface observation system appreciably exceeds the RSS in the summer season (Fig. 1a). In the tropical zone atmospheric IR gives the minimum RAE values. Here the solar UV has an RAE close to that which is characteristic for the surface observation system.

In the middle latitudes, due to the increase in measurement errors, the informativeness of atmospheric IR becomes lower than for the solar UV system. Only in the polar zone is it possible to note the advantages of RSS over SOS. During winter (Fig. 1b) the RAE values for solar UV and SOS systems are close in the middle latitudes. In the tropics there is an indisputable advantage of RSS. The solar ultraviolet system is more informative than the atmospheric IR system. Due to the absence of UV measurements in the polar zone of the winter hemisphere the RAE values for solar UV here rarely increase. This circumstance ensures an advantage of atmospheric IR. However, the SOS and atmospheric IR are close in their informativeness in the polar zone due to the relatively low accuracy of the atmospheric IR method.

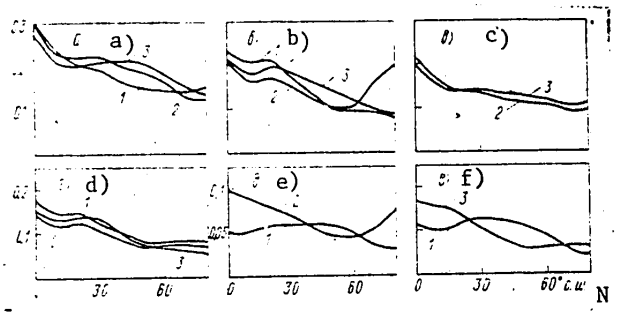

Fig. 1. Latitudinal dependences of RAE d^2_θ. a) season II: 1) SOS, 2) solar ultraviolet ($\Delta\theta$= 05°), 3) atmospheric IR ($\Delta\theta$ = 2.5°); b) season I: SOS, 2) solar UV ($\Delta\theta$ = 2.5° ($\Delta\theta$= 2.5°, without polar region), 3) atmospheric IR ($\Delta\theta$= 2.5°); c) season II: 2) SOS + solar UV ($\Delta\theta$ = 5°), 3) SOS + atmospheric IR ($\Delta\theta$ = 2.5°); d) season I: 1)SOS + solar UV ($\Delta\theta$ = 5° without polar region), 2) SOS + solar UV ($\Delta\theta$ = 2.5°, without polar region), 3) SOS + atmospheric IR ($\Delta\theta$ = 2.5°); e) season II: 1) Δd^2_θ (SOS), 2) Δd^2_θ (solar UV); f) season I: 1) Δd^2_θ (SOS), 3) Δd^2_θ (atmospheric IR).

An analysis on the basis of SOS and RSS data is of maximum practical interest. The dependence of RAE on latitude for two variants of combined observation systems SOS + atmospheric IR and SOS + solar UV (Fig. 1,c,d) make it possible to draw several conclusions. The SOS + atmospheric IR system has a considerable advantage in summer in the tropics and in winter in the polar zone. The solar UV system in combination with the SOS in summer is more informative in the middle and high latitudes. Since the measurements of solar UV have a lesser spatial density than the atmospheric IR, the combined SOS + atmospheric IR is preferable for winter season conditions (Fig. 1d).

In the analysis of the informativeness of the combined observation system it is important to evaluate the individual informative contribution of its individual components in different latitude zones. For this purpose we computed the data increments arising in the creation of combined observation systems. It is natural to determine them using the formulas: Δd^2_θ (atmospheric IR) = d^2_θ (SOS) $-d^2_\theta$ (atmospheric IR + SOS); Δd^2_θ (solar UV) = d^2_θ (SOS) $-d^2_\theta$ (solar UV + SOS); Δd^2_θ (SOS/atmospheric IR) = d^2_θ (atmospheric IR) $-d^2_\theta$ (atmospheric IR + SOS); Δd^2_θ (SOS/solar UV = d^2 (solar UV) $-d^2$ (solar UV + SOS). Latitudinal increments of information show that the SOS has information advantages in the middle latitudes for both seasons. In summer the advantages of the SOS are limited to the range 40-60°N (Fig. 1e). The solar UV system considerably dominates in the tropical and polar zones. In winter the advantages of the atmospheric IR system also remain important in the tropical zone (Fig. 1f). In the high latitudes the role of satellite observations is somewhat less appreciable.

An examination of the latitudinal aspect of the problem of informativeness of the planned RSS makes it possible to conclude that the solar UV and atmospheric IR systems mutually supplement one another. They also supplement SOS data. In summer in the tropical zone it is desirable that the atmospheric IR system be used. In the middle and high latitudes it is necessary to make measurements using the solar UV system. During winter, on the other hand, the solar IR system can provide useful information in the polar zone. In the tropics and temperate zones the solar UV system can have advantages over the atmospheric IR system.

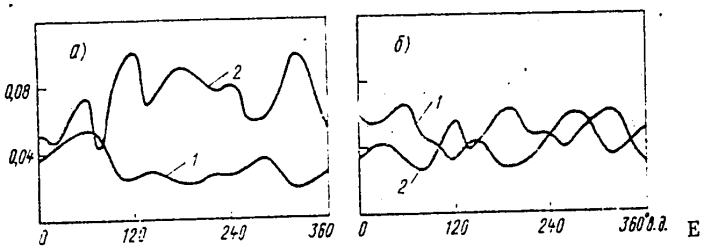

Fig. 2. Zonal dependences of information increments Δd^2_λ. a) season II: 1) SOS, 2) solar UV, b) season I: 1) SOS, 2) atmospheric IR.

Zonal Structure of Characteristics of Informativeness of Measurement Systems

RSS have a characteristic feature: measurements along polar orbits close to meridional circles. Obvious limitations on the volume of storage of the information collected by means of on-board memory devices dictate the timeliness of the problem of optimum planning of observations. An examination of the meridional aspect of the problem made it possible to formulate recommendations on measurements in different latitude zones. The investigation of latitudinally averaged RAE values d^2_λ, being a function of longitude λ, creates a prerequisite for the detection of the most informative orbits. For SOS the informational contribution Δd^2_λ (SOS/solar UV) = d^2_λ (solar UV) $-d^2_\lambda$ (solar UV + SOS) (Fig. 2a,b) attains maximum values along the continental regions, and the minimum values -- for longitudes corresponding to the location of the Pacific and Atlantic Oceans. The western coast of North America and East Asia (excluding the Japanese islands) are poorly supplied with data. In order to study the role of RSS it is desirable to examine the increments of the informativeness indices attributable to the contribution of satellite observations: Δd^2_λ (solar UV) = d^2_λ (SOS) $-d^2_\lambda$ (solar UV + SOS);

Δd^2_λ (atmospheric IR) = d^2_λ (SOS) $-d^2_\lambda$ (atmosoheric IR + SOS). The curves of the mentioned data increments shown in Fig. 2a,b give some idea concerning the relative effectiveness of measurements in relation to different longitude values. The maximum values of the information contributions Δd^2_λ (solar UV) and Δd^2_λ (atmospheric IR) fall in the central regions of the Pacific and Atlantic Oceans. In addition, a region of East Asia is defined where the ozone variations are significant both in summer and in winter and the network of surface ozonometric stations is inadequately dense, as is indicated by the Δd^2_λ minimum (surface observation network) at $\lambda = 120^\circ$E (Fig. 2a,b)

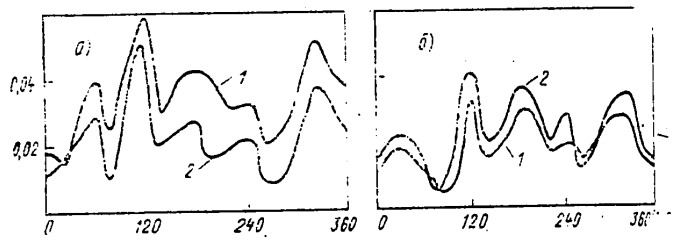

Fig. 3. Information contribution in individual orbits $\Delta d^2_{\lambda_i}$ (dependence on longitude of orbit λ_i). a) season II: 1) solar UV; 2) atmospheric IR; b) season I: 1) solar UV, 2) atmospheric IR

These estimates relate to the influence of the entire set of observations on refinement of the zonal component of the ozone field. However, for the purposes of planning it is important to study the information contributions of measurements in individual orbits. Since the measurements in a particular orbit with $\lambda = \lambda_i$ make the principal contribution to evaluation of the field at the subsatellite points, it is desirable to examine the values $\Delta d^2_{\lambda_i}$ (atmospheric IR (λ_i) = $d^2_{\lambda_i}$ (surface observation network) $-d^2_{\lambda_i}$ (surface observation network + atmospheric IR (λ_i)); $\Delta d^2_{\lambda_i}$ (solar UV (λ_i)) = $d^2_{\lambda_i}$ (surface observation network) $-d^2_{\lambda_i}$ (surface observation network + solar UV (λ_i)). The maximum values of the functions describing the contributions of the measurements in individual orbits (Fig. 3a,b) relate to the already mentioned central regions of both oceans and also to the eastern part of Asia. The effectiveness of the measurements in the indicated regions is 1.5-2 times greater than for other orbits. The minimum values of the information contribution relate to orbits passing over Western Europe ($\lambda = 0$-10°E), Central Asia ($\lambda = 80$-90°E) and North America ($\lambda = 80$-100° W). In addition to these zones, having extremal indices of effectiveness of satellite measurements, it is necessary to note the adequately informative orbits passing over the western part of North America and the eastern sector of the Pacific Ocean ($\lambda = 120$-140°W). During summer it is desirable to carry out remote measurements at $\lambda = 60^\circ$E, which supply information on considerable fluctuations of the ozone field caused by the peculiarities of the dynamics of air masses associated with the Asiatic monsoon in the northwestern sector of the Indian Ocean. The similarity of the dependence Δd^2 (solar UV (λ)) and Δd^2_λ (solar UV) on λ, and also the similar characteristics for atmospheric IR again confirm the conclusions in [3] that the horizontal correlation of the ozone field has a spatial scale similar to that which is characteristic for temperature and geopotential. Thus, the informative orbits are situated not only over the waters of the oceans, where there are almost no surface observation stations,

but also over regions covered by measurements where there is a great variability of the total ozone content.

Principal Conclusions

The systems for remote indication of the field of total ozone content in the northern hemisphere in their informativeness are close to the surface network. The principal contribution of data from satellite observations is from the high and tropical latitudes. The IR system is most effective in winter, primarily in the temperate and polar latitudes. The UV system has appreciable advantages in summer in the middle and high latitudes. In the tropical zone the desirability of using IR measurements is related to the possibilities of attaining a high spatial resolution (30-50 km). The most informative orbits are those passing not only over the central part of the waters of the Pacific and Atlantic Oceans, but also over regions of East Asia (λ= 120°E) and the western part of North America (λ= 80-100°W). In summer it is desirable that measurements be made in an Asiatic orbit at λ= 60°E. Observations with allowance for the cited recommendations and with use of satellite systems will supply information which to a substantial degree is not dependent on data from the surface network of stations.

BIBLIOGRAPHY

1. Kaygorodtsev, A. Ye. and Pokrovskiy, O. M., "Natural Components of the Field of Total Ozone Content in the Northern Hemisphere," METEOROLOGIYA I GIDROLOGIYA (Meteorology and Hydrology), No 8, 1980.

2. Pokrovskiy, O. M. and Kaygorodtsev, A. Ye., "Informational Content of IR Ozone Measurements in the Atmosphere," IZV. AN SSSR: FIZIKA ATMOSFERY I OKEANA (News of the USSR Academy of Sciences: Physics of the Atmosphere and Ocean), Vol 14, No 8, 1978.

3. Pokrovskiy, O. M., Ivanykin, Ye. Ye. and Kaygorodtsev, A. Ye., "Numerical Modeling of Systems for Observing and Analyzing the Ozone Field," METEOROLOGIYA I GIDROLOGIYA, No 1, 1979.

4. CIAP MONOGRAPH 1. THE NATURAL STRATOSPHERE. DOT-TST-75-51, 1975.

5. Dutsch, H. U., "The Ozone Distribution in the Atmosphere," CAN. J. CHEM., Vol 52, No 6, 1974.

6. London, J., et al., ATLAS OF THE GLOBAL DISTRIBUTION OF TOTAL OZONE. July 1957-June 1967, NCAR TECHN. NOTE. NCAR (TN), 113, 1976.

7. Lovill, J. E., et al., TOTAL OZONE RETRIEVAL FROM SATELLITE MULTICHANNEL FILTER RADIOMETER MEASUREMENTS, L. L. L., UCRL 52473, 1978.

8. Mateer, C. L., et al., "Estimation of Total Ozone From Satellite Measurements of Backscattered Ultraviolet Radiance," J. ATMOS. SCI., Vol 28, No 6, 1971.

9. Penndorf, R., ANALYSIS OF OZONE AND WATER VAPOR FIELD MEASUREMENT DATA, REP. FAA-EE-78-29, 1978.

10. Prior, E. J. and Oza, B. J., "First Comparison of Simultaneous IRIS, BUV and Ground-Based Measurements of Total Ozone," GEOPHYS. RES. LETTER, Vol 5, No 5, 1978.

11. Reiter, E. R. and Lovill, J. E., "The Longitudinal Movement of Stratospheric Ozone Waves as Determined by Satellite," ARCH. METEOROL. GEOPHYS. BIOCLIMATOL., Vol A23, No 1, 1974.

UDC 551.(558.1:576.11:509.616)

AXISYMMETRIC PROBLEM OF FREE CONVECTION AND NUMERICAL EXPERIMENTS FOR DYNAMIC MODIFICATION OF A CUMULUS CLOUD

Moscow METEOROLOGIYA I GIDROLOGIYA in Russian No 7, Jul 81 (manuscript received 30 Sep 80) pp 46-53

[Article by A. S. Kabanov, candidate of physical and mathematical sciences, and A. Ye. Klykov, Institute of Experimental Meteorology]

[Text]

Abstract: It is demonstrated by a comparison of an analytical solution of a simplified and numerical solution of the axisymmetric problem of dry convection with a constant turbulence coefficient that the development of convection into multilevel convection is a result of a stable stratification of the atmosphere. On the basis of an axisymmetric model of a cumulus cloud both with variable and constant turbulence coefficients the authors carried out a series of numerical experiments for the dynamic modification of a cumulus cloud for the purpose of ascertaining the most favorable modification conditions.

In [5] we compared the results of a numerical axisymmetric model of convection with the results of analytical solution of a plane problem, which could cause doubts as to the admissibility of such a comparison. Accordingly, the purpose of this article is first and foremost a demonstration that in the case of stable stratification there is an effect of development of atmospheric convection into multilevel convection. The proof is presented using an analytical solution of a simplified axisymmetric problem of dry convection and comparison of the analytical solution with the numerical solution of the axisymmetric problem with a constant turbulence coefficient. A knowledge of the analytical solution of the axisymmetric problem and its comparison with the numerical solution also made it possible to solve a number of important methodological problems for ascertaining the extent of the reckoning region undistorted by boundary conditions (simulating conditions at infinity) when formulating a numerical model of a cumulus cloud. Earlier this model was used in studying the thermal effect on a cloud [5].

Recently much attention has been devoted to dynamic methods for modifying cumulus clouds for suppressing cloud activity. As is well known, descending movements favor the evaporation of droplets and thereby the destruction of clouds. Among the

methods responsible for the formation of descending currents are the helicopter modification method, the flight of aircraft over clouds, the maneuvering of jet aircraft with large pitching angles, and the dropping of powders of different composition from aircraft: talc, sodium chloride, etc.

When powder is introduced into the region of the tops of convective clouds, in addition to the powder there is downward entrainment of the surrounding air with the moisture and cloud droplets present in it [4]. Unstable stratification in clouds accelerates the descending flows, in which the air temperature is below that of the ambient atmosphere and there is an intensive evaporation of cloud droplets. The dispersal of a cloud occurs as a result of the outflow and settling of its peak and "peeling off" and evaporation of the cloud at its base. The effect of the powder is associated with the destruction of ascending flows in the clouds, which leads to a cessation of its development and dispersal.

It was demonstrated in [2, 3] that in an unstably stratified atmosphere, under the influence of the momentum of the descending air movement, the development of stationary jets is possible. The results of the theory of stationary descending flows demonstrate that under real conditions the velocity of the descending jet can be equal to the velocity of the ascending flow and even exceed it. The destruction of the most vigorously developing clouds should occur more intensively, which is associated with the more unstable stratification of the atmosphere. With the artificial formation of stationary descending jets it is necessary to take into account the intensity and duration of the downward-directed force.

Below, on the basis of the nonstationary problem, using numerical methods for solution of the nonlinear equations of thermohydrodynamics with variable turbulence coefficients, a study is made of the influence of the effect of the downward-directed force on the development of a cumulus cloud.

Linear axisymmetric problem of free convection in a stably stratified atmosphere. without viscosity and thermal conductivity. We will examine the convection of an ideal fluid in a cylindrical coordinate system when boundaries, humidity, viscosity and thermal conductivity are absent and the nonlinear terms are negligible. In this case the system of equations of free convection can be written in the form:

$$\frac{\partial \eta}{\partial t} = \frac{g}{T_0}\frac{\partial T'}{\partial r}, \tag{1}$$

$$\frac{\partial T'}{\partial t} + (\gamma_a - \gamma) V_z = \frac{q(r,z,t)}{\rho c_p}, \tag{2}$$

where the tangential component of vorticity is

$$\eta = \frac{\partial V_z}{\partial r} - \frac{\partial V_r}{\partial z} = \frac{1}{r}\left(\frac{\partial^2 \Psi}{\partial r^2} - \frac{1}{r}\frac{\partial \Psi}{\partial r} + \frac{\partial^2 \Psi}{\partial z^2}\right). \tag{3}$$

Ψ is a function of the Stokes current, $V_r = -\frac{1}{r}\frac{\partial}{\partial z}$ is the radial velocity component, $V_z = \frac{1}{r}\frac{\partial \Psi}{\partial r}$ is the vertical velocity component, g is the acceleration of free falling, T' is temperature deviation from the background T_0, $\gamma_a = g/c_p$ is the dry adiabatic temperature gradient, $\gamma = -\partial T_0/\partial z$ is the background temperature gradient $\gamma_a - \gamma > 0$, c_p is the specific heat capacity of air at a constant pressure, ρ is air density, q is the stipulated density of the heat source.

At the initial moment in time motion is absent and an arbitrary local temperature disturbance $T'_0(r, z)$ is stipulated such that

$$\int_0^{\infty}\int_{-\infty}^{\infty} rT'_0 dr\,dz = \infty. \tag{4}$$

With (3) taken into account, the system of equations (1) and (2) can be represented in the form

$$\frac{\partial}{\partial t}\frac{1}{r}\left(\frac{\partial^2\Psi}{\partial r^2}-\frac{1}{r}\frac{\partial\Psi}{\partial r}+\frac{\partial^2\Psi}{\partial z^2}\right)=\frac{g}{T_0}\frac{\partial T'}{\partial r}, \tag{5}$$

$$\frac{\partial T'}{\partial t}+(\gamma_a-\gamma)\frac{1}{r}\frac{\partial\Psi}{\partial r}=\frac{q}{\rho c_p}. \tag{6}$$

We apply the Laplace transform to (5) and (6). We have

$$p\frac{1}{r}\left(\frac{\partial^2\Phi}{\partial r^2}-\frac{1}{r}\frac{\partial\Phi}{\partial r}+\frac{\partial^2\Phi}{\partial z^2}\right)=\frac{g}{T_0}\frac{\partial\theta}{\partial r}, \tag{7}$$

$$p\theta+(\gamma_a-\gamma)\frac{1}{r}\frac{\partial\Phi}{\partial r}=T'_0+\frac{1}{\rho c_p}\tilde{q}, \tag{8}$$

where p is the Laplace transform parameter,

$$\Phi=\int_0^{\infty}\Psi e^{-pt}dt,\quad \theta=\int_0^{\infty}T'e^{-pt}dt,\quad \tilde{q}=\int_0^{\infty}qe^{-pt}dt.$$

Solving the system of equations (7), (8) relative to Φ, we obtain

$$\frac{\partial^2\Phi}{\partial r^2}-\frac{1}{r}\frac{\partial\Phi}{\partial r}+\frac{1}{a^2}\frac{\partial^2\Phi}{\partial z^2}=\frac{1}{p^2a^2}\frac{g}{T_0}r\left(\frac{\partial T'_0}{\partial r}+\frac{1}{\rho c_p}\frac{\partial\tilde{q}}{\partial r}\right), \tag{9}$$

where

$$a^2=\frac{p^2+\omega_0^2}{p^2},\quad \omega_0^2=(\gamma_a-\gamma)\frac{g}{T_0}.$$

With $r\to\infty$ and $z\to\infty$ $\Phi\to 0$. Applying Green's function, the expansion of the $\delta(z)$ function into the Fourier integral and Hankel transform for the $\delta(r)$ function, the solution of equation (9) can be represented in the form

$$\Phi=\frac{rg}{2T_0}\frac{1}{p^2a^2}\int_0^{\infty}\int_{-\infty}^{\infty}\left(T'_0+\frac{1}{\rho c_p}\tilde{q}\right)\times \tag{10}$$

$$\times\int_0^{\infty}kr'J_1(kr)J_0(kr')e^{-ak(z-z')}dk\,dr'\,dz,$$

where k is the Hankel transform parameter; J_0 and J_1 are Bessel functions of the first kind of the zero and first orders respectively.

If the heat is released at the origin of coordinates, then

$$T'_0=\frac{Q}{2\pi r\rho c_p}\delta(r')\delta(z'),\quad \tilde{q}=\frac{\tilde{q}_*}{2\pi r'}\delta(r')\delta(z'). \tag{11}$$

Here Q is the total quantity of heat released at the initial moment in time; q_* is the Laplace transform of $\tilde{q}_*$ -- the quantity of heat released in a unit time at the origin of coordinates.

Substituting (11) into (10) and carrying out integration in the derived expression, we find that

$$\Phi = \frac{g}{4\pi\rho c_p T_0}\frac{r^2}{R^3}\frac{p}{(p^2+\omega_0^2)(p^2+\omega^2)^{3/2}}(Q+\tilde{q}_*). \tag{12}$$

Here $R = \sqrt{r^2+z^2}$, $\omega^2 = \frac{z^2}{R^2}\omega_0^2$. Performing the inverse Laplace transform, we find an expression for the Stokes stream function

$$\Psi = \frac{g}{4\pi\rho c_p T_0}\frac{r^2}{R^3}\left[Qf(t)+\int_0^t f(t-\tau)\,q_*(\tau')\,d\tau'\right], \tag{13}$$

where

$$f(t) = tJ_0(\omega t) - \omega_0\int_0^t (t-\tau)\,J_0[\omega(t-\tau)]\,J_1(\omega_0\tau)\,d\tau. \tag{14}$$

Expressions (13) and (14) represent the general spatial asymptotic solution of the convection problem, which reflects the real variation of the process at distances R considerably exceeding the dimension $R_0(t)$ of the region within which is concentrated all the heat from the source. With $R \gg R_0$ the heat source can be considered a point source, the current velocity with increasing distance from the source tends to zero and the scales of the inhomogeneities of the velocity and temperature fields increase. Accordingly, a solution at great distances from a source can be obtained by neglecting the nonlinear terms and the terms taking viscosity and thermal conductivity into account in the free convection equations. When $R \gg R_0$ the nature of the attenuation of the velocity amplitude in conformity to the law $\beta(t, \cos\varphi)\frac{1}{R^3}$ follows from (13) and (14), where the φ function is not dependent on R and the φ angle is reckoned from the vertical axis. However, expressions (13) and (14) still do not contain a definite final answer concerning the details of the flow structure. By stipulating one or another specific form of the heat source it is possible to penetrate without limit into the study of the formulated problem.

Comparison of results of numerical and analytical solution of the dry convection problem. If in equation (13) the second term on the right-hand side, corresponding to the constantly operative heat source, is assumed equal to zero and one leaves only the first term with the initial temperature momentum different from zero only at the origin of coordinates, the stream function of the analytical solution of the linear problem of free convection assumes the form

$$\Psi = \frac{g}{4\pi\rho c_p T_0}\frac{r^2}{R^3}Qf(t). \tag{15}$$

The basis of the numerical model of dry convection is a system of equations in thermohydrodynamics in the Boussinesq approximation: to the right-hand sides of equations (1) and (2) we added the expressions

$$-V_r\frac{\partial\eta}{\partial r} - V_z\frac{\partial\eta}{\partial z} + \frac{V_r\eta}{r} + k\left(\frac{\partial^2\eta}{\partial r^2} + \frac{1}{r}\frac{\partial\eta}{\partial r} + \frac{\partial^2\eta}{\partial z^2} - \frac{\eta}{r^2}\right),$$

$$-V_r\frac{\partial T'}{\partial r} - V_z\frac{\partial T'}{\partial z} + k\left(\frac{\partial^2 T'}{\partial r^2} + \frac{1}{r}\frac{\partial T'}{\partial r} + \frac{\partial^2 T'}{\partial z^2}\right)$$

respectively. The initial conditions had the following form:

$$V_r = V_z = \Psi = \eta = 0, \qquad T'(r,z,0) = \begin{cases} T_0' e^{-\frac{r}{r_0}}\sin^2\frac{\pi z}{z_0}, & r \leq r_0 = 1000\ м,\ z \leq z_0 = 600\ м, \\ 0, & r > 1000\ м,\ z > 600\ м, \end{cases}$$

$$T_0' = 1\text{K},\ T_0(z) = T_0(0) - \gamma z,\ T_0(0) = 298\ \text{K}.$$

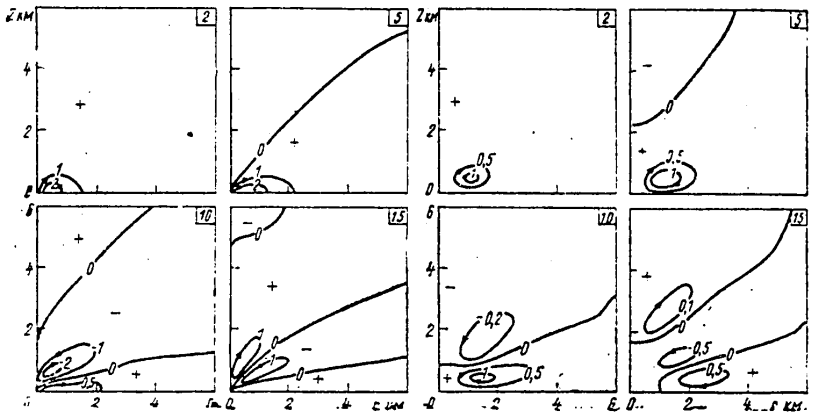

Fig. 1. Evolution of Stokes stream function Ψ (10^5 m^3/sec) of analytical (at left) and numerical (at right) solutions of the dry convection problem.

In the numerical solution there was satisfaction of the axial symmetry condition, attachment condition at the lower boundary and heat absorption condition at the lateral, lower and upper boundaries. The values of the parameters at the lateral and upper boundaries corresponded to conditions at infinity for a motionless atmosphere. The turbulence coefficient k = 40 m^2/sec. The initial thermal impulse coincided in value with the thermal impulse of the analytical problem. In both the numerical and analytical solutions γ= 0.008 K/m.

The calculations were made in an explicit scheme with variable right differences. The Arakawa scheme [1] was used for the nonlinear terms and the remaining terms were approximated by central differences. Equation (3) was solved by the method of a decrease in dimensionalities [8]. The calculation region fell in the range of 6,000 m along the r and z axes. The time interval was equal to 10 sec and the spatial interval along both axes was 200 m.

An analysis of the analytical and numerical solutions indicates that nonstationary oscillations with the frequency ω arise in the medium; the frequency is dependent on the coordinates. The dependence of frequency ω on coordinates leads with time to stratification of the current into a number of eddies whose number after each time interval, equal to the Brent-Väisälä period $2\pi/\omega_0$, increases by unity. This effect was also described in [5, 6].

Figure 1 shows the stream function for the analytical and numerical solutions of the dry convection problem. The numbers at the upper right corners of the rectangles denote the corresponding moments in time (in minutes) from the beginning of development of convection. It can be seen from a comparison of these figures that as might be expected, convection in the greater part of the space, excluding the boundaries of the reckoning region and the region where the heat from the initial impulse is concentrated, has an almost identical character. Naturally, the

quantitative characteristics of the field of the convective current, described analytically and numerically, differ somewhat. It should not be forgotten here that in the numerical model the initial impulse occupies some spatial region with its center situated on the z-axis and at an altitude of 300 m from the underlying surface, whereas in the analytical model the initial impulse is situated at the origin of coordinates and the underlying surface is absent. We note also that in the analytical model the heat spot at all times remains at the origin of coordinates, whereas in the numerical model it rises in the process of development of convection, cooling as it rises, and is scattered as a result of turbulent diffusion. The principal objective of the comparison is the proof (as can be seen from the figure) that the number of eddies is approximately identical in the analytical and numerical models, as was already indicated in [5], where the results of the numerical model were compared with the results obtained in analytical solution of the plane problem. Thus, nonlinear effects, viscosity, thermal conductivity and the underlying surface exert an influence only on the configuration of the eddies, whereas their number is determined by the degree of stability (that is, the ω_0 value) in the atmosphere and the time elapsing from the onset of development of convection.

In earlier studies [7, 9] it was also possible to note the well-expressed character of multilevel convection, but the authors there did not reveal the reasons for this phenomenon and the authors themselves did not devote due attention to this problem.

The finding of new properties of already known phenomena and a description of the patterns to which these properties conform can be considered successes of the theory. In this case using the generally accepted equations it was possible to detect an interesting property of free convection -- the stratification of a current into a series of eddies in a stably stratified medium.

In addition, a comparison was made of a methodological development of a numerical model of a cumulus cloud. This made it possible to select such dimensions of the reckoning region in which the current zone, distorted by the upper and lateral boundaries of the reckoning region, did not intersect the region ($R_0(t)$) during the time of development of the entire convection cycle -- from rest to the moment of activation of the temperature impulse to the maximum development of convection and its subsequent attenuation. For the case represented in Fig. 1 at the right, the development of convection from its beginning to the stage of maximum development is 10 minutes, then after 5 minutes the current velocity (in the zone of action of the source) decreased by half. In this case the R_0 dimension differed insignificantly from the dimension (10^3 m) of the initial heat impulse.

Dynamic modification of cumulus cloud. With dynamic modification there is clarification of the problem of the possibility of cloud dispersal using a concentrated downward-directed force imparted to one part or another of a cloud or cloudless space and operative at all times from the beginning of modification to cloud disappearance. The investigation was carried out on the basis of the equations of thermohydrodynamics in a cylindrical coordinate system with a variable turbulence coefficient:

$$\frac{\partial \eta}{\partial t} + V_r \frac{\partial \eta}{\partial r} + V_z \frac{\partial \eta}{\partial z} = \frac{V_r \eta}{r} + \frac{\partial F}{\partial r} + \frac{1}{r} \frac{\partial}{\partial r} kr \frac{\partial \eta}{\partial r} + \\ + \frac{\partial}{\partial z} k \frac{\partial \eta}{\partial z} - k \frac{\eta}{r^2}, \tag{16}$$

$$\frac{\partial A}{\partial t} + V_r \frac{\partial A}{\partial r} + V_z \frac{\partial A}{\partial z} + (\gamma_a - \gamma) V_z = \frac{1}{r} \frac{\partial}{\partial r} kr \frac{\partial A}{\partial r} + \frac{\partial}{\partial z} k \frac{\partial A}{\partial z}, \tag{17}$$

$$\frac{\partial B}{\partial t} + V_r \frac{\partial B}{\partial r} + V_z \frac{\partial B}{\partial z} - \Gamma V_z = \frac{1}{r} \frac{\partial}{\partial r} kr \frac{\partial B}{\partial r} + \frac{\partial}{\partial z} k \frac{\partial B}{\partial z}, \tag{18}$$

$$F = \left(\frac{T'}{T_0} + 0{,}61\, s' - \delta c_w \right) g + F_s(r, z, t),$$

where

[B = modification]

$F_{mod} = \theta(t) F_f(r, z)$ is the force of dynamic modification

$$\theta(t) = \begin{cases} 0 \text{ when } t < t_{mod}, \\ 1 \text{ when } t \geqslant t_{mod}, \end{cases}$$

t_{mod} is the time elapsing from the beginning of convection to the time of activation of dynamic modification, F_f is a constant downward-directed force stipulated at two points: on the axis and alongside the axis in such a way that the magnitude of the integral

$$\int_0^{2\Delta} \int_0^{2\Delta} 2\pi \rho F_f \, r dr dz$$

is equal to $4.9 \cdot 10^5$H. F_f at the grid points at which it differs from zero is of the same order of magnitude as the maximum value of the buoyancy force.

$$F_{buoy} = \left(\frac{T'}{T_0} + 0{,}61\, s' - \delta c_w \right) g,$$

s' is the deviation of specific humidity from the background value s_0, c_w is specific liquid-water content,

$$\Gamma = -\frac{\partial s_0}{\partial z},$$

$$\delta = \begin{cases} 1 \\ 0 \end{cases}, \quad A = \begin{cases} T' - \frac{L}{c_p} c_w \\ T' \end{cases}, \quad B = \begin{cases} s' - c_w & \text{in a cloud} \\ s' & \text{outside a cloud} \end{cases}$$

L is the latent heat of water condensation, Δ is the grid interval, ρ is air density.

In order to compute Ψ we used equation (3), and for the turbulence coefficient we employed expression [10]:

$$k = (c\Delta)^2 \left\{ \left(\frac{\partial V_z}{\partial r} + \frac{\partial V_r}{\partial z} \right)^2 + 2 \left[\left(\frac{\partial V_r}{\partial r} \right)^2 + \left(\frac{\partial V_z}{\partial z} \right)^2 + \left(\frac{V_r}{r} \right)^2 \right] \right\}^{1/2}, \tag{19}$$

where c is a constant coefficient which was selected empirically.

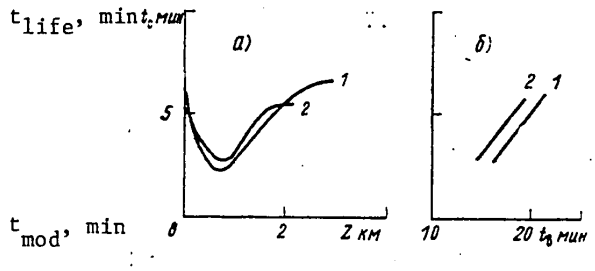

Fig. 2. Dependence of lifetime of cloud on altitude of source of dynamic modification (a) and on the moment of onset of modification (b). 1) for model with variable turbulence coefficient; 2) for model with constant turbulence coefficient.

In the model with a constant turbulence coefficient k = 40 m^2/sec. The initial and boundary conditions, reckoning region and also other parameters were the same as in our preceding study [5]. We employed the same numerical method as in the dry convection model.

Figure 2a shows the dependence of cloud lifetime on the distance between the underlying surface and the point of imparting of the concentrated force beginning to operate in the first minute of cloud existence. The dimensions of a cloud in models with both variable and constant turbulence coefficients did not exceed 10^3 m. In both models a cloud without modification attained its maximum development in the fourth minute of its existence. Curve 1 illustrates the dependence of cloud lifetime on altitude of application of the modification source in a model with a variable turbulence coefficient. Curve 2 in this figure shows the results of a numerical experiment with dynamic modification of a cumulus cloud in a model with a constant turbulence coefficient. It must be noted that in a model with a variable turbulence coefficient the lifetime of a cloud without modification is 7 minutes and its center is situated at an altitude of 600 m. However, in the model with a constant turbulence coefficient the lifetime is 6 minutes, whereas the center of the cloud is situated at an altitude of 800 m. A maximum effect is obtained in both cases if the modification is carried out at an altitude of about 800 m, that is, between the peak and the middle part of the cloud.

Figure 2b shows that in models with both a constant and variable turbulence coefficient there is a directly proportional dependence between the lifetime of the cloud and the time of onset of the dynamic mofification. The modification effect is the smaller the closer to the end of cloud existence it is activated. Evidently, such a dependence is related to the small size of the cloud and its short lifetime. In the case of well-developed clouds with a long lifetime this dependence, if it can be established, will possibly have a somewhat different character.

In our numerical experiments the great intensity of the imparted force under natural conditions can be identified from a helicopter hovering at a definite altitude.

In conclusion the authors express appreciation to V. I. Bekryayev for useful discussions.

BIBLIOGRAPHY

1. Arakawa, A., "Scheme for Numerical Integration of the Equations of Motion of a Fluid Over a Long Time: Case of a Two-Dimensional Flow of an Incompressible Fluid," CHISLENNYYE METODY RESHENIYA ZADACH DINAMIKI ATMOSFERY I OKEANA (Numerical Models for Solution of Problems in Dynamics of the Atmosphere and Ocean), Leningrad, Gidrometeoizdat, 1968.

2. Vul'fson, N. I., Levin, L. M. and Cherenkova, Ye. P., "Destruction of Developing Convective Clouds Artificially Created by Descending Jets," IZV. AN SSSR: FIZIKA ATMOSFERY I OKEANA (News of the USSR Academy of Sciences: Physics of the Atmosphere and Ocean), Vol 6, No 1, 1970.

3. Vul'fson, N. N. and Levin, L. M., "Destruction of Developing Cumulus Clouds Using Explosions," IZV. AN SSSR: FIZIKA ATMOSFERY I OKEANA, Vol 8, No 2, 1972.

4. Gayvoronskiy, I. I., Zadelina, L. P. and Seregin, Yu. A., "Results of Experiments for the Modification of Convective Clouds," IZV. AN SSSR: FIZIKA ATMOSFERY I OKEANA, Vol 6, No 3, 1970.

5. Kabanov, A. S. and Klykov, A. Ye., "Model of Convection in the Atmosphere With a Cloud and Numerical Experiments for Modification of a Cumulus Cloud," METEOROLOGIYA I GIDROLOGIYA (Meteorology and Hydrology), No 3, 1978.

6. Kabanov, A. S., "Plane Free Convection Arising From a Local Heat Source in a Stably Stratified Medium," PRIKLADNAYA MATEMATIKA I MEKHANIKA (Applied Mathematics and Mechanics), Vol 43, 1970.

7. Arnason, G. and Greenfield, R., "Micro- and Macro-structure of Numerically Simulated Convective Clouds," J. ATMOS. SCI., Vol 29, No 2, 1972.

8. Ogura, M. A., "A Direct Solution of Polson's Equation by Dimension Reduction Method," J. METEOROL. SOC. JAPAN, Vol 47, No 4, 1969.

9. Ogura, Y., "The Evolution of a Moist Convective Element in a Shallow Conditionally Unstable Atmosphere: A Numerical Calculation," J. ATMOS. SCI., Vol 20, No 5, 1963.

10. Soon Su-Tzai and Ogura Yoshimitsu, "A Comparison Between Axisymmetric and Slab-Symmetric Cumulus Cloud Models," J. ATMOS. SCI., Vol 30, No 5, 1973.

UDC 551.(576+507.362)(-062.1.45°:-062.2.45°)

CLOUD EXTENT IN ZONE 45°N-45°S OVER PLANET

Moscow METEOROLOGIYA I GIDROLOGIYA in Russian No 7, Jul 81 (manuscript received 30 Oct 80) pp 54-60

[Article by O. A. Avaste, doctor of physical and mathematical sciences, and O. Yu. Kyarner and S. Kh. Keevallik, Institute of Astrophysics and Atmospheric Physics, Estonian Academy of Sciences]

[Text]

Abstract: Assuming the albedo of clouds in the indicated latitudinal zone of the planet to be constant, and employing published data on albedo of the earth's surface, mean monthly estimates of cloud cover are made on the basis of two satellite measurements of albedo. Employing simple stochastic analysis, the climatic mean value of cloud albedo is estimated. The conclusion is drawn that the proposed method gives satisfactory results in determining cloud coverage over a homogeneous underlying surface and regions with a relatively small albedo.

Many studies have been made to determine the mean cloud coverage over the earth*. Most of these investigations have been based on surface observations. They have given exaggerated values for rather extensive regions. Among the estimates made on the basis of satellite data, the most thorough are given in the atlas of Miller and Feddes [10] and in studies carried out under the direction of Sadler [14, 15]. The first gives maps of the mean monthly cloud cover for the period 1967-1970. The data taken from this atlas will henceforth be called M-F estimates. The studies of the Sadler group characterize the period 1965-1975. These results will henceforth be called S estimates.

A comparison of these studies reveals a considerable discrepancy in the climatological estimates: the S-estimates exceed the M-F estimates by a factor of approximately 1.5 [4]. A far lesser scatter is indicated by a comparison of the mean zonal albedos obtained on the basis of different satellite measurements (Fig. 1). Accordingly, in determining the quantity of clouds of this type the data could serve as a point of departure. Here the principal difficulty arises in that an identical

* A review of the corresponding literature can be found in [1] and [3].

planetary albedo value is formed by several methods: with a small albedo of clouds and a great cloud coverage, and also with a great cloud albedo and their small coverage.

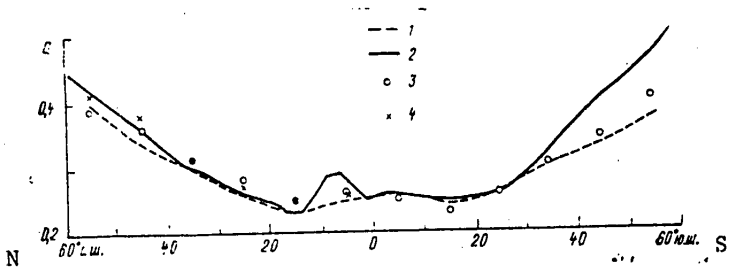

Fig. 1. Zonal distribution of mean annual albedo values for the earth-atmosphere system according to different studies. 1) [12, 13], 2) computations by authors on the basis of NOAA data, 3) [17], 4) [6].

In this study it is assumed that the climatological cloud albedo value is constant and on this basis an evaluation of the mean monthly quantity of clouds is made on the basis of data from two satellite experiments. Using a simple stochastic analysis the conclusion is drawn that in the zone 45°N-45°S a relatively small quantity of clouds and a great albedo of clouds are more realistic.

Approximation. In evaluating the quantity of clouds use is made of the simple relationship

$$a=(1-x)\,a_0+x\,a_1. \tag{1}$$

Here a is the measured albedo, to be more precise, that determined using data on the measured brightnesses at different wavelengths and for known solar altitudes, a_0 is the albedo of the earth-atmosphere system in the case of a cloudless sky, a_1 is the albedo of clouds, x is the quantity of clouds in fractions of total sky coverage ($0 \leqslant x \leqslant 1$).

In our approximation we will consider a_0 to be constant in a definite region of a particular latitude zone in the course of one month, that is, we will use the data mass a^i_{0jk}, where k is the month, j is the zone, i is the region. Each zone is divided into three regions. The ocean is denoted i = 1; the coastal areas and the land with a low albedo are denoted i = 2 and the land with a high albedo is denoted i = 3.

We will assume that a_1 is not dependent on latitude and is constant in time. Then, using (1), for the mean monthly data for a in squares 2.5 x 2.5° we obtain the mean monthly quantities of clouds in the corresponding squares:

$$x=\frac{a-a_0}{a_1-a_0}. \tag{2}$$

In the squares where $a \leqslant a_0$ we will assume that x = 0, and where $a \geqslant a_1$, we will assume that x = 1.

Initial data for a. The study is based on estimates of planetary albedo using data from two satellite experiments.

In an experiment with the "Nimbus-4" satellite there were ten 15-day cycles with transit of the equator at approximately 1100 LT. The processing of data for finding estimates of albedo was described in detail in [12] and [13]. As a result, we had at our disposal 15-day mean albedo values in the zone 30°N-30°S in squares measuring 2.5 x 2.5°, as well as the minimum albedo values for each cycle in these same squares.

From the results of measurements from satellites of the NOAA system (intersection of the equator at approximately 0900 LT) we used the mean monthly albedo values in the zone 60°N-60°S in squares measuring 2.5 x 2.5° during the period from July 1974 to June 1977. The method for obtaining these evaluations was described in [7]. The zonal variation of the mean annual planetary albedo according to these data, together with the results obtained by other authors, is indicated in Fig. 1, from which it can be seen that the albedo values according to NOAA for the zone 40-50°S greatly exceed other similar albedo estimates. This can be attributed to earlier intersection of the equator [7].

Evaluations of a_0. In order to find the albedo of the earth-atmosphere system a_0 we use published data on albedo of the earth's surface α_0 and a formula from [2]

$$a_0 = A\alpha_0 + B.$$

On the basis of data for the entire earth Budyko found for the coefficients the values A = 0.66, B = 0.1. Here we are interested for the most part in the region 30°N-30°S, where the albedo of the underlying surface is small ($\alpha_0 \leqslant 0.35$). For this region, employing the least squares method, we found the values of the coefficients A and B from the following data. The $\{\alpha_0\}$ data were interpolated for each month using the maps from [8], which give the mean monthly albedo values for the earth's surface for squares 10 x 10° for four months: February, May, August, November. The $\{a_0\}$ data were obtained using data on minimum albedo according to measurements from the "Nimbus-3" satellite. These data were used in obtaining values of the coefficients A = 0.85 and B = 0.05.

Table 1

Frequency of Cases $a \geqslant a_1$ for Different a_1 Values

a_1	"Nimbus-3" 30°N-30°S	NOAA 30°N-30°S	NOAA 45°N-45°S
0.60	0.0005	0.0007	0.0012
0.55	0.0009	0.0030	0.0044
0.50	0.0028	------	------

The determined coefficients were used in preparing tables of the mean regional albedo values a^i_{0jh}. The separation of the land into parts with small and large albedo values α_0 was carried out on the basis of the maps in [8]. The coastal squares were those where the seas were less than 75% in area.

Choice of a_1. The use of the proposed method for evaluating cloud coverage on the basis of albedo values for the earth-atmosphere system requires a predetermined constant cloud albedo value a_1. It is impossible to use climatological evaluations of albedo a_1 obtained on the basis of a priori zonal cloud cover distribution.

Table 2

Mean Zonal Cloud Cover Data According to NOAA. $a_1 = 0.60$

Zone	I	II	III	IV	V	VI	VII	VIII	IX	X	XI	XII	Year
45—42.5° N	50	50	45	41	39	38	36	33	33	35	42	45	41
42,5—40	48	46	43	39	38	35	34	29	29	33	38	43	38
40—37,5	43	42	39	36	32	24	29	25	28	30	34	40	34
37,5—35	39	39	35	34	31	29	27	24	28	28	30	36	32
35—32,5	38	36	33	35	33	29	27	23	26	27	30	35	31
32,5—30	35	33	33	34	32	28	28	25	27	25	29	33	29
30—27,5	31	29	29	30	30	25	27	25	26	22	25	28	27
27,5—25	29	27	27	27	26	25	29	28	26	22	24	26	26
25—22,5	29	26	26	25	24	24	30	32	27	22	23	25	26
22,5—20	28	26	24	24	22	26	32	35	29	24	24	25	27
20—17,5	24	23	24	23	22	26	32	35	31	25	23	23	26
17,5—15	21	20	21	20	21	25	31	34	30	25	22	20	24
15—12,5	20	19	21	19	21	27	33	36	34	28	23	20	25
12,5—10	22	21	22	22	27	33	39	42	41	36	29	23	30
10—7,5	27	27	29	29	36	40	45	45	46	43	39	32	37
7,5—5	33	34	37	36	40	41	42	40	39	40	38	37	38
5—2,5	35	39	38	35	38	32	35	33	33	34	33	34	34
2,5—0	34	37	37	31	25	26	30	29	31	32	31	32	31
0—2,5° S	38	39	39	31	23	23	28	27	30	32	32	33	31
2,5—5	40	39	39	31	23	23	27	27	31	35	35	35	32
5—7,5	41	39	36	27	21	22	27	27	31	35	36	35	31
7,5—10	40	38	32	25	21	22	25	26	29	34	36	36	30
10—12,5	40	38	31	25	21	22	25	26	29	34	37	37	31
12,5—15	38	38	30	24	22	23	24	27	29	32	36	36	30
15—17,5	36	36	30	24	24	23	24	27	30	32	35	35	30
17,5—20	34	34	27	24	24	24	25	27	31	33	34	34	29
20—22,5	31	30	25	23	24	25	26	27	31	31	31	31	28
22,5—25	30	29	26	24	28	25	27	27	32	32	32	30	28
25—27,5	30	30	27	26	29	27	30	30	35	34	32	31	30
27,5—30	31	32	28	28	32	31	35	33	36	36	33	32	32
30—32,5	35	36	32	33	36	35	39	38	41	41	38	35	37
32,5—35	39	41	38	37	41	39	41	41	43	43	43	40	41
35—37,5	44	46	46	43	44	44	46	44	47	47	48	46	45
37,5—40	49	50	52	47	48	48	50	47	50	51	52	51	50
40—42,5	54	54	55	51	50	51	54	52	52	54	56	55	53
42,5—45	59	60	57	54	52	55	56	54	54	57	58	58	56

Since model computations reveal a great variation of cloud albedo as a function of types [16], in this study we have presented computations for several a_1 values: 0.55 and 0.60 for NOAA data and 0.45-0.70 with an interval of 0.05 for "Nimbus-3" data. With each a_1 value we registered the number n_1 of cases where $a \geqslant a_1$. The corresponding frequencies n_1/M, where M is the number of all the cases in the experiment, are regarded as the probabilities that the entire month there will be a continuous cloud cover over some square. We evaluate this same probability, taking into account the asymptotically normal distribution of the sample means $N(m, \sigma)$ and using evaluations of the mean cloud coverage and the cloud cover dispersions obtained in other studies [4, 14, 15].

We will assume that the observations are independent. This assumption, which is sufficiently correct in the case of squares 10 x 10° [4] may "not work" here with squares of 2.5 x 2.5°. Taking this into account, we will evaluate the probability of

observing a continuous cloud cover in the course of eight independent observations. The maximum evaluations for the mean m value are obtained with squares 2.5 x 2.5° in the zone 45°N-45° in the interval 0.65-0.70 (S evaluations for an average of 11 years). For the standard deviation from these same data we obtain $\sigma = 0.1$. Then the probability that the sample monthly cloud cover mean is equal to 1 is found to be in the range

$$0{,}00003 < P\,(x=1) \leqslant 0{,}0014,$$

since the 1 - m value falls in the range

$$3\sigma \leqslant 1-m < 4\sigma.$$

The assumption with respect to squares with large mean quantities of cloud according to S evaluations leads to the same results. For squares in the entire zone the corresponding probability is still less.

The experimental frequencies n_1/M in our computations with different a_1 values are given in Table 1. It can be seen that the best coincidence between the two assumptions concerning the probability of a continuous cloud cover over the course of a month is obtained with the following a_1 values: 0.60 according to NOAA data and 0.55-0.60 according to "Nimbus-3" data.

It is important to note that the latitude dependence of cloud albedo obtained in many studies [5, 11] according to our computations is manifested in latitudes above 45° where the experimental frequencies n_1M increase sharply.

Results. The mean monthly estimates of the quantity of clouds, according to NOAA data, averaged for zones with a width of 2.5° in the zone 45°N-45°S, are represented in Table 2. Tables 3 and 4 give these same estimates separately for the sea; Table 3 applies to NOAA data, whereas Table 4 applies to the experiment with the "Nimbus-3." In all the tables the quantity of clouds is represented in hundredths of total sky coverage, that is, 61 should be read as 0.61.

Figure 2 represents the annual mean zonal estimates of the quantity of clouds according to different studies. Here the curves 1, 3 and 4 represent cloud cover over the sea and 2, 5, 6 reflect the total mean zonal estimates. In this figure the values 6 give cloud cover estimates made on the basis of surface observations.

An analysis of the frequencies n_0/M, where n_0 is the number of cases, when $a \leqslant a_0$, indicates that for the sea $n_0/M < 10^{-3}$. Most of the cases $a \leqslant a_0$ relate to land squares with a high albedo. The maximum discrepancy is obtained for the mountainous regions of Asia in the zone 30-40°N, where the albedo of the earth-atmosphere system [8] is greater than that measured from satellites. Accordingly, it can be anticipated that the estimates of the mean zonal quantity of clouds for 20-45°N and 20-30°S are artificially reduced due to the high albedo a_0 for some part of the land. Therefore, it is necessary to refine the albedo a_0 and divide the land into a greater number of regions with a definite value of the above-mentioned parameter. The necessity for such a refinement is also indicated by the fact that according to [8] the a_0 variations between different squares can be considerable. Bearing in mind the noted variations, it can be said that the determined frequencies n_0M cannot be interpreted as evaluations of the probability of cloudless weather in the course of a month.

Table 3

Mean Zonal Cloud Coverage Over World Ocean According to NOAA Data for $a_1 = 0.60$

Zone	I	II	III	IV	V	VI	VII	VIII	IX	X	XI	XII	Year
45—42,5° N	54	57	56	55	54	57	57	49	48	48	51	53	53
42,5—40	56	57	53	51	49	52	49	40	39	45	51	54	50
40—37,5	56	54	51	47	45	33	40	33	32	43	47	52	44
37,5—35	52	50	48	45	42	41	33	30	29	38	44	48	42
35—32,5	46	43	41	40	38	36	30	26	25	30	39	45	37
32,5—30	43	39	39	37	38	33	28	26	26	28	35	39	34
30—27,5	38	34	35	33	32	27	26	26	26	24	30	33	30
27,5—25	34	32	32	30	29	24	26	27	26	24	27	31	29
25—22,5	30	29	28	27	24	22	26	29	26	22	23	27	26
22,5—20	29	28	27	27	23	23	28	34	28	24	23	26	27
20—17,5	25	24	26	24	21	24	28	34	30	25	22	24	26
17,5—15	24	24	24	22	21	23	27	32	31	27	25	23	25
15—12,5	25	23	24	23	23	27	30	36	36	31	28	25	28
12,5—10	27	25	26	25	29	33	37	40	42	39	35	30	32
10—7,5	33	31	30	29	36	40	43	42	45	45	44	39	38
7,5—5	38	37	37	36	41	39	40	37	37	38	39	42	38
5—2,5	35	40	37	34	30	30	31	29	30	32	30	34	33
2,5—0	32	34	33	26	19	21	25	25	27	28	27	28	27
0—2,5° S	32	32	34	26	17	18	24	23	26	27	34	26	27
2,5—5	34	33	35	26	18	21	27	27	29	31	30	28	28
5—7,5	36	34	31	24	19	24	30	31	31	34	34	30	30
7,5—10	37	33	28	23	22	26	30	31	32	36	37	33	31
10—12,5	38	34	29	23	23	25	29	30	31	36	37	35	31
12,5—15	38	35	29	25	25	26	29	31	32	34	37	35	31
15—17,5	37	34	29	26	26	26	28	32	32	34	37	35	32
17,5—20	36	34	29	27	26	28	29	31	33	35	36	35	32
20—22,5	36	33	29	28	29	30	31	33	34	36	37	35	33
22,5—25	35	33	30	30	30	30	32	33	37	37	38	35	33
25—27,5	35	34	30	32	32	32	36	36	40	39	39	36	35
27,5—30	37	36	33	34	35	36	39	39	42	42	40	38	38
30—32,5	40	40	37	38	38	38	42	43	45	45	44	41	41
32,5—35	44	45	43	40	40	41	44	44	47	47	47	45	44
35—37,5	47	49	48	45	44	45	47	46	50	49	51	49	48
37,5—40	52	53	55	49	47	49	52	49	52	53	54	53	52
40—42,5	55	56	56	52	50	52	54	52	53	55	57	56	54
42.5—45	60	59	58	55	53	55	58	54	55	58	59	58	57

Table 4

Mean Zonal Cloud Coverage Over World Ocean According to "Nimbus-3" Data $a_1 = 0.60$

Zone	II	V	VI	VII	VIII	X
30—20° N	23	24	24	21	22	18
20—10	15	19	22	28	27	23
10—0	24	31	28	26	26	22
0—10° S	21	20	20	21	25	22
10—20	23	21	19	24	26	23
20—30	23	23	27	24	25	27

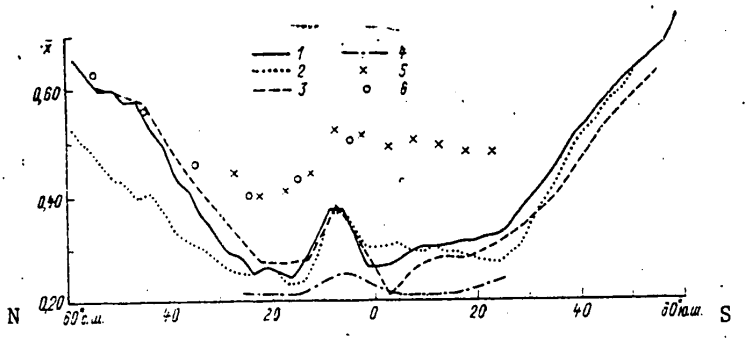

Fig. 2. Zonal distribution of mean annual cloud coverage according to different studies. 1) mean according to NOAA data; 2) mean zonal according to NOAA data; 3) mean according to [10]; 4) mean according to "Nimbus-3" data; 5) mean zonal according to [14, 15], 6) mean zonal according to [9].

Using formula (2) we can also estimate the variation Δx of the quantity of clouds. For the sea albedo a_0 in this latitude zone is 0.08-0.12. Then

$$\Delta x = 2\Delta a.$$

Since in different studies (Fig. 1) the variation Δa of mean zonal albedo attains 0.03, then $\Delta x = 0.06$. Interpreting this result as the width of the zone of uncertainty of cloud coverage, we can say that our results for the most part coincide with the M-F cloud cover estimates over the ocean. Accordingly, we note in conclusion that the proposed method gives satisfactory climatic estimates of the quantity of clouds over a uniform underlying surface and regions with a relatively low albedo.

This investigation is a continuation of the joint work with scientists of Colorado State University at Fort Collins [4]. The authors express sincere appreciation to Professor T. H. Vonder Haar and Professor S. K. Cox for numerous productive discussions.

BIBLIOGRAPHY

1. Avaste, O. A. and Vaynikko, G. M., "Influence of Resolution of Television Cameras and Radiometers on the Accuracy in Determining the Quantity of Clouds From Satellites," METEOROLOGIYA I GIDROLOGIYA (Meteorology and Hydrology), No 3, 1973.

2. ATLAS TEPLOVOGO BALANSA ZEMNOGO SHARA (Atlas of the Earth's Heat Balance), edited by M. I. Budyko, Moscow, 1963.

3. Kondrat'yev, K. Ya. and Timofeyev, Yu. M., METEOROLOGICHESKOYE ZONDIROVANIYE ATMOSFERY IZ KOSMOSA (Meteorological Sounding of the Atmosphere From Space), Leningrad, Gidrometeoizdat, 1978.

4. Avaste, O. A., Campbell, G. G., Cox, S. K., DeMasters, D., Karner, O. U., Shifrin, K. S., Smith, E. A., Steiner, E. J. and Vonder Haar, T. H., "On the Estimation of Cloud Amount Distribution Above the World Oceans," COLORADO STATE UNIVERSITY, ATMOS. SCI. PAP., No 309, 1979.

5. Cess, R. D., "Climate Change: an Appraisal of Atmospheric Feedback Mechanisms Employing Zonal Climatology," J. ATMOS. SCI., Vol 33, No 10, 1976.

6. Ellis, J. and Vonder Haar, T. H., "Zonal Average Earth Radiation Budget Measurements From Satellites for Climate Studies," COLORADO STATE UNIVERSITY, ATMOS. SCI. PAP., No 240, 1976.

7. Gruber, A., "Determination of the Earth-Atmosphere Radiation Budget From NOAA Satellite Data," NOAA TECHNICAL REPORT NESS 76, Washington, D. C., 1978.

8. Hummel, J. R. and Reck, R. A., "A Global Surface Albedo Model," J. APPL. METEOROL., Vol 18, No 3, 1979.

9. London, J., "A Study of the Atmospheric Heat Balance," REPORT CONTRACT AF 19 (122)-165, College of Engineering, New York University, 1957.

10. Miller, D. B. and Feddes, R. G., GLOBAL ATLAS OF RELATIVE CLOUD COVER 1967-1970, Washington, D. C., 1971.

11. Paltridge, G. W., "Global Dynamics and Climate -- a System of Minimum Entropy Exchange," QUART. J. ROY. METEOROL. SOC., Vol 101, No 429, 1975.

12. Raschke, E., Vonder Haar, T. H., Pasternak, M. and Bandeen, W. R., "The Radiation Balance of the Earth-Atmosphere System From Nimbus-3 Radiation Measurements," NASA TECHN. NOTE TN D-7249, Washington, D. C. 1973.

13. Raschke, E., Vonder Haar, T. H., Bandeen, W. R. and Pasternak, M., "The Annual Radiation Balance of the Earth-Atmosphere System During 1969-1970 From Nimbus-3 Measurements," J. ATMOS. SCI., Vol 30, No 3, 1973.

14. Sadler, J. C., "Average Cloudiness in the Tropics From Satellite Observations," INTERN. INDIAN OCEAN EXPEDITION, Honolulu, East-West Center Press, METEOROL. MONOGR., No 2, 1969.

15. Sadler, J. C., Oda, L. and Kilonsky, B. J., "Pacific Ocean Cloudiness From Satellite Observations," REPT. METEOROL. UNIV. HAWAII, 1976.

16. Welch, R. M., Cox, S. K. and Davis, J. M., "Solar Radiation and Clouds," Boston, Mass., American Meteorological Society, 1980. METEOROL. MONOGR., Vol 17, No 39.

17. Vonder Haar, T. H. and Suomi, V. E., "Measurements of the Earth's Radiation Budget From Satellites During a Five-Year Period. Part I: Extended Time and Space Means," J. ATMOS. SCI., Vol 28, No 3, 1971.

UDC 551.(507.362+526.6)

RESULTS OF CHECKING METHODS FOR DETERMINING WATER SURFACE TEMPERATURE FROM 'METEOR' ARTIFICIAL EARTH SATELLITES

Moscow METEOROLOGIYA I GIDROLOGIYA in Russian No 7, Jul 81 (manuscript received 22 October 80) pp 61-69

[Article by L. I. Koprova, candidate of physical and mathematical sciences, Ye. F. Utkin and A. Ye. Bakhmatov, State Scientific Research Center for the Study of Natural Resources]

[Text]

Abstract: The authors tested two methods for remote determination of water surface temperature on the basis of measurements of IR radiation in the spectral interval 8-12μm received from the "Meteor" artificial satellite. In one of these methods computations are made of the atmospheric transfer function; the other is based on writing of a regression equation. The accuracy of the results of temperature determinations is estimated under cloudless conditions. Illustrative examples are given: maps of temperature of the water surface constructed on the basis of satellite data.

The remote determination of ocean surface temperature, which exerts an enormous influence on the processes transpiring in the atmosphere, is a timely problem in satellite meteorology [13, 17]. The "Meteor" artificial earth satellite is used in making regular measurements in the IR spectral region λ = 8-12μm and their primary processing is carried out in an operational regime. As a result of the primary processing it was possible to obtain data on the radiation temperature t_r measured with a spatial resolution 8 x 8 km and the corresponding thermal radiation of the earth-atmosphere system in this spectral range. This value differs substantially (up to 15°C) from the water surface temperature t_0, which must be determined on the basis of satellite measurements. The accuracy in determining t_0 is evaluated by comparing it with the temperature of the surface water layer t_{lay}, measured on shipboard by the standard method. The principal factors responsible for the difference in the t_r and t_{lay} values, as follows from [7, 18, 19], are: absorption of radiation by atmospheric gas components; absorption by aerosol;

errors in geographical tie-in of satellite data; difference between the temperature of the radiating surface of the water film measured from the artificial earth satellite and the temperature of the surface water layer measured on shipboard; errors in the registry of t_r using a measurement system.

In this article we examine two methods for interpreting data for the existing make-up of measurements from an artificial earth satellite of the "Meteor" system, making it possible to obtain quantitative information on the temperature t_0 of the water surface.

Determination of Water Surface Temperature Using the Atmospheric Transfer Function Method

One of the methods for taking into account the influence of the atmosphere on measurements is the atmospheric transfer function method. The transfer function has the form [12]

$$P_{\Delta\lambda} = \frac{\int_{\lambda_1}^{\lambda_2} A_\lambda \, I_\lambda \, d\lambda}{\int_{\lambda_1}^{\lambda_2} \varepsilon_\lambda A_\lambda B_\lambda (t_0) \, d\lambda} = \frac{I_{\Delta\lambda}(t_p)}{B_{\Delta\lambda}(t_0)}, \quad (1)$$

where I_λ is the intensity of thermal radiation at the wavelength λ at the upper boundary of the atmosphere, B_λ is the Planck function, t is temperature, ε_λ is the emissivity of the underlying surface ($\varepsilon_\lambda \approx 1$ for a water surface), A_λ is instrument spectral response.

As indicated by (1), on the basis of the characteristic radiation $I_{\Delta\lambda}$ measured from the satellite and the known value of the transfer function $P_{\Delta\lambda}$ it is possible, using the instrument calibration dependence $B_{\Delta\lambda}(t)$, to determine the temperature t_0.

The transfer function, dependent on both absorption and radiation characteristics of the atmosphere (vertical distributions of temperature, principal absorbing components and their spectral properties) at the measurement time, is usually unknown. However, according to [1-4], it is possible to determine t_0 with an accuracy acceptable for some practical problems if use is made of values of the atmospheric transfer function computed on the basis of climatic data on meteorological parameters.

With the above considerations taken into account, the transfer function from (1) was computed using the radiation transfer equation [8] on the basis of the radiation model and climatic data. The radiation model was selected after carrying out a number of methodological computations and evaluations. We will give a brief description of the mentioned computations and the results obtained.

As an atmospheric model, in the computations we used global climatic data on the vertical profiles of meteorological elements (temperature, geopotential, specific humidity, ozone) for the four central months of seasons of the year [9, 11] present in the electronic computer machine catalogue. We took into account only absorption by gas components (water vapor H_2O and ozone O_3). Allowance was not introduced for absorption by aerosol since at present there are no reliable data on aerosol absorption.

Table 1

Latitude Variation of Transmission Function $\tau_{\Delta\lambda}$(W, m — Total Moisture Content and Ozone Content, cm). 1) Computations by Leningrad State University Employing Method in [22, 24], 2) Computations by State Scientific Research Center for Study of Natural Resources Using Data in [14], 3) Computations by State Center Employing the Coefficients in [5]

$\varphi°$	W	m	$\tau_{\Delta\lambda}$		
			1	2	3
60	0,9	0,314	0,802	0,788	0,835
45	1,3	0,310	0,770	0,753	0,797
30	1,3	0,258	0,783	0,772	0,809
0	4,7	0,226	0,584	0,512	0,561
—30	3,3	0,245	0,611	0,603	0,644
—45	1,9	0,279	0,719	0,709	0,748
—60	1,1	0,234	0,794	0,790	0,829

In the computations an evaluation was made of the influence of different factors on the atmospheric transfer function, such as the spectral characteristics of the satellite instrument and absorption by the atmospheric gases H_2O and O_3, the content of the absorbing components H_2O and O_3 and their variability relative to the climatic values. The data cited below relate to a series of computations with the use of climatic data on the meteorological parameters along fixed meridional sections for the Atlantic and Pacific Oceans.

The atmospheric transmission function $\tau_{\Delta\lambda}$ was computed by three methods using the very same climatic data (Table 1).

The first method was precise quantum-mechanical computations made at Leningrad State University by Yu. M. Timofeyev, employing the methods and data in [22, 24]. Computations by the second and third methods were made in this study. In the second method use was made of logarithmic (for H_2O) and generalized (for O_3) absorption coefficients, averaged taking into account the structure of the absorption bands, obtained by the processing of experimental data [14]. In the third method use was made of the H_2O and O_3 absorption coefficients averaged for the interval $\Delta\lambda = 8\text{-}12\mu m$ [5]. The data in Table 1 show that the results of computations by the method in [14] are closest to precise computations. The maximum $\tau_{\Delta\lambda}$ differences, observed in equatorial regions with a high humidity, lead to differences of about 0.3°C in determining water surface temperature t_0. Accordingly, as the radiation model we thereafter employed the simplest second method for computing $\tau_{\Delta\lambda}$.

The standard instrumentation aboard artificial earth satellites of the "Meteor" system contains two duplicating instruments for measuring IR radiation which are interexchangeable in the process of flight of an artificial earth satellite. The spectral responses of these instruments A_λ are somewhat different. Computations of $P_{\Delta\lambda}$, made without allowance for the spectral response ($A_\lambda = 1$) and with allowance for different A_λ (for three satellites of the "Meteor" system), indicated

that failure to take A_λ into account can lead to errors in determining t_0 as great as 1°C. Accordingly, for each instrument operating on the artificial earth satellite it is desirable to take into account the influence of A_λ on the transfer function.

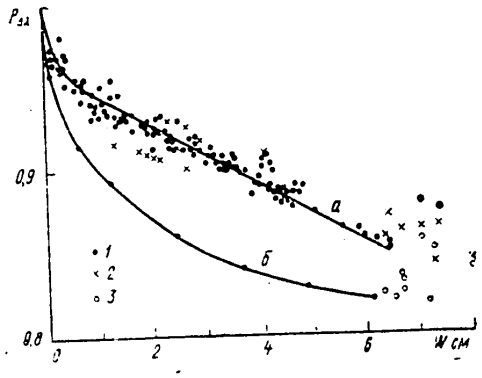

Fig. 1. Dependence of the atmospheric transfer function $P_{\Delta\lambda}$ on moisture content W. 1) computations on the basis of climatic data on meteorological parameters along meridional sections 30 and 170°E (curve a -- averaged data) and using data from [2] (curve b); 2) computations using radiosonde data over the surfaces of the White and Baltic Seas and the Indian Ocean; 3) computations on the basis of data from the "Meteor-2" - No 2" artificial earth satellite and on the basis of shipboard data in northern part of Indian Ocean obtained during the "Musson-77" period.

The $P_{\Delta\lambda}$ transfer function is dependent on the total atmospheric moisture content W. This dependence, computed on the basis of climatic data in this study and in [2], is illustrated in Fig. 1 (curves a and b respectively). This same figure shows the $P_{\Delta\lambda}$ values of two types which were computed on the basis of synchronous data for different types of observations of the actual state of the atmosphere: according to radiosonde data, according to data from observations of ozone content (2) and according to data from satellite and shipboard measurements of temperature (3). The first type of transfer function, obtained on the basis of experimental data, was computed by the method described above. The second type of transfer function was computed using formula (1), in which t_r is the radiation temperature measured on the "Meteor-2 - No 2" artificial earth satellite, and $t_0 = t_{lay}$ is the temperature of the ocean surface measured on shipboard. A comparison of the $P_{\Delta\lambda}$ values computed and determined on the basis of independent experimental data demonstrated that the experimental $P_{\Delta\lambda}$ values were close to the a curve. The latter is evidence in support of the selected model for computing the transfer function.

The atmospheric transfer function is also dependent on the ozone content. In some studies, such as [5], it is asserted that the transformation of radiation in the spectral range 8-12 μm is determined primarily by the absorption of water vapor and ozone absorption must be taken into account in the case of low moisture content values. We will evaluate the influence of ozone on the atmospheric transfer function. We will represent the water surface temperature determined on the basis of satellite measurements in the form

$$t_0 = t_p + \Delta t, \tag{2}$$

$$\Delta t = \Delta t_{H_2O} + \Delta t_{O_3}, \tag{3}$$

where Δt_{H_2O}, Δt_{O_3} are temperature corrections taking into account the influence of the atmosphere on measurements and dependent on the transfer function. They can be computed on the basis of climatic or real data on meteorological parameters using the radiation transfer equation. Such computations, carried out by the authors of this article, indicated that despite the conclusions drawn in [5], ozone exerts an influence on the transfer function at all latitudes and in both the warm and cold half-years. The relationship of the corrections Δt_{H_2O} and Δt_{O_3} can be different: depending on the latitude zone, one or another correction prevails, or they are comparable in absolute value.

Evaluations of the error in determining t_0 as a result of failure to take into account variations in meteorological parameters relative to their climatic values were made on the basis of data from 40 radiosondes, obtained for different ocean areas during summer -- in the White and Baltic Seas and the Indian Ocean. This error was 1.1°C.

Model computations made it possible to develop a machine catalogue of the global distribution of climatic values of the transfer function in the atmosphere. The catalogue of $P_{\Delta\lambda}$ values, registered on a "YeS-1022" magnetic tape, is used as a priori information in determining water surface temperature on the basis of measurements from the "Meteor" artificial earth satellite.

Determination of Water Surface Temperature Using the Regression Method

In a number of studies [6, 20, 21, 23, 25] water surface temperature was determined using the statistical relationships between satellite measurements (intensity of outgoing radiation or radiation temperature t_r) and the parameters of the underlying surface (its temperature or radiation) or between the correction taking into account the influence of the atmosphere and atmospheric moisture content. In order to find the regression coefficients in the correlation equations it is necessary to have a large sample of synchronous values of the initial parameters. The regression coefficients can be determined on the basis of real satellite and surface data, but such an approach requires that a special subsatellite experiment be carried out on a global scale, which is difficult to accomplish. For this reason the regression equations used in [6, 20, 21, 23, 25] were obtained by model computations.

In this study we derived regression equations in the form

[p = r]

$$t_0 = \sum_{i=0}^{\infty} a_i t_r^i. \tag{4}$$

In computing a_i we used models of the atmosphere with climatic data on the vertical profiles of meteorological parameters [9-11]. From the entire mass of climatic data for the surface of the world ocean we selected only those which applied to a cloudless situation. This choice was made using the following test: in a cloudless situation the dew point spread t_d at all isobaric levels exceeded the

critical t_d values [15]. The t_r values were computed using the radiation transfer equation on the basis of the already described radiation model. Table 2 gives the a_i coefficients computed for N cases relating to the entire ocean area in the temperate and tropical latitudes. The values of the residual dispersions of these equations with standard deviations t_0 of about 7°C were 0.7-2.3°C.

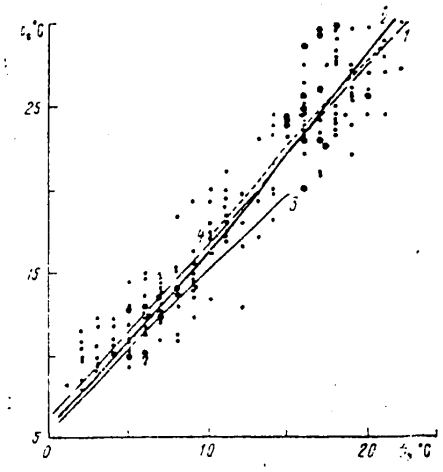

Fig. 2. Dependence of water surface temperature t_{lay} on radiation temperature t_r. The dots represent data from simultaneous measurements on ships and IR measurements from the "Meteor-2 - No 2" and "Meteor-2 - No 4" artificial earth satellites; 1, 2) approximation of real data using regression equations for entire ocean area (N = 224) and for Baltic Sea (N = 110); 3, 4) approximation of climatic data for temperate and tropical latitudes (N = 500).

Regression equations of the form (4) were also derived on the basis of a sampling of real measurements. The sampling included measurements of the t_r value from the "Meteor" artificial earth satellite during the summer from 1977 through 1979 and measurements of the water surface temperature t_{lay} on shipboard and at shore stations in the regions of the White, Baltic, Black and Caspian Seas and the Indian and Pacific Oceans. Satellite and surface data differed in time by not more than three hours and in space by ±30 km; the total number of pairs N is 244 (Fig. 2, dots). On the basis of this sample we computed the a_i coefficients in equation (4) for the entire ocean area and on the basis of the part of this sample relating to the Baltic Sea (N = 110) we computed the a_i coefficients for the middle latitudes (Table 2). The residual dispersions of the regression equations were 2°C and 1.2°C respectively. Figure 1 and Table 2 show that regression equations in the form (4), obtained on the basis of climatic and real data, give results differing by less than 1°C.

Another method for determining temperature t_0 is based on the existence of a stable statistical correlation between the temperature correction for the atmospheric influence Δt and total atmospheric moisture content W in the temperate and tropical latitudes:

$$\Delta t = \sum_{i=0}^{2} a_i W^i, \qquad (5)$$

where a_i are the regression coefficients. The t_0 value is found using formula (2).

Table 2

Coefficients a_i of Regression Equations and Evaluation of Accuracy in Determining Water Surface Temperature t_0 by the Transfer Function Method (1) and Regression Method (2)

Region	A	B			C			N	1		2		n
		a_0	a_1	$-a_2$	a_0	a_1	$-a_2$		Δ °C	f %	Δ °C	f %	
Using climatic data													
All ocean area	4	7.5	1.02	0.008	5,2	1,17	0,004	1000	2,5	98	2,1	98	244
	5	2.2	1.15	0,021				1000			2,0		40
Middle latitudes	4	5.4	1.05	0,006	8,8	1,19	0,002	500	1,8	99	1,5	96	165
Tropics	4	9.2	1.02	0,008	5,9	1,17	0,004	500	3,1	96	2,6	97	79
Using measurement data													
Baltic Sea	4	5.6	1.05	0,006				110	1,9	96	2,2	112	55
All ocean area	4	6.3	1.07	0,004				244	1,9	96	1,9	113	55
	5	4.5	0.08	0.14				40					

KEY:

A) Number of equation
B) "Meteor-2--No 2"
C) "Meteor-2--No 4"

An equation of type (5) was used in an interpretation of measurements from the NOAA operational satellite in the United States [19]. Data on W synchronous with t_r values can in principle be found by means of model computations or by employing satellite measurements in the IR or in the SHF ranges of the spectrum (from which W is determined) or use is made of radiosonde data (which are usually absent for the seas and oceans). In this study, on the basis of a sufficiently great sample of climatic data (N = 1000), relating to a cloudless situation and four seasons of the year, we computed the t_r values and the corresponding values Δt and W. The a_i coefficients are given in Table 2.

The same regression equation was derived by computing the t_r and W parameters using data from 40 radiosondes in the regions of the White and Baltic Seas and the Indian Ocean (Table 2). The residual dispersions of the determined regression equations according to climatic and real data were close and do not exceed 1°C.

Evaluation of Accuracy in Determining Water Surface Temperature

The evaluation of the accuracy of the proposed methods for remote determination of t_0 was made on the basis of synchronous satellite and subsatellite measurements relating to different ocean areas (see Figure 1, dots). The results of the evaluations are given in the right-hand side of Table 2.

As a measure of accuracy in determining t_0 using different interpretation methods we used the parameter

$$\Delta = \frac{\sqrt{\sum_{i=1}^{n} \delta_i^2}}{n}, \tag{6}$$

where $\delta = t_{lay} - t_0$, n is the volume of the sample.

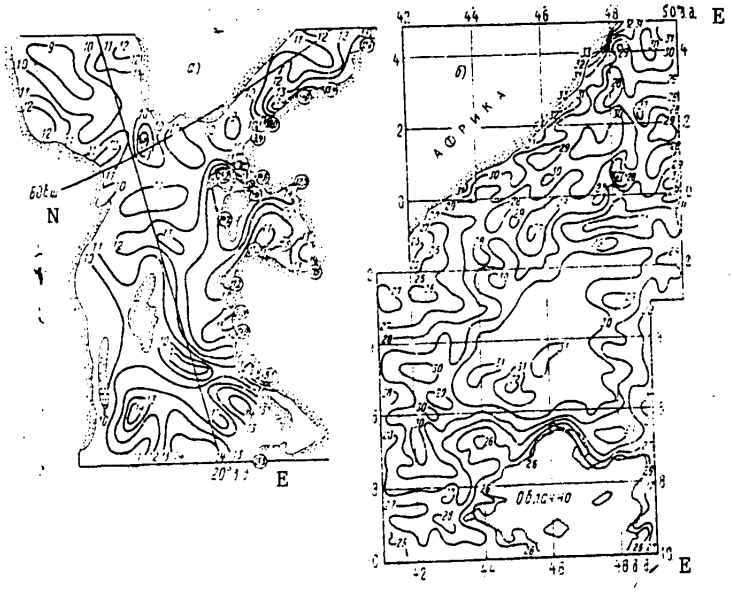

Fig. 3. Examples of maps of water surface temperature according to data from artificial earth satellites "Meteor-2 - No 2" (a) and "Meteor-2 - No 4" (b). In circles -- water temperature according to data from standard observations on ships and at shore stations.

The effectiveness of the interpretation method employed can be determined using the parameter

$$f = \frac{1}{n} \sum_{i=1}^{n} \frac{|t_0 - t_p|}{t_c - t_p} \cdot 100\%, \tag{7}$$

which indicates what fraction (in %) of the true difference $t_{lay} - t_r$ can be taken into account with the employed method for determining t_0. Values $f > 100\%$ mean that the determined temperature t_0 is exaggerated in comparison with the true value.

A comparison of the Δ values for t_0, determined using the climatic transfer function and regression equations of type (4) and (5), obtained on the basis of climatic data, indicated that the employed methods give close results. For example, for the regions of the temperate latitudes an accuracy of 1.5-1.8°C is attained, in the tropics -- about 2.6°C, for the entire ocean -- 2.0°C. The f value varies in the range 96-99%. The t_0 values were determined with the same error using

regression equations derived using real data (see Table 2).

The regression equations (4), (5) were derived on the basis of a limited sample of real data and require additional checking.

The regression method makes it possible to assimilate cm or SHF data on the moisture content W in the interpretation of IR measurements. However, if together with W there are simultaneous data from thermal sounding from a satellite it is desirable to use the first method and compute the transfer function on the basis of data on the actual state of the atmosphere.

The transfer function method was introduced into the routine practice of processing and interpretation of IR measurements (in the first stage in a climatic variant), as a result of which quantitative information is obtained on t_0, the accuracy of which is constantly checked. For example, according to data from 12 revolutions of the "Meteor-2 No 6" artificial earth satellite over the Pacific and Atlantic Oceans during the period 19-21 September 1980 relating to the latitude zone $\pm 40°$ and synchronous shipboard data (a sample of 100 cases) the accuracy in determining temperature was about 1°C. A further improvement in the technical means and methods of interpretation will increase the quality and reliability of satellite information.

Examples of satellite maps of water surface temperature for the northern ocean area and the tropics, constructed as a result of interpretation of data from IR measurements from the "Meteor" artificial earth satellite with the use of the atmospheric climatic transfer function, are given in Fig. 3. In order to construct such maps we carried out a joint analysis of data from IR measurements (radiation temperature maps) and TV photographs, as a result of which it was possible to discriminate cloudy and cloudless sectors on the t_r maps, on which the numerical values apply to an area of about 20 x 20 km. For the purpose, to some degree, of excluding the influence of measuring system noise and partial cloud cover on the measurements (without smoothing nonuniformities of some hundreds of kilometers), we carried out averaging of radiation temperatures for areas of 40 x 40 km (for the Baltic Sea) and 60 x 60 km (for the tropics). It should be noted that the problem of averaging the t_r field is a special problem and is not considered in this article. After the mentioned averaging we introduced to the t_r values a correction by means of the transfer function and then drew isolines of the restored field t_0. On the t_0 map we plotted data on water temperature obtained by standard methods at observation times differing by not more than three hours from satellite observations.

A map of the surface temperature of the Baltic Sea, constructed by this method on the basis of data from IR measurements from the artificial earth satellite "Meteor-2--No 2" on 2 June 1978 at 0832 hours is shown as Fig. 3a. The temperature field of the Baltic Sea is characterized by a considerable variability. Thermal inhomogeneities with clearly expressed regions of heat and cold, which are characteristic for the Baltic Sea during the considered period, are defined. Data on standard water temperature measurements are available only for coastal stations. Their comparison with the restored temperatures indicates that the sea temperature, according to data from contact and remote measurement methods, is in good agreement. The range of temperature variability over the area of the Baltic Sea, constituting 8-15°C for the two types of measurements, also coincides.

Figure 3b is a satellite map of the surface temperature of the Indian Ocean constructed for the period of implementation of "MONEKS-79" on 27 April 1979 at 1251 hours. The thermal inhomogeneities on this map are oriented from southwest to northeast, which corresponds to the directions of the currents in this region. The examined area of the Indian Ocean (1500 x 800 km) is virtually not covered by meteorological data. The only ocean temperature value close in time to the measurement was at a point with the coordinates 4.5°S and 42°E, measured on a ship; it was 1°C higher than the temperature of the ocean surface reconstructed on the basis of satellite data.

Satellite maps give virtually instantaneous detailed information on the structure of the water surface temperature field having distinguishing characteristics in each ocean area. The cited examples graphically illustrate the possibilities of satellite methods for investigating water surface temperature.

A further improvement in methods for the processing and interpretation of satellite measurements will make it possible to obtain more precise and reliable data on the global distribution of water surface temperature.

The authors express appreciation to I. A. Chetverikov and A. B. Uspenskiy for valuable comments on implementation of the study and M. S. Lyubanskiy for assistance in the work.

BIBLIOGRAPHY

1. Boldyrev, V. G., Koprova, L. I. and Malkevich, M. S., "Allowance for Variations in the Vertical Profiles of Temperature and Humidity in Determining Temperature of the Underlying Surface on the Basis of Outgoing Radiation," IZV. AN SSSR: FIZIKA ATMOSFERY I OKEANA (News of the USSR Academy of Sciences: Physics of the Atmosphere and Ocean), Vol 1, No 7, 1965.

2. Boldyrev, V. G., "Computation of the Atmospheric Transfer Function in the Spectral Interval 8-12μm for the Territory of the Northern Hemisphere," IZV. AN SSSR: FIZIKA ATMOSFERY I OKEANA, Vol 1, No 7, 1965.

3. Boldyrev, V. G., "Problem of the Use of Measurements of Outgoing Radiation for Computing the Temperature of the Earth's Surface and the Altitude of the Upper Cloud Boundary," TRUDY MMTs. VOPROSY SPUTNIKOVOY METEOROLOGII (Transactions of the World Meteorological Center. Problems in Satellite Meteorology), No 8, 1965.

4. Boldyrev, V. G., Koprova, L. I., Medvedeva, L. V. and Yakovleva, E. A., "Use of the Statistical Characteristics of the Vertical Structure of the Temperature Fields of the Underlying Surface Using Radiation Measurements From a Satellite," AKTINOMETRIYA I OPTIKA ATMOSFERY. (TRUDY VI MEZHVEDOMSTVENNOGO SOVESHCHANIYA PO AKTINOMETRII I OPTIKE ATMOSFERY, 1966 god, g. Tartu) (Actinometry and Atmospheric Optics. (Transactions of the Sixth Interdepartmental Conference on Actinometry and Atmospheric Optics, 1966, Tartu), Tallin, 1968.

5. Komarov, V. S., "Statistical Parameters of the Total Moisture Content of the Atmosphere and Their Application in Some Practical Problems," TRUDY VNIIGMI-MTsD (Transactions of the All-Union Scientific Research Institute of Hydrometeorological Information-World Data Center), No 28, 1976.

6. Komarov, V. S., "Parameterization of the Vertical Macroscale Structure of the Temperature and Humidity Fields Applicable to Solution of Problems in Remote Sounding of the Atmosphere," TRUDY VNIIGMI-MTsD, No 71, 1980.

7. Kondrat'yev, K. Ya., Grigor'yev, A. A., Rabinovich, Yu. I. and Shul'gina, Ye. M., METEOROLOGICHESKOYE ZONDIROVANIYE PODSTILAYUSHCHEY POVERKHNOSTI IZ KOSMOSA (Meteorological Sounding of the Underlying Surface From Space), Leningrad, Gidrometeoizdat, 1979.

8. Kondrat'yev, K. Ya. and Timofeyev, Yu. M., METEOROLOGICHESKOYE ZONDIROVANIYE ATMOSFERY IZ KOSMOSA (Meteorological Sounding of the Atmosphere From Space), Leningrad, Gidrometeoizdat, 1978.

9. Koprova, L. I., "Catalogue of Global A Priori Information for Routine Processing of Spectrometric Measurements From Artificial Earth Satellites," TRUDY GosNITsIPRa (Transactions of the State Scientific Research Center for the Study of Natural Resources), No 4, 1977.

10. Koprova, L. I., "Global Distribution of Ozone for Different Seasons of the Year," TRUDY GosNITsIPRa, No 9, 1978.

11. Koprova, L. I. and Uranova, L. A., "Latitudinal and Seasonal Variation of the Total Ozone Content During 1964-1975," METEOROLOGIYA I GIDROLOGIYA (Meteorology and Hydrology), No 5, 1978.

12. Malkevich, M. S., OPTICHESKIYE ISSLEDOVANIYA ATMOSFERY SO SPUTNIKOV (Optical Investigations of the Atmosphere From Satellites), Moscow, Nauka, 1973.

13. Nelepo, V. A., SOVREMENNYYE PROBLEMY SPUTNIKOVOY OKEANOLOGII. ISSLEDOVANIYE ZEMLI IZ KOSMOSA (Modern Problems in Satellite Oceanology. Investigation of the Earth From Space), No 1, 1980.

14. Niylisk, Kh. Yu. and Norma, R. O., "Spectral Distribution of the Intensity and Fluxes of Thermal Radiation in the Free Atmosphere," ISSLEDOVANIYA RADIATSIONNOGO REZHIMA ATMOSFERY (Investigations of the Atmospheric Radiation Regime), AN ESSR, Institut Fiziki i Atmosfery, Tartu, 1967.

15. RUKOVODSTVO PO KRATKOSROCHNYM PROGNOZAM POGODY (Manual on Short-Range Weather Forecasting), Part II, Chapter III, Leningrad, Gidrometeoizdat, 1965.

16. RUKOVODSTVO PO GIDROLOGICHESKIM RABOTAM V OKEANAKH I MORYAKH (Manual on Hydrological Studies in the Oceans and Seas), Leningrad, Gidrometeoizdat, 1977.

17. Fedorov, K. N., "Hopes and Realities of Satellite Oceanology," ISSLEDOVANIYE ZEMLI IZ KOSMOSA (Investigation of Earth From Space), No 1, 1980.

18. Breaker, L., Klain, G. and Pitts, M., "Quantitative Measurements of Sea Surface Temperature at Several Locations Using the NOAA-3 Very High Resolution Radiometer," NOAA TECH. MEM. NESS, Vol 98, 1978.

19. Brower, R. L., Dohrband, H. S., Pichel, W. G., Signore, T. L. and Walton, C. C., "Satellite-Derived Sea-Surface Temperatures From NOAA Spacecraft," NOAA TECH. MEM., NESS 78, 1976.

20. Cogan, I. L. and Willand, I. H., "Measurement of Sea Surface Temperature by the NOAA-2 Satellite," J. APPL. METEOROL., Vol 15, No 2, 1976.

21. Martin, P. L. and Salomonson, V. V., "A New Statistical Method of Estimating Surface Radiances From Corresponding Satellite Window Channel Radiances," MON. WEATHER REV., Vol 98, No 9, 1970.

22. McClatchey, R. A., et al., ATMOSPHERIC ABSORPTION LINE PARAMETERS COMPILATION, AFCRL-TR-73-0096, 1973.

23. Pastre, C. and Tournier, B., NOTES INTERNES DE L'ESTABLISSEMENT D'ETUDES ET DE RECHERCHES METEOROLOGIQUES, No 350, 1974.

24. Roberts, R. E., Selby, I. E. A., Biberman, L. M., "Infrared Continuum Absorption by Atmospheric Water Vapor in the 8-13 Window," APPL. OPT., Vol 15, No 9, 1976.

25. Smith, W. L. and Rao, P. K., "The Determination of Surface Temperature From Satellite Window Radiation Measurements," PROC. FIFTH SYMP. ON TEMPERATURE, Washington, D. C., June 21-24, 1971. Repr. Pittsburg, Pa., Instrum. Soc. Amer., 1972.

UDC 551.465.7

COMPARATIVE ANALYSIS OF METHODS FOR CALCULATING TURBULENT HEAT AND MOISTURE FLOWS FROM THE OCEAN TO THE ATMOSPHERE

Moscow METEOROLOGIYA I GIDROLOGIYA in Russian No 7, Jul 81 (manuscript received 13 Jan 81) pp 70-76

[Article by N. R. Nuriakhmetova, USSR Hydrometeorological Scientific Research Center]

[Text]

Abstract: The article gives the results of a cross-comparison of the heat and moisture flows obtained using different parameterizations. Because of the peculiarities in the mechanism of interaction between the ocean and the atmosphere, and specifically the presence of a surface "film," evaporation and heat transfer with the spray, the analysis is made separately for cases of low and high wind velocities. It is shown that the surface "film" is one of the reasons for the disagreement between the results of computations by indirect methods and methods based on direct measurements of turbulent flows. Recommendations are given concerning the applicability of some methods. Conclusions are drawn concerning the consistency of different parameterizations.

Vertical turbulent flows of heat and moisture are important quantitative characteristics of interaction between the ocean and the atmosphere. A knowledge of these parameters is necessary for solving a wide range of problems in meteorology and oceanology. They can be determined either by direct fluctuation measurements or by indirect computations.

The indirect computation method is based on the following premise. It is assumed that the principal mechanism determining the vertical distribution of properties from the underlying surface to a height of several tens of meters above it is turbulent exchange. Therefore the turbulent flows are related to the vertical gradient of the transferred property and the coefficient of turbulent exchange and are described by the equation

$$F_a = -k_a \frac{da}{dz}.$$

Here F_a is the flow of the property a, da/dz is the vertical gradient of the property, k_a is the coefficient of turbulent exchange. However, over the sea the temperature and humidity gradients are very small. Correct gradient observations can be made only by the use of special buoys. On the basis of shipboard hydrometeorological measurements it is possible to obtain information on the wind velocity at a fixed level and the temperature and humidity differentials between the water surface and a fixed level in the air. Accordingly, the following formulas are the basis for all the used methods:

$$H = \rho c_p c_H V_z (t_0 - t_z), \quad (1)$$

$$E = \rho c_E V_z (q_0 - q_z), \quad (2)$$

$$F = \rho c_D V_z^2. \quad (3)$$

where c_H is the heat exchange coefficient; c_E is for the moisture exchange; c_D is the drag coefficient; ρ is air density; V_z is wind velocity at the level z; t_0, t_z is water temperature at the ocean surface and air temperature at the level z; q_0, q_z is the saturating specific humidity of the air at the temperature of the water surface and air specific humidity at the level z; c_p is the specific heat capacity of air at a constant pressure; H is the heat flow; E is the moisture flow; F is the momentum flux.

As is well known, the exchange coefficients are not constant parameters. Accordingly, the question arises of the methods for their parameterization through the measured parameters. Specifically these procedures distinguish one method for computing the flows from another. In our analysis we selected the Arakawa [6] and Louis [9] parameterizations, used in models of general circulation of the atmosphere, and also the method proposed by R. S. Bortkovskiy, et al. [1], which takes into account the humidity stratification of the near-water layer and heat and moisture transfer with the spray during storms. In order to parameterize such parameters as dynamic velocity and roughness level we used the results of the investigations of Garrat [8] and S. A. Kitaygorodskiy [4].

Until very recently there were only a few cases of direct measurements of atmospheric flows. However, despite the complexity and limits of application of this method, recently a definite quantity of data has been accumulated on the fluctuation measurements of flows. The authors of [7] proposed a parameterization based on these data which was used for computations of the heat and moisture flows in this study.

We would like to note that a need arose for this investigation despite the existence of such studies on the comparison of methods for determining turbulent flows. This is attributable to the appearance of new methods, both based on recent experimental data and those used successfully in models of general circulation of the atmosphere.

Review of Employed Parameterizations of Processes of Interaction Between the Atmosphere and the Ocean

We will begin the review with the Friehe and Schmitt parameterization [7]. On the basis of direct fluctuation measurements the turbulent flows of heat and moisture can be computed using the formulas

$$H = \rho c_p \overline{w'\theta'}, \tag{4}$$

$$E = \overline{w'q'}. \tag{5}$$

Here $\overline{w'\theta'}$ is the mean covariation of vertical velocity and temperature, $\overline{w'q'}$ is the mean covariation of vertical velocity and water vapor density, θ' are temperature fluctuations, q' are water vapor density fluctuations, w' are fluctuations of vertical wind velocity.

The authors of [7] systematized the data available in the literature on direct measurements of the vertical turbulent flows of heat and moisture in the near-water layer of the atmosphere over the ocean available in the literature. Using the least squares method the data were represented in the form of the following dependences for different stratification conditions:

$$\text{with} \quad 0 \leqslant V_z(T_{ст} - T_z) < 25$$
$$\overline{w'\theta'} = 0{,}002 + 0{,}97 \cdot 10^{-3} V_z(T_{ст} - T_z), \quad \sigma = 2{,}2 \cdot 10^{-3}; \tag{6}$$

[Here and in the text which follows the subscript "CT" denotes stratification.]

$$\text{with} \quad V_z(T_{ст} - T_z) > 25$$
$$\overline{w'\theta'} = 1{,}46 \cdot 10^{-3} V_z(T_{ст} - T_z), \quad \sigma = 14{,}8 \cdot 10^{-3}; \tag{7}$$

$$\text{with} \quad V_z(T_{ст} - T_z) < 0$$
$$\overline{w'\theta'} = 0{,}0026 + 0{,}86 \cdot 10^{-3} V_z(T_{ст} - T_z), \quad \sigma = 3{,}2 \cdot 10^{-3}; \tag{8}$$

$$\overline{w'q'} = 1{,}32 \cdot 10^{-3} V_z(Q_{ст} - Q_z), \quad \sigma = 6{,}4 \cdot 10^{-3}. \tag{9}$$

Here T_{CT} is water temperature at a depth of approximately 1 m from the sea surface (K), T_z is the potential temperature of air at the level z (K), Q_z is water vapor density at the level z, Q_{CT} is the saturating density of water vapor at the temperature T_{CT}, σ is the standard deviation of the approximation of the measured values.

Formula (6) was derived on the basis of 75 measurements, (7) -- 14, (8) -- 41.

The recommended interval for the use of these formulas is $20 < V_z(T_{CT} - T_z) < 160$. With respect to the applicability of formula (9) in computing the moisture flows, the authors of [7] indicate an absence of data from measurements for high wind velocities. We will note a peculiarity of this parameterization. With a zero difference between the water and air temperatures the heat flow is not equal to zero but has small positive values.

In a model of circulation of the atmosphere [6] Arakawa uses the well-known parameterization of Deacon and Webb [3] for computing the drag coefficient under neutral conditions ($t_0 - t_z = \Delta t = 0$)

$$c_D = (1 + 0{,}07\, V_z) \cdot 10^{-3}. \tag{10}$$

For computing the exchange coefficients the author proposes the following formulas:

$$\text{with} \quad \Delta t > 0 \quad c_H = c_E = c_D \left(1 + \sqrt{\frac{\Delta t}{V_z^2}}\right), \tag{11}$$

$$\text{with} \quad \Delta t < 0 \quad c_H = c_E = c_D \frac{1}{1 - 7\frac{\Delta t}{V_z^2}}. \tag{12}$$

Garrat in his review of studies published during the last ten years, whose purpose was to find the values of the drag coefficient, proposes a refinement of formula (10)

$$c_{DG} = (0{,}75 + 0{,}067\, V_z) \cdot 10^{-3}. \tag{13}$$

We will now examine the parameterization proposed by Louis. The author of [9], like Arakawa, proposes analytical formulas for describing the dependence of the exchange coefficient on the measured parameters in the following form:

$$\text{with} \quad T_0 - T_z = \Delta T = 0 \quad c_D = \varkappa^2 \Big/ \left(\ln \frac{z}{z_0}\right)^2, \tag{14}$$

$$\text{with} \quad \Delta T > 0 \quad c_H = c_E = c_D \frac{1}{0{,}74}\left[1 + \frac{3{,}1\frac{\Delta T}{V_z^2}}{1 + 15{,}9\, c_D \sqrt{\frac{z}{z_0}}\sqrt{\frac{\Delta T}{V_z^2}}}\right], \tag{15}$$

$$\text{with} \quad \Delta T < 0 \quad c_H = c_E = c_D \frac{1}{0{,}74}\left[1 + \frac{1{,}6\,\Delta T}{V_z^2}\right]^2. \tag{16}$$

With values of the Richardson number above the critical level the flows are assumed equal to zero, that is

$$\text{with} \quad -\frac{gz}{T}\frac{\Delta T}{V_z^2} \geq 0{,}212 \quad H = 0, \quad E = 0, \tag{17}$$

where g is the acceleration of free falling, T = 300 K.

A new parameter appears in formulas (14)-(16): the roughness level z_0. In [9] there are no recommendations concerning the choice of its value. Accordingly, in this study we used the well-known Charnok formula

$$\frac{z_0 g}{u_*^2} = \alpha. \tag{18}$$

Here α is a constant whose values are different in the publications of different authors. In this study we used the values $\alpha = 0.035$ [4] and $\alpha = 0.0144$ [8]. However, in formula (18) there is still another unknown parameter -- dynamic velocity. Garrat [8] proposes the following parameterization for its computation:

$$u_* = 0{,}023\, V_z^{1.23}. \tag{19}$$

We will examine the following method for computing the flows. In source [1] the authors propose nomograms expressing the dependence of the exchange coefficients on wind velocity V_Z and the so-called effective temperature differential

$$\Delta T_z^{\text{эф}} = t_0 - t_z + 0{,}108\,(E_0 - e_z),$$

where E_0 is saturation elasticity at the water temperature, e_Z is water vapor elasticity.

The introduction of the effective temperature differentials ensures allowance for humidity stratification. The expressions on the basis of which the nomograms were constructed were derived from a theoretical model of the atmospheric boundary layer generalized for different stratification conditions. These nomograms are applicable for wind velocities up to 14 m/sec. The authors indicate a qualitatively different mechanism of exchange between the ocean and the atmosphere for high wind velocities, and specifically the existence of heat transfer and evaporation with a spray. Due to the small number of experimental investigations providing data for high wind velocities a table is given with the approximate values of the exchange coefficients as a function of wind velocity. The authors also deem it possible to neglect the influence of stratification under storm conditions.

There is still another circumstance which governs the separation of situations with low and high wind velocities on the basis of exchange mechanism: the existence of a surface "film" on the water. The authors of [2] by the term "film" mean some surface water layer for which the quantities of absorbed solar radiation, changes in heat content and advective heat influxes are small in comparison with the total heat flow through this layer. This leads to the formation of a layer of great water temperature gradients. It follows from [10] that the temperature gradient in the "film" is directed in such a way that it favors a decrease in the total water-air temperature differential.

Comparative Analysis of Results of Computations of Heat and Moisture Flows

In this article we used a two-month sample (January and November 1975) of on-ship hydrometeorological data, which constituted 1,306 points for the ocean area of the northern part of the Atlantic Ocean. Before proceeding to a comparative analysis of the results of computations by all the above-mentioned methods, we will examine the significance of the Garrat corrections [8]. A comparison of the results of computations by the Louis method with different α values in formula (18) indicates a systematic exaggeration of the values of the exchange coefficients with $\alpha = 0.035$ by 16-25%. The use of (13) instead of (10) in the computations by the Arakawa method gives lesser values of the exchange coefficients by 18-25%. Thereafter computations were made in agreement with the Garrat recommendations.

Graphs were constructed for an analysis of the sensitivity of the methods to a change of various exchange conditions. The Arakawa method was most sensitive to changes in wind velocity. However, in the case of velocities greater than 22.5 m/sec allowance for heat transfer and evaporation with spray leads to the largest

exchange coefficients by the method described in [1]. The Arakawa method reacts to changes in temperature stratification most strongly in the case of instability, whereas the Louis method reacts most strongly in the case of stability. The humidity stratification, as pointed out above, exerts an influence on the value of the exchange coefficient when using the method described in [1].

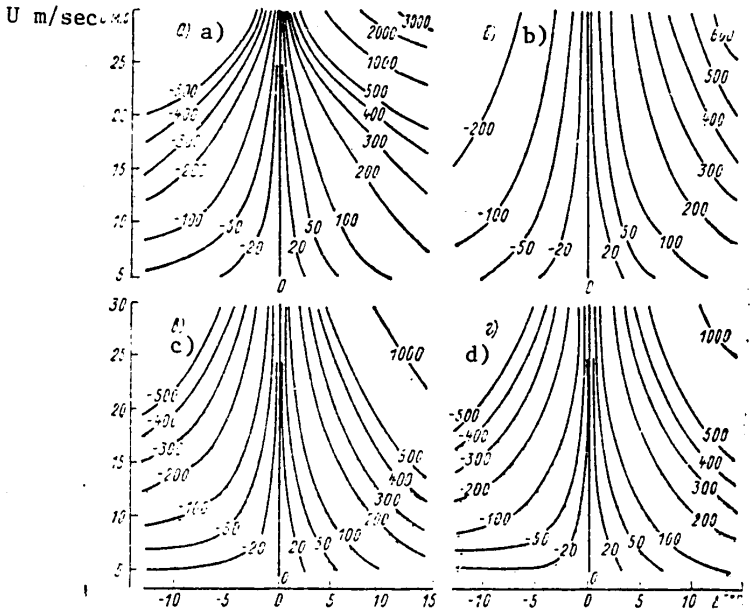

Fig. 1. Flows of apparent heat (W/m^2), computed using the methods developed by R. S. Bortkovskiy, et al. (a), Friehe and Schmitt (b), Arakawa (c) and Louis (d). U is the wind velocity at the level 10 m, ΔT is the water-air temperature differential.

In accordance with what has been set forth above, the analysis of the results of the computations was carried out separately for cases with low wind velocities and separately for storms.

A comparative analysis [5] of the results of direct measurement of turbulent flows and the results of indirect computations revealed that the computed data are higher on the average by 25%. The use of the Friehe and Schmitt method, based on the results of direct measurement of flows, confirms such a relationship (see Fig. 1). In this article an attempt was made to attribute this discrepancy to the presence of a surface "film."

In all methods, other than [7], it is necessary to know the temperature of the ocean surface. However, in actual practice use is made of data on water temperature deeper than the surface. It was stated above that the "film" favors a decrease in the water-air temperature differential, that is, a decrease in the flows of heat and moisture. If it was possible to compute the value of the correction for the "film" on the basis of the measured parameters, for example, on the basis of atmospheric

stratification and the wind, its introduction could lead to a better consistency between the results of direct measurements and computations on the basis of theoretical methods. Due to the impossibility of taking into account the influence of stratification on the value of the gradient in the "film," in this study we used a dependence derived by G. N. Panin in [10] (Fig. 2). The scatter of points is attributable to failure to take stratification into account.

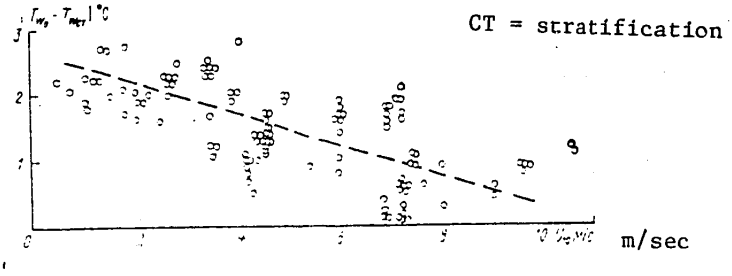

Fig. 2. Dependence of difference $T_{w0} - T_{wCT}$ on wind velocity at height 10 m. T_{w0} -- temperature of water surface; T_{wCT} -- water temperature below sea surface, U_{10} -- wind velocity at level 10 m.

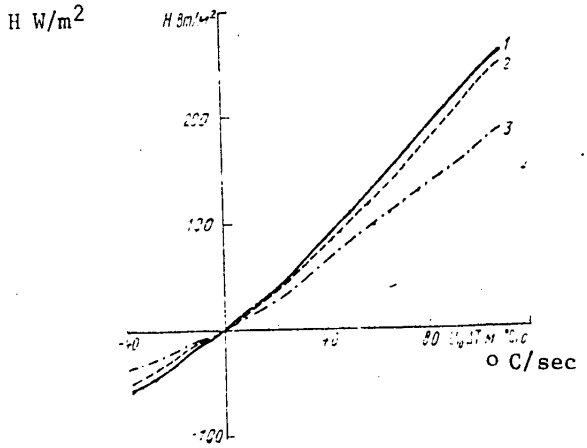

Fig. 3. Flows of apparent heat computed by Arakawa method (1), Arakawa method with allowance for correction for "film" (2), Friehe and Schmitt (3). H -- flow of apparent heat, U_{10} -- wind velocity at level 10 m, ΔT water-air temperature differential.

The results of computations by the Arakawa method with use of the correction for the "film" are cited in Fig. 3. It follows from the figure that the allowance for the influence of the "film" leads to some decrease in the difference between these two methods. However, computation of the correction only as a function of

wind velocity does not lead to a satisfactory consistency of methods in the case of great water-air temperature differentials. It is necessary to ascertain the dependence of the water temperature gradient in the "film" on stratification of the near-water layer, the use of which with the introduction of a correction could give a satisfactory result.

With respect to cases of storm wind velocities, Fig. 1 shows an appreciable discrepancy of the results of computations based on the different methods. The Friehe-Schmitt method gives low values for the flows of apparent and latent heat and the magnitude of the discrepancy is comparable with the flows themselves. It was stated above that for storms there is no great number of cases of direct measurement of the flows and therefore the parameterization [7] is based on a limited volume of data and the standard deviation of the approximation from the real values is rather great. A comparison of the results of computations by the three remaining methods reveals a consistency of the methods within the limits of accuracy indicated in [1], except for the region of a wind of hurricane force ($V_z > 25$ m/sec). In the latter there is discrimination of very high values of turbulent flows computed by the method in [1]. However, it is necessary to take into account the approximate character of the exchange coefficient values for velocities greater than 14 m/sec and a relatively low frequency of recurrence of velocities greater than 25 m/sec.

Conclusions

1. In the region of low wind velocities the minimum values of the turbulent flows of heat and moisture are given by the Friehe and Schmitt method, based on the results of direct measurement of the flows.

2. The assumption of an influence of the surface temperature "film" and the introduction of a corresponding correction leads to some improvement in the consistency of the methods.

3. In the region of great wind velocities the Friehe and Schmitt parameterization is doubtful because it is based on the results of only 14 measurements, which give a great scatter.

4. For wind velocities from 14 to 25 m/sec the parameterizations [1, 6, 9] agree within the limits of 30% accuracy with an unstable stratification, and in the case of a stable stratification -- within the limits of a 40% accuracy.

BIBLIOGRAPHY

1. Ariel', N. Z., Bortkovskiy, R. S. and Byutner, E. K., "Fundamental Principles in Constructing Tables for Determining Turbulent Flows in the Lower Air Layer Over the Sea," METEOROLOGIYA I GIDROLOGIYA (Meteorology and Hydrology), No 11, 1975.

2. Bortkovskiy, R. S., Byutner, E. K., Malevskiy-Malevich, S. P. and Preobrazhenskiy, L. Yu., PROTSESSY PERENOSA VBLIZI POVERKHNOSTI RAZDELA MORYA I ATMOSFERY (Transfer Processes Near the Sea-Atmosphere Discontinuity), Leningrad, Gidrometeoizdat, 1974.

3. Deacon, I. L. and Webb, I. K., "Microscale Interaction," MORE (The Sea), Leningrad, Gidrometeoizdat, 1965.

4. Kitaygorodskiy, S. A., FIZIKA ATMOSFERY I OKEANA (Physics of the Atmosphere and Ocean), Leningrad, Gidrometeoizdat, 1970.

5. Malkus, Zh., "Macroscale Interaction," MORE, Leningrad, Gidrometeoizdat, 1965.

6. Arakawa, A., "Design of the UCLA General Circulation Model," Univ. of California, Los Angeles, Department of Meteorology, TECHNICAL REPORT No 7, 1972.

7. Friehe, C. A. and Schmitt, K. F., "Parameterization of Air-Sea Interface Fluxes of Sensible Heat and Moisture by the Bulk Aerodynamic Formulas," J. PHYS. OCEANOGR., Vol 6, 1975.

8. Garrat, J. R., "Review of Drag Coefficients Over Oceans and Continents," MON. WEATHER REV., Vol 105, 1977.

9. Louis, J. F., "Parameterization of the Surface Fluxes," European Center for Medium-Range Weather Forecasts, Research Dep., Internal Report, No 4, Feb 77.

10. Panin, G. N., Volkova, S. V. and Foken, T. H., "On Heat Exchange of Surface Layer of Water Reservoir With Atmosphere. XVIII Congresso IAHR Italia 1979, HYDRAULIC ENGINEERING IN WATER RESOURCES DEVELOPMENT AND MANAGEMENT PROCEEDINGS, Vol 3, Subject B, Cagliari, Italia, Sep 1979.

UDC 551.465.(152+53)(261.2)

NUMERICAL EXPERIMENTS USING A MODEL OF THE OCEAN'S UPPER LAYER

Moscow METEOROLOGIYA I GIDROLOGIYA in Russian No 7, Jul 81 (manuscript received 8 Jul 80) pp 77-85

[Article by G. Friedrich, doctor, V. P. Kochergin, professor, V. I. Klimok, A. V. Protasov and V. A. Sukhorukov, candidates of physical and mathematical sciences Institute of Oceanography, Hamburg University, and Computation Center, Siberian Department, USSR Academy of Sciences]

[Text]

Abstract: The article presents meteorological and oceanological data from measurements made in the FLEX experiment. On the basis of a mathematical model of the upper layer of the ocean with the use of FLEX data in the boundary conditions it was possible to carry out numerical computations for reconstruction of hydrodynamic characteristics of the sea. The results of the computations are compared with the experimental data. The sensitivity of solution of the problem to the model parameters is evaluated.

Measurement Data From FLEX

During 1978 West German oceanographers carried out measurements under the program of the FLEX experiment in a polygon in the North Sea. The authors had at their disposal the following filtered data obtained during the period 6 April-13 June with a discreteness of 4 hours: wind velocity components u_a and v_a, near-water pressure P, air temperature T_a and wet-bulb thermometer T_w, total flux of short-wave radiation F_I, flux of outgoing long-wave radiation F_B and temperature of the sea surface T_s. Meteorological measurements were made at a standard horizon. Figure 1 represents these data by days corresponding to measurements at midday. A peculiarity of this period is the heating of the upper layer of the sea and the near-water layer of the atmosphere.

The measurements were made from the scientific research ships "Meteor" and "Anton Dorn," which operated alternately. On individual days the measurements were made outside the polygon: 5-7 May and 5-8 June -- the "Meteor" operated approximately 100 km and on 12-14 May the "Anton Dorn" operated 80 km.

We carried out a series of numerical experiments in which the FLEX data were introduced into the boundary conditions of the problem. The parameters of wind frictional stress at the sea surface τ_x, τ_y were computed for the two wind velocity components:

$$\tau_x = C_\tau \rho_a u_a |u_a|, \quad \tau_y = C_\tau \rho_a v_a |v_a|. \tag{1}$$

The fluxes of apparent F_H and latent heat of evaporation F_E at the sea surface can be computed on the basis of the BULK method:

$$F_H(T_s) = \rho_a C_D |\vec{v}_a| c_p (T_s - T_a), \tag{2}$$

$$F_E(T_s) = \rho_a C_D |\vec{v}_a| L [q_s(T_s) - q_a]. \tag{3}$$

Here ρ_a is air density; c_p is the specific heat capacity of air; L is the latent heat of evaporation; $q_s(T_s)$ is the specific humidity of saturated air at the temperature of the sea surface T_s; q_a is specific humidity; C_τ, C_D are the drag coefficient and the heat exchange coefficient.

The specific humidity q_s (T_s) is determined on the basis of the equation of state of an ideal gas and Dalton's law

$$q_s(T_s) = \frac{0{,}622\, e_s}{P - 0{,}378\, e_s}. \tag{4}$$

Here e_s is the partial pressure of saturated water vapor. The pressure e_s, according to the Clausius-Clapeyron equation with a constant mean latent heat of evaporation L, is approximately determined as follows:

$$e_s(T_s) = e(T_0) \exp\left\{\frac{L}{R_v}\left(\frac{1}{T_0} - \frac{1}{T_s}\right)\right\} = 6{,}108 \exp\left\{19{,}85\left(1 - \frac{T_0}{T_s}\right)\right\}. \tag{5}$$

Here T_0 = 273.16 K, R_v is the gas constant for water vapor, T_s is temperature in Kelvin.

Formula (5) gives the e_s value in millibars, differing by less than 2% from the precise values at a temperature below 30°C [2]. Formula (5) does not take into account the salinity of sea water, which exaggerates the pressure value e_s by 2% [2].

The specific humidity q_a was determined through the temperature of the wet-bulb thermometer T_w

$$T_w = T_a - \frac{L}{c_p}(S_s - S), \tag{6}$$

where S_s, S are the mixture ratios for air saturated and unsaturated with vapor respectively. According to definition of the S value, it is the ratio of vapor density to the density of dry air and the equation of state of an ideal gas

$$S_s = \frac{0{,}622\, e_s(T_w)}{P - e_s(T_w)}. \tag{7}$$

By definition, the mixture ratio is related to specific humidity by the expression

$$q_a = \frac{S}{1 + S}. \tag{8}$$

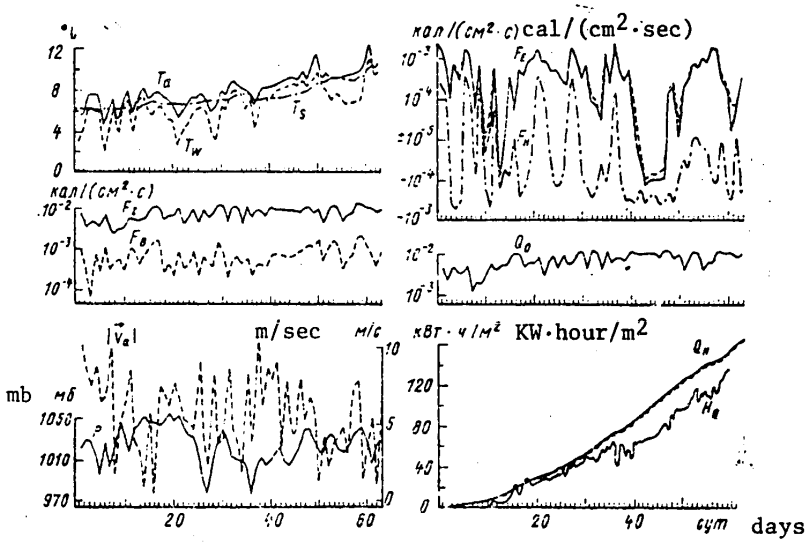

Fig. 1. FLEX data.

From expressions (6), (7) we obtain

$$S = (T_w - T_a)\frac{c_p}{L} + \frac{0{,}622\, e_s(T_w)}{P - e_s(T_w)}. \tag{9}$$

Substituting the S value from expression (9) into formula (8), we find the specific humidity q_a. In computations of the flux of latent heat using formula (3) the L(T) value was determined using the expression [2]

$$L(T) = 597{,}3 - 0{,}56(T - T_0) \text{ cal/g}. \tag{10}$$

In numerical experiments the flux of latent heat was computed using the formula proposed in [8],

$$F_E(T_s) = \rho_a C_D |\vec{v}_a| L\left[q_s(T_a) - q(T_a) + \frac{\partial q_s}{\partial T}\Big|_{T_a}(T_s - T_a)\right], \tag{11}$$

which is expansion of formula (3) into a series in powers of $(T_S - T_a)$. Comparative computations with formulas (3) and (11) indicated that the total heat flux into the sea over a two-month period

$$Q_H = \int_{t_1}^{t_2} (F_I - F_B - F_E - F_H)\, dt$$

differs from the results of computations using different formulas by less than 1%, although the quantity of latent heat of evaporation at some times differs up to 50% and sometimes also changes sign. During this period of observations the heat balance at the surface was determined by the flux of short-wave radiation and therefore different methods for computing the flux of latent heat were not reflected in the total entry of heat into the sea.

Figure 1 shows the change in the heat content of the 80-m layer in the sea during this period

$$H_Q = \int_{t_1}^{t_2} \int_0^H \rho_0 C \frac{\partial T}{\partial t} dz\, dt,$$

which was computed by West German specialists using data on the vertical distribution of temperature. The difference between the entry of heat and heat content increases with time and was caused by the error in computing the total heat flux at the surface and horizontal advection. The error in computing the heat flux is related to the inaccuracy of the computation formulas and the error in measuring the initial parameters.

In the computations the input constants assumed the following values:

$$C_z = C_D = 1{,}3 \cdot 10^{-3},\ \rho_a = 1{,}2 \cdot 10^{-3}\ \text{g/cm}^3,\ c_p = 0{,}24\ \text{cal/(g·degree)},$$
$$C = 1\ \text{cal/(g·degree)},\ L = 595\ \text{cal/g}.$$

Formulation of Problem

A study was made of the one-dimensional boundary layer of the ocean:

equations of drift movements

$$\frac{\partial u}{\partial t} - fv = \frac{\partial}{\partial z} K \frac{\partial u}{\partial z}, \tag{12}$$

$$\frac{\partial v}{\partial t} + fu = \frac{\partial}{\partial z} K \frac{\partial v}{\partial z}, \tag{13}$$

thermal conductivity equation

$$\frac{\partial T}{\partial t} = \frac{\partial}{\partial z}\left(K \frac{\partial T}{\partial z} - F_I e^{-\beta z}\right), \tag{14}$$

formula for determining the coefficient of vertical turbulent exchange

$$K = (C_k h)^2 \sqrt{\left(\frac{\partial u}{\partial z}\right)^2 + \left(\frac{\partial v}{\partial z}\right)^2 - g \frac{1}{\rho_0} \frac{\partial \rho}{\partial z}}, \tag{15}$$

and equation of state

$$\frac{\partial \rho}{\partial z} = -\alpha \frac{\partial T}{\partial z}. \tag{16}$$

The boundary-value conditions of problem (12)-(14) are as follows:

$$z = 0: \quad K \frac{\partial u}{\partial z} = -\frac{\tau_x}{\rho_0}, \quad K \frac{\partial v}{\partial z} = -\frac{\tau_y}{\rho_0}, \tag{17}$$

$$C \rho_0 K \frac{\partial T}{\partial z} = F_B + F_E + F_H,$$

if the last term $F_I e^{-\beta z}$ is absent in equation (3), then

$$C\rho_0 K\frac{\partial T}{\partial z} = F_B + F_E + F_H - F_I = -Q_0,$$

$$z = H = 100\ м: \quad u = v = 0, \quad T = T_H. \tag{18}$$

Here u, v are the velocity components of sea currents; T is temperature; $f = 2\omega\sin\varphi$ is the Coriolis parameter; ω is the angular velocity of the earth's rotation; φ is latitude ($\varphi = 59^{\circ}$N); h is the depth of the surface turbulent layer, which is determined from the computation point z_k, the first from the surface, at which the following condition is satisfied

$$(C_k z_k)^2 \Big/ \overline{\left(\frac{\partial u}{\partial z}\right)^2 + \left(\frac{\partial v}{\partial z}\right)^2 - \frac{g}{\rho_0}\frac{\partial \rho}{\partial z}} \leq \min K = K_0; \tag{19}$$

α is the coefficient of thermal expansion of sea water; $\alpha = 1.5\cdot10^{-4}$ degree^{-1}; β is the index of absorption of short-wave radiation in the water medium; the z-axis is directed downward.

The formulated problem was solved numerically on an electronic computer produced by the "Telefunken" Corporation at Hamburg University. The boundary-value conditions were computed on the basis of FLEX data. The equations of motion (12)-(13) were approximated in time by an implicit difference scheme and a spatial central-difference approximation. The derived system of algebraic equations is solved by matrix factorization. The thermal conductivity equation (14) was approximated in time using an implicit scheme and was approximated in space by central differences. The derived system of algebraic equations is solved by a modification of the difference schemes method [6] which makes possible more careful computation of the difference solution gradients in the neighborhood of the temperature jump. The entire system of equations (12)-(15) with the boundary conditions (17)-(18) was solved successively in time with a time interval of 24 minutes -- 10 steps between the measurement data with linear interpolation between them. Vertically use was made of a uniform computation grid with an interval of 2.5 m. The details of the solution method for such a formulation were given in [1].

Results of Numerical Experiments

There are a number of free parameters in the problem: the C_k coefficients in formula (15) and the absorption coefficient K_0, the drag coefficient C_τ and the heat exchange coefficient C_D. The sensitivity of the solution to these parameters was checked in the numerical experiments.

In the first series of computations the short-wave radiation was taken into account by the boundary conditions of the thermal conductivity equation. The following experiments were carried out in this series: with a constant value of the coefficient of vertical turbulent exchange K, with different values of the coefficients C_k and K_0. In the second series of computations short-wave radiation was taken into account as a source on the right-hand side of the thermal conductivity equation (14). The influence of the coefficients β and K_0 was evaluated in this series.

1) Figure 2a represents the computed surface temperature with constant values of the coefficient of turbulent viscosity K. On the basis of these results it is possible to estimate the characteristic value of the K coefficient which was equal approximately to 10 cm^2/sec. The use of the model for the K coefficient considerably improved the result. This can be seen from a comparison of Figures 2a and 2b.

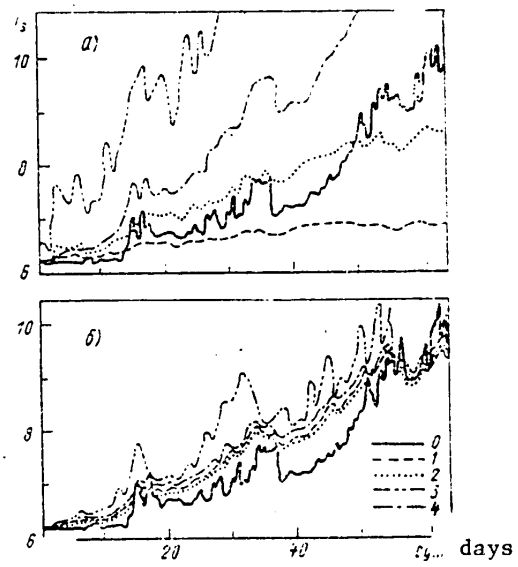

Fig. 2. Temperature of sea surface. 0) FLEX data, a) computations with constant K coefficient: 1) K = 50; 2) K = 10; 3) K = 1 cm^2/sec; 4) K variable, C = 0.05, K_0 = 1 cm^2/sec, b) computations with value K_0 = 8-7.9 $(z/H)^{1/2}$: 1) C_k = 0.21-0.2 z/H; 2) C_k = 0.41-0.4 z/H; 3) C_k = 0.11-0.1 z/H, Δz = 10 m; 4) C_k = 0.11-0.1 z/H.

The formula for determining the K coefficient (15) is a special case of the dynamic turbulence equations [1]. The C_k coefficient was found by solution of the dynamic turbulence equations and in the case of weak stable stratification can be assumed equal to 0.05 [1]. In a general case the C_k value is dependent on the thickness of the surface turbulent layer [3]. The analytical solutions of the stationary equations (12)-(14), obtained with the a priori coefficient K, are substituted into the left- and right-hand sides of formula (15): K = K_1 and K = $K_1(1-z/H)^2 = K_1x^2$ (K_1 = const) [4] and the C_k coefficient is evaluated using this method:

$$(C_k h)^2\left[\left(\frac{\partial u}{\partial z}\right)^2+\left(\frac{\partial v}{\partial z}\right)^2-\frac{g}{\rho_0}\frac{\partial \rho}{\partial z}\right]^{1/2}=(C_k h)^2\sqrt{\frac{\varepsilon}{K}}, \qquad (20)$$

$$K^3=(C_k h)^4\varepsilon, \quad C_k=\left(\frac{K^3}{\varepsilon}\right)^{1/4}\frac{1}{h}.$$

Substituting the known solution obtained with a constant value of the K coefficient into the right-hand side of formula (20) [4], we obtain

$$C_k=\frac{(2e^{-\pi}\mu^{-1})^{1/2}}{\pi(e^{-2\gamma z}-e^{-\pi})^{1/4}}\underset{z=0}{\approx}\frac{(2e^{-\pi}\mu^{-1})^{1/2}}{\pi}. \qquad (21)$$

With a variable K coefficient, K = K_1x^2

$$C_k=\frac{(2e^{-\pi}\mu^{-1})^{1/2}}{A(\mathrm{Re}_T)(1-\mathrm{Re}_T^{-1/2})}\frac{x^{3/2}}{(x^{2m}-e^{-\pi})^{1/4}}\underset{z=0}{\approx}\frac{(2e^{-\pi}\mu^{-1})^{1/2}}{A(\mathrm{Re}_T)(1-\mathrm{Re}_T^{-1/2})}. \qquad (22)$$

Here $\mu = \lambda/L$, $\lambda = u_*/f$, $u_*^2 = |\vec{\tau}|/\rho_0$, $L = u_*^3/g\alpha Q_0$,

$$\gamma = (fe^{\pi}\mu/2u_*\lambda)^{1/2}, \quad \mathrm{Re}_T = u_* Le^{-\pi}/K_0, \quad A(\mathrm{Re}_T) = \\ = \{[2(1 + 2\pi/\ln \mathrm{Re}_T)^2 - 1]^3 - 1\}^{1/4},$$

ε is the rate of turbulent dissipation.

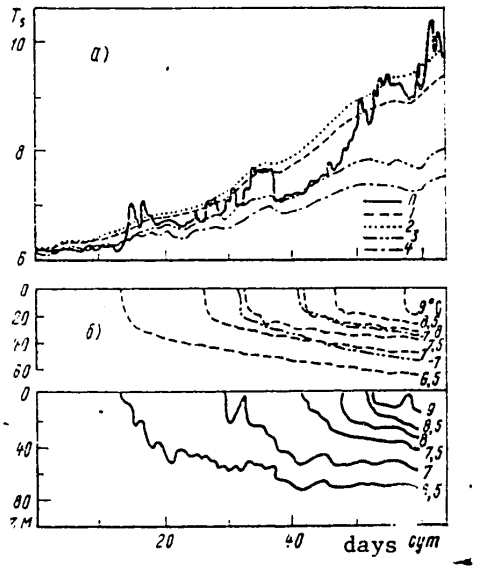

Fig. 3. Temperature of sea surface (a) and temperature isolines (b). 1) $\beta = 75\cdot10^{-5}$, $K_0 = 1$; 2) $\beta = 75\cdot10^{-5}$, $K_0 = 0.1$; 3) $\beta = 75\cdot10^{-5}$, $K_0 = 8$; 4) $\beta = 3\cdot10^{-3}\mathrm{cm}^{-1}$, $K_0 = 8\ \mathrm{cm}^2/\mathrm{sec}$. 0) FLEX data.

A decrease in the stratification parameter $\mu(\mu \geq 0)$ under the influence of a decrease in wind stress or an increase in stable stratification leads to a decrease in depth h and an increase in the C_k coefficient, formulas (21), (22). For the characteristic μ-values in the ocean, equal to 10^{-1}, 1, 10, in formula (21) C_k = 0.29; 0.09; 0.029; and in formula (22) C_k = 0.13; 0.035; 0.009 respectively.

Figure 2b shows the results of computations with a variable C_k coefficient. A considerable increase in the C_k coefficient is poorly reflected in the evolution of sea surface temperature. The principal parameter to which surface temperature is sensitive was the value of the K_0 coefficient and to a lesser degree the value of the C_k coefficient.

The reconstructed surface temperature variation is exaggerated, especially after 37 days. At this time a storm occurred in the polygon and there was a marked decrease in heat content of the sea (see Fig. 1). This effect is not noted in the

computed entry of heat into the sea. This difference can be caused by the measurement error and the inaccuracy in the computation formulas for the heat flow. At this time the measurements were made 80 km from the polygon. With an increase in wind velocity the C_ζ and C_D coefficients increase; failure to take this effect into account gives up to a 15% understatement for the computed flow of apparent heat and an understatement of the latent heat of evaporation up to 7% [5]. In addition, frictional stress can be understated up to 40% due to the averaging of wind velocity, and not its square. The mean value of the drag coefficient, evaluated for FLEX data using the formula [7]

$$C_* = (1{,}0 + 0{,}07|\vec{v}_a|)\,10^{-3}, \quad \vec{v}_a \text{ in m/sec}, \tag{23}$$

is correct in the case of a neutral stratification, equal to $1.4 \cdot 10^{-3}$. The total heat influx, computed with this C_D value, differs from the preceding by approximately 1%.

Another distinct difference in the data was noted in the neighborhood of 60 days. The surface temperature was below the data. The reason is also attributable to the difference between measurement of heat content of the sea and heat entry into the sea. At this time there was a high level of heat entry into the sea when there was a very weak wind. Under such conditions the errors in measuring meteorological parameters and computations of heat balance components at the sea surface should be small. Accordingly the difference between the heat content and heat influx into the sea was attributable to horizontal advection.

Figure 2b also shows the role of vertical resolution. The conclusion follows from this that the result can be improved by making the computation grid more detailed.

An analysis of the computations shows that a particularly strong discrepancy with the data is noted during the time of heating of the sea when there is no wind. At such moments turbulent exchange is absent and therefore the surface temperature increases sharply in comparison with the data. A smoothing of this effect is attained by an increase in the a priori K_0 coefficient ($K_0 \simeq 10$ cm^2/sec) or the distribution of the short-wave radiation with depth.

2) Four computations were made taking into account short-wave radiation in equation (14) (see Fig. 3). The C_k coefficient in these computations is equal to 0.05. The characteristic value of the K_0 coefficient in this case is 0.1-1 cm^2/sec. With an increase in the K_0 parameter the surface temperature values decrease and the isotherms are deepened (Fig. 3b). In these computations the surface temperature is less sensitive to the a priori coefficient K_0, as was the case in the preceding computations.

The absorption coefficient β exerts an influence on the surface temperature field and the depth of the isotherms (Fig. 3). An increase in the absorption coefficient β unexpectedly reduced the surface temperature. We will examine the stationary solution of the thermal conductivity equation (14) with the constant coefficient K:

$$C\rho_0 K T_z(z) = F_J(e^{-\beta z} - 1) + (F_B + F_E + F_H), \tag{24}$$

$$T(z) = T_H + \frac{H-z}{KC\rho_0} Q_0 - \frac{F_I}{\beta KC\rho_0}(e^{-\beta z} - e^{-\beta H}), \tag{24}$$

$$F_I,\ F_E,\ F_H,\ F_B > 0.$$

The surface temperature value

$$T_s = T_H + \frac{H}{KC\rho_0} Q_0 - \frac{F_I}{\beta KC\rho_0}(1 - e^{-\beta H}) \tag{25}$$

decreases with a decrease in the β parameter:

$$\frac{\partial T_s}{\partial \beta} = \frac{F_I}{\beta^2 KC\rho_0}(1 - e^{-\beta H}) - \frac{F_I H}{\beta KC\rho_0} e^{-\beta H} > 0. \tag{26}$$

The computations indicated an inverse effect. This can be attributed to a change in the K value with a change in the β parameter:

$$\frac{\partial T_s}{\partial K} = -\frac{H}{K^2 C\rho_0} Q_0 + \frac{F_I}{\beta K^2 C\rho_0}(1 - e^{-\beta H}). \tag{27}$$

The sign of this expression is not dependent on the K value and is determined by the expression

$$\frac{F_I}{\beta}(1 - e^{-\beta H}) - H(F_I - F_B - F_E - F_H) \gtrless 0. \tag{28}$$

If $F_I \gg F_B + F_E + F_H$ (this is correct during the daytime), then expression (28) can be simplified:

$$\frac{F_I}{\beta} - HF_I = F_I\left(\frac{10^5}{75} - 10^4\right) < 0,$$

and with characteristic β values with an increase in the K coefficient there is a decrease in the T_S value.

If $F_B + F_E + F_H \gg F_I$ (this condition is satisfied at nighttime), then $\partial T_S/\partial K > 0$ and with an increase in the K coefficient there is an increase in the T_S value. A change in the absorption coefficient β leads to a change in the K coefficient and it determined the variation of surface temperature.

The distribution of short-wave radiation with depth improved the result, especially the profiles of the isotherms in depth-time coordinates. There was no further improvement in the temperature regime by careful choice of the β and K_0 coefficients. The reason for this is the discrepancy in data on the change in heat content and the computed entry of heat into the sea. In this connection it is desirable to improve the formulas for computing the heat balance components at the sea surface using FLEX data.

The authors express appreciation to Professor Yu. Sunderman for kindly affording the opportunity for carrying out this study.

BIBLIOGRAPHY

1. Kochergin, V. P., Klimok, V. I. and Sukhorukov, V. A., "Homogeneous Layer of the Ocean Within the Framework of 'Differential' Models," CHISLENNYYE METODY MEKHANIKI SPLOSHNOY SREDY (Numerical Methods in Mechanics of a Continuous Medium), Novosibirsk, Vol 8, No 5, 1977.

2. Kraus, Ye., VZAYMODEYSTVIYE ATMOSFERY I OKEANA (Interaction Between the Atmosphere and Ocean), Leningrad, 1976.

3. Marchuk, G. I., et al., MATEMATICHESKIYE MODELI TSIRKULYATSII V OKEANE (Mathematical Models of Circulation in the Ocean), Novosibirsk, Nauka, 1980.

4. Marchuk, G. I., Kochergin, V. P., Klimok, V. I. and Sukhorukov, V. A., "Analytical Solutions for Ekman Turbulent Layer in the Ocean," DOKLADY AN SSSR (Reports of the USSR Academy of Sciences), Vol 247, No 1, 1979.

5. OKEANOLOGIYA. FIZIKA OKEANA (Oceanology. Oceanic Physics), Vol 1, GIDROFIZIKA OKEANA (Oceanic Hydrophysics), Moscow, Nauka, 1978.

6. Samarskiy, A. A., TEORIYA RAZNOSTNYKH SKHEM (Theory of Difference Schemes), Moscow, Nauka, 1977.

7. Deacon, E. L. and Webb, E. K., "Interchange of Properties Between Sea and Air," THE SEA: IDEAS AND OBSERVATIONS, Vol 1, 1962.

8. Haney, R. L., "Surface Thermal Boundary Condition for Ocean Circulation Models," J. PHYS. OCEANOGR., Vol 1, No 4, 1971.

UDC 551.465.4(262.5)

HYDROLOGICAL STRUCTURE AND ENERGY RESERVES OF RINGS IN THE MAIN BLACK SEA CURRENT

Moscow METEOROLOGIYA I GIDROLOGIYA in Russian No 7, Jul 81 (manuscript received 8 May 80) pp 86-93

[Article by A. S. Blatov, candidate of geographical sciences, Moscow State University]

[Text]

Abstract: It was established on the basis of data from two synchronous hydrological surveys in the zone of the main Black Sea current that the process of ring formation in the Black Sea is associated with the meandering of the main Black Sea current. It is shown that the vertical hydrological structure of the rings, discovered along the coast of Anatolia and in the southeastern part of the sea, is similar in structure to the rings of intensive boundary currents. The author gives an evaluation of the available potential and kinetic energy of the rings, on the basis of which it is concluded that the rings are expressed less intensively in the Black Sea.

Due to the implementation of numerous oceanographic expeditions ("Poligon-70," MODE, POLIMODE), as well as the successes of satellite oceanology, the study of mesoscale and synoptic eddy (ring) formations in the ocean has considerably advanced. Researchers working in this field are faced with the task of generalizing available observational data on such oceanic formations for the purpose of formulating physically valid models of the formation and evolution of rings in the ocean, standardization and classification of their spatial-temporal parameters. In contrast to the ocean, in internal seas, such as the Black Sea, there has been very little study of these formations. However, in water bodies of this type (great depths, considerable extent, presence of an intensive well-developed main pycnocline and intermediate layers) the ring-formation processes can transpire the same as in the ocean. The authors of [1], on the basis of data from two hydrological surveys in the zone of the main Black Sea current in the neighborhood of the Anatolian coast, carried out in July-August 1976 under the national program for Joint Multisided Investigations of the Black Sea (SKOICh -- Sovmestnyye Kompleksnyye Issledovaniya Chernogo Morya), as well as data from observations of currents at three buoy stations, employing hydrological criteria, defined a powerful anticyclonic eddy and proposed an explanation of the mechanism of

its formation, related to intensive meandering of the Black Sea current. The hypotheses expressed in [1] concerning the mechanism of formation of this eddy are more rigorously confirmed by additional in situ observations, and this constitutes the subject of this study, in which we subject to further analysis the hydrological observations used in [1], process and analyze data from a hydrological survey made in the southeastern part of the Black Sea carried out during November-December 1977. In addition, we employed generalized data from synchronous hydrological surveys in the 1950's and long-term instrumental observations of currents carried out in the Black Sea.

A generalization of all the available observations of currents in the zone of the main Black Sea current, and also the processing of the long-term mass of hydrological data available at the Department of Oceanology at Moscow State University, made it possible to confirm the prevailing idea that the main Black Sea current, propagating along the coast, occupies the entire sea as a cyclonic ring. It was found that a cyclonic character of the circulation is observed over the course of the entire year; the main characteristic of the seasonal restructuring of the field of currents is attenuation of the cyclonic flow from winter to summer. This is somewhat contradictory to current concepts that a cyclonic circulation is observed in 70% of the cases, whereas in 30% of the cases there is an anticyclonic circulation. Restructuring to the latter is most probable in summer [5].

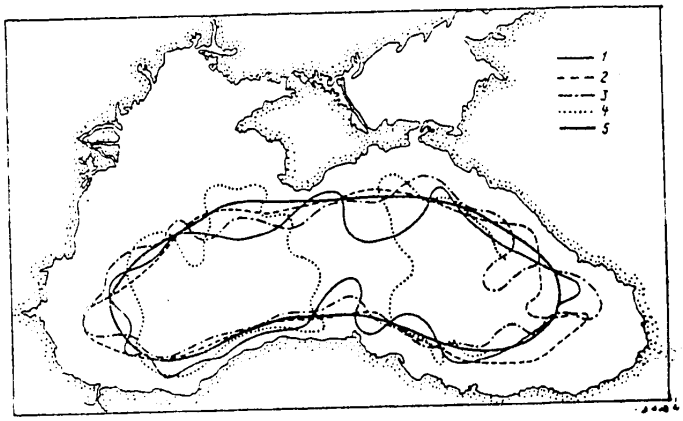

Fig. 1. Position of axis of main Black Sea current according to data from synchronous surveys in the 1950's. 1) 1951; 2) 1952; 3) 1953; 4) 1957; 5) mean position.

It was established on the basis of repeated surveys of currents with the EMIT* apparatus that the main Black Sea current has the form of a narrow jet whose width is 40-80 km. The maximum velocities in the jet (current axis) can attain 100-150 cm/sec. A comparison of the position of the current axis with the data from synchronous hydrological surveys revealed that the main Black Sea current at depth is associated with regions of increased gradients of thermohaline characteristics and can be regarded as a boundary jet current separating the freshened waters of

* The EMIT survey data were provided through the courtesy of V. I. Zats.

the coastal regions from the relatively saline waters of the abyssal zone of the Black Sea. It was found that on the basis of hydrological criteria it is possible to identify the position of the main Black Sea current, in particular, to discriminate the axis of the current at a depth of 100 m on the basis of the 20°/oo isohaline.

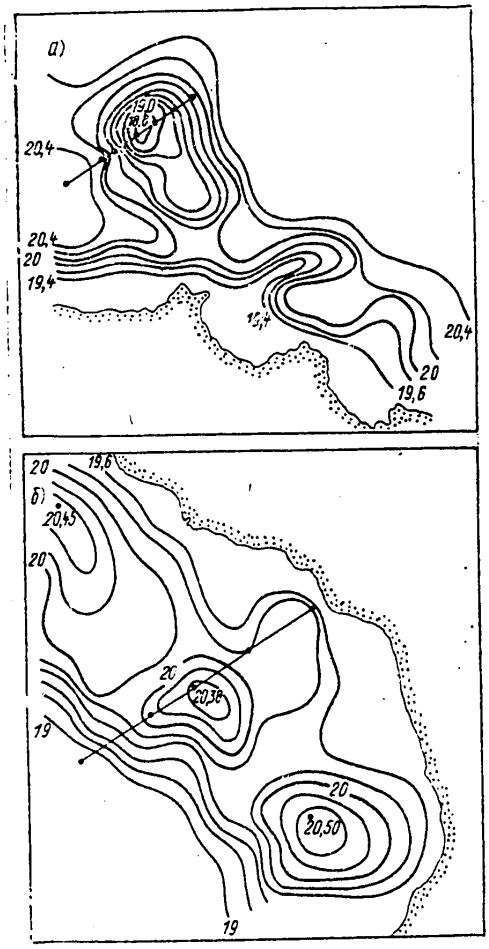

Fig. 2. Salinity field at the 100-m horizon. a) in July 1976 along the shores of Anatolia; b) in November-December 1977 in the southeastern part of the sea.

Figure 1 shows the position of the axis of the main Black Sea current at the 100-m horizon obtained on the basis of data from synchronous surveys of the 1950's. Figure 1 shows the "wandering" of the main Black Sea current, which experiences wavelike fluctuations, approaching the shore and withdrawing from it. Three regions of the strongest meandering of the main Black Sea current are defined: the region of the Anatolian coast (to the east of Cape Sinop), the southeastern region of the Caucasus coast and the region of dropoff of the depths of

the northwestern part of the Black Sea.

According to the hypothesis proposed in [1], the main reason for the meandering is the baroclinic instability of the main Black Sea current. Under definite conditions (with an increase in wave disturbances of the main Black Sea current) individual rings similar to those discovered in [1] can be formed in its zone. Therefore, the process of meandering and ring formation in the zone of the main Black Sea Current can be regarded as a manifestation of frontal instability of the type of the Gulf Stream instability to the east of Cape Hatteras and other boundary currents. It therefore follows that the rings in the zone of the main Black Sea current must have properties similar to the properties of the Gulf Stream rings.

It is well known [4] that one of the principal properties of the rings is an asymmetry of the formation relative to the flow axis: along one side of the current there is formation of only anticyclonic rings, whereas along the other side only cyclonic rings are formed. Still another important property of the rings is that the waters within these rings have an origin which differs from the waters surrounding them. Accordingly, on the basis of data from hydrological surveys they can be discriminated on the basis of the difference in temperature and salinity of their internal parts and the surrounding water. In addition, in the vertical hydrological structure of the rings there is a substantial increase or decrease (depending on the vorticity sign) in the vertical thickness of the intermediate layers in comparison with the surrounding waters (for example, the presence of a vertically thick interlayer of "18°" water in the anticyclonic rings of the Gulf Stream).

We will attempt to trace whether the noted properties are observed in the horizontal and vertical structure of ring formations in the Black Sea. Figure 2 shows the salinity fields at the 100-m horizon along the shores of Anatolia (Fig. 2a) and in the southeastern part of the sea (Fig. 2b). Along the coast of Anatolia in July of 1976 it was easy to trace two meanders, one of which is in a stage of detachment from the main Black Sea current and in actuality constitutes an anticyclonic eddy in which the salinity is 0.70-1.00°/oo less than the salinity of the surrounding waters. In the southeastern part of the sea (Fig. 2b) there are two cyclonic eddies detached from the main Black Sea current, whose axis corresponds to 20°/oo. The eddies are characterized by increased salinity values, which at their centers differ from the salinity of the surrounding waters by 0.5-0.9°/oo.

The ring along the Anatolian coast has an ellipsoidal configuration; the degree of elongation of the eddy (the ratio of its greater axis (92 km) to its lesser axis (52 km)) is 1.80. This ring, as was indicated in [1], is traced on the basis of hydrological characteristics to the horizons 400-500 m.

The rings in the southeastern part of the sea have an almost regular circular configuration with mean radii for the first ring of 28 km and for the second -- 30 km; the degrees of elongation are 1.15 and 1.18 respectively. Vertically the rings are elongated to a considerably lesser degree than along the Anatolian coast and are traced in the upper layer to a depth of 200 m.

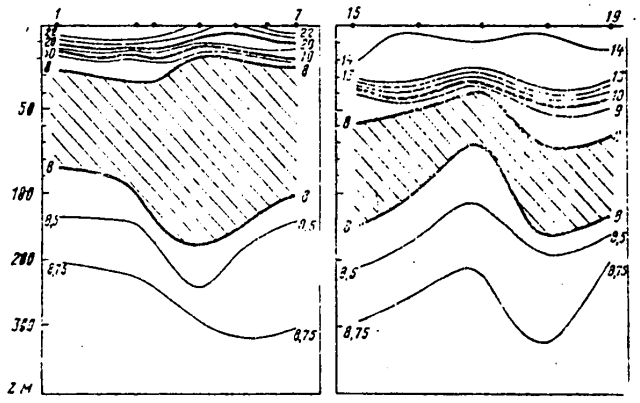

Fig. 3. Vertical temperature sections. a) along lesser axis of anticyclonic eddy along coast of Anatolia; b) through cyclonic eddy in southeastern part of sea. The position of the sections is shown in Fig. 2. The cold intermediate layer is represented by shading.

The anticyclonic ring along the coast of Anatolia was formed to the left of the main Black Sea current (looking along the current), whereas the cyclonic rings in the southeastern part of the sea were formed on the right side of the current. In addition, the anticyclonic ring was formed from less saline waters of the coastal zone, whereas the cyclonic rings were formed from the more saline waters of the abyssal regions of the sea, that is, apparently there is an analogy with oceanic frontal eddies-rings. This is also confirmed by the characteristics of the vertical hydrological structure. It is well known that a distinguishing characteristic of the distribution of the cold intermediate layer (CIL) over the surface of the Black Sea is a decrease in its thickness in the abyssal regions and an increase in the thickness of the CIL in the coastal regions. Accordingly, in the anticyclonic ring formed from the coastal waters there should be an increase in the thickness of the CIL, whereas in the cyclonic rings this thickness should decrease. Figure 3 shows the vertical temperature sections for an anticyclonic ring (Fig. 3a) and a cyclonic ring (Fig. 3b); it is shown that there is a corresponding increase and decrease in the thickness of the CIL in comparison with its thickness in the surrounding waters. In addition, the noted characteristics of propagation of cold intermediate waters in the observed eddy formations are evidence of intensive vertical movements in ring zones*. Thus, on the basis of the correspondence between the characteristics of the rings discovered in the Black Sea and the main properties of the rings in the Gulf Stream it can be concluded that the formation of rings of the mentioned spatial scales (about 60-90 km) occurs as a result of frontal instability of the main Black Sea current, having a jetlike character.

---

* The possibility of the existence of such movements in the southeastern part of the sea was for the first time noted by A. D. Dobrovol'skiy in [3].

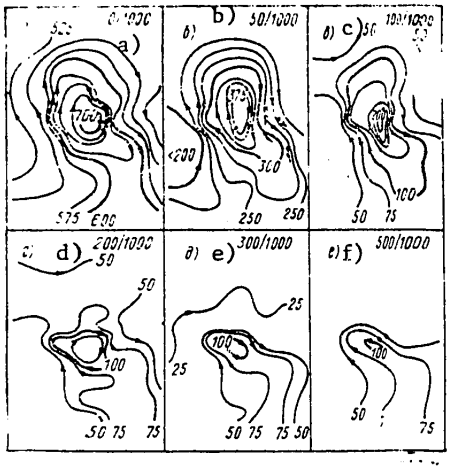

Fig. 4. Relative dynamic topography in zone of anticyclonic ring for different surfaces. a) sea surface; b) 50-decibar surface; c) 100 db; d) 200 db; e) 300 db; f) 500 db. The zero surface is 1000 db. The arrows indicate the mean vectors of current velocities measured at automatic buoy stations.

In many studies devoted to investigation of rings in the Gulf Stream and other boundary currents it has been demonstrated that the field of currents in the eddies is in a quasigeostrophic regime. In order to check this point for the rings of the main Black Sea current we carried out dynamic processing of data for the used synchronous surveys and then made a comparison of the dynamic maps with the results of instrumental observations of currents carried out at this same time in this same region. As the zero reference surface the 1000-db surface was selected. Figure 4 shows maps of the relative dynamic topography for different surfaces in the region of ring propagation along the coast of Anatolia, from which it can be seen that the anticyclonic ring discriminated earlier on the basis of the distribution of salinity and temperature is very clearly traced in the field of geostrophic currents and is most clearly expressed at the 50 and 100 db surfaces; at the sea surface the ring is traced somewhat less clearly (it occupies a lesser area), evidently due to the distorting influence of the intensive seasonal thermocline, whose formation in the zone of the main Black Sea current leads to a decrease in the differences in dynamic heights at the sea surface in summer. The area occupied by the ring and the differentials in dynamic heights at the 200-db surface are considerably less than at 0, 50 and 100 db, whereas at the 300 and 500 db surfaces there is only one closed dynamic contour line, outlining a still lesser area than at the 200-db surface. All this is evidence that vertically the anticyclonic ring has a conical configuration.

Estimates of geostrophic velocities were made for sections along the longer and shorter axes of the ring. These revealed that the velocities on the periphery for the shorter axis at the surface attained 60 cm/sec, and at the 50-m horizon even 65 cm/sec; the mean weighted velocity in this section of the upper 200-m layer was 50 cm/sec, whereas on the greater axis of the eddy it was less (20 cm/sec).

A comparison of the velocities of the geostrophic currents with the parameters of currents averaged for the entire time of observations at the automatic buoy stations in the eddy zone indicated their good correspondence with respect to both absolute value and direction of the velocity vector at the horizons 25, 50, 75 and 100 m (Fig. 4). This is evidence of quasigeostrophicity of the field of currents in the anticyclonic ring. Similar dynamic computations were made using survey data for the southeastern part of the sea. These computations indicated the presence of cyclonic rings at the surface and in the water layer to the 200-db surface, but the intensity of the geostrophic circulation attenuated considerably in comparison with the anticyclonic ring. The maximum velocities of the geostrophic currents on the periphery of the rings are 23 cm/sec.

It is of great interest to estimate the kinetic energy (KE) and available potential energy (APE) of the rings and also the relationship between them because such estimates can tell about the stage in development of the rings and then also about their lifetime, without drawing upon data from long-term observations of the hydrological structure of such eddy formations.

The kinetic energy of the rings was estimated without taking into account the kinetic energy of the transfer movement, that is, only the KE of rotational motion was computed:

$$\mathrm{KE} = \frac{1}{2}\int_{(V)} \rho V^2\, dV \approx \frac{1}{2}\sum_{j=1}^{N}\left(\sum_{i=1}^{M}\left[\frac{\Delta m_i}{2}(R_i^2 + R_{i-1}^2)\right]\omega_i^2\right)\Delta z_j, \tag{1}$$

where i is the number of ring "circles" included in the computations, j is the number of layers vertically, Δz_j is the thickness of the layer in dimensionless units, Δm_i is the mass of a ring circle of a unit thickness, R_i and R_{i-1} are the external and internal radii of the ring circle, ω_i^2 is the mean (angular) velocity of rotation of the ring circle i.

The available potential energy was computed using the formula

$$\mathrm{APE} = \frac{1}{\rho_0 g}\int_{(S)}\left(\int_{p_0}^{0} p\,(\delta\rho)\, dp\right) dS \approx \frac{1}{\rho_0 g}\sum_{i=1}^{M}\left[\sum_{j=1}^{N} p_j\,(\delta\rho)_j\,\Delta p_j\right]\Delta S_i, \tag{2}$$

where i and j are the same as for (1), Δp_j is the thickness of the layers in pressure units, ΔS_i is the area of the ring circle, $(\delta\rho)_j$ is the mean density anomaly for a ring circle and p_j is pressure at the j horizon; g is the acceleration of free falling, ρ_0 is the mean density of sea water.

In the computations it was assumed that M = 3, N = 11 for an anticyclonic ring and M = 2 and N = 8 for cyclonic rings, that is, the entire volume occupied by rings was broken down into three circles "imbedded" in one another and 11 vertical layers for an anticyclonic ring; and for cyclonic rings -- 2 circles and 8 layers.

The mean density anomalies $(\delta\rho)_j$ for the circle were obtained by averaging the density anomalies at hydrological stations falling in the area of the corresponding circle. The density anomalies for an anticyclonic ring were computed as deviations from the undisturbed density field in the abyssal part of the Black Sea, and for a cyclonic ring -- from the undisturbed density field in the coastal regions of the southeastern part of the sea.

Table 1 gives computed data for APE and KE in several layers for an anticyclonic ring along the Anatolian coast and one cyclonic ring in the southeastern part of the sea.

The table shows that more than 85% of the total mechanical energy of an anticyclonic ring can be assigned to APE and the ratio of KE to APE is 0.13, that is, APE exceeds KE by approximately an order of magnitude. More than 90% of the APE is contained in the main pycnocline (between the contour lines 75 and 150 meters), whereas 59% of the KE is concentrated in the 100-m layer. In the upper 200-m layer there is concentration of more than 90% of the KE in the ring. Such a relationship of APE and KE and their vertical distribution are in good agreement with similar estimates made for Gulf Stream rings [6, 7]. However, with respect to absolute values the estimates obtained differ from those cited in [6, 7] by two orders of magnitude: APE values of about 10^{24} erg were obtained for Gulf Stream rings. This is an indication that less intensive rings are formed in the Black Sea during meandering of the main flow.

Table 1

Distribution of Available Potential Energy (APE, 10^{20} erg) and Kinetic Energy KE, 10^{20} erg) With Depth in Anticyclonic and Cyclonic Rings

Thickness of layer, m	KE	APE	Thickness of layer, m	KE	APE
Anticyclonic ring			Cyclonic ring		
0-100	7.50	27.9	0-50	1.16	1.53
100-200	4.32	56.7	50-100	0.73	2.68
200-300	0.68	6.3	100-150	0.29	0.82
300-400	0.12	2.2	150-200	0.18	0.35
400-500	0.07	0.9	200-300	0.05	0.10
Total energy	12.69	94.0		2.41	5.48

For cyclonic rings in the southeastern part of the Black Sea, which had lesser dimensions and vertical thickness, an estimate of total mechanical energy was obtained (10^{20} erg). For the ring situated closer to the zore of the main Black Sea flow the relationship between KE and APE is 0.44. The APE accounts for 70% of the entire energy in this ring and in the second cyclonic ring, more distant from the main Black Sea current, APE already accounts for 55% of the entire energy of the ring; more than 50% of the KE is concentrated in the upper 50-m layer.

Since the anticyclonic ring along the Anatolian coast was in a stage of detachment from the main Black Sea current, it can be considered a young dynamic formation. It is characterized by a low value of the KE-APE ratio -- 0.13. The rings in the southeastern part are completely separated from the main Black Sea current eddies. The ring formation conditions in this region are such that the region of propagation of the rings is limited on one side by the main Black Sea current, and on the other by the shoreline. This gives basis for assuming that the ring situated at a greater distance from the zone of the main Black Sea current was formed earlier than the ring situated closer to the main Black Sea current. The ratio of KE to APE for the

less old ring was 0.44 and for the older ring was 0.81.

A comparison of these estimates of KE and APE and their relationships makes it possible to propose the following mechanism of redistribution of energy during the evolution of the rings: in the process of meandering of the jet streams and ring formation a definite reserve of both KE and APE is created in the rings. The initial vertical distribution of KE and APE is similar to that obtained for an anticyclonic ring along the Anatolian coast. In the course of evolution of the rings the KE dissipates due to friction (and possibly due to the excitation of internal wave processes [2]), but the reserves of APE are constantly replenished, the ratio of KE to APE constantly increases and the KE is concentrated in a surface layer which is increasingly thin vertically. In the absence of additional sources of energy of meteorological or topogenic character the rings, expending the entire reserve of APE, degenerate. To be sure, the cited scheme for energy redistribution during the evolution of rings is a qualitative picture and requires further confirmation by experimental data and theoretical computations.

Thus, as a result of detailed processing and analysis of the materials from two surveys it was possible to confirm the hypothesis expressed earlier [1] that in the Black Sea there can be a process of ring formation as a result of frontal instability of the main Black Sea current, having a jet character. It was noted that in the vertical structure of the rings and the distribution of kinetic energy and available potential energy in them in the Black Sea there is much in common with the Gulf Stream rings and rings in other boundary currents. However, in the Black Sea the rings are expressed less intensively.

In conclusion the author expresses appreciation to A. D. Dobrovol'skiy, A. N. Kosarev and Yu. A. Ivanov for comments and advice given in discussion of the work.

BIBLIOGRAPHY

1. Blatov, A. S. and Ivanov, V. A., "Ring Formation in the Black Sea," KOMPLEKSNYYE ISSLEDOVANIYA CHERNOGO MORYA (Multisided Investigations in the Black Sea), Sevastopol', 1979.

2. Vlatov, A. S. and Ivanov, V. A., "Problem of the Mesoscale Variability of Oceanological Characteristics in the Black Sea," KOMPLEKSNYYE ISSLEDOVANIYA CHERNOGO MORYA, Sevastopol', 1979.

3. Dobrovol'skiy, A. D., "Dynamic Map of the Eastern Part of the Black Sea," IZV. GIDROMET. INSTITUTA CHERNOGO I AZOVSKOGO MOREY (News of the Hydrometeorological Institute of the Black Sea and Sea of Azov), No 1, 1933.

4. OKEANOLOGIYA. FIZIKA OKEANA. GIDROFIZIKA OKEANA (Oceanology. Ocean Physics. Ocean Hydrophysics), Vol 1, Moscow, Nauka, 1978.

5. Filippov, D. M., TSIRKULYATSIYA I STRUKTURA VOD CHERNOGO MORYA (Circulation and Structure of Black Sea Waters), Moscow, Nauka, 1968.

6. Barrett, J. R., "Available Potential Energy of Gulf Stream Rings," DEEP-SEA RES., Vol 18, No 12, 1971.

7. Richardson, P., "Gulf Stream Rings," OCEANUS, Vol 19, No 3, 1976.

UDC 556.(556.2+072)(474.2)

NUMERICAL MODELING OF WIND-DRIVEN CURRENTS IN LAKES

Moscow METEOROLOGIYA I GIDROLOGIYA in Russian No 7, Jul 81 (manuscript received 28 Oct 80) pp 94-101

[Article by A. G. Bogachev, G. B. Volkova, V. I. Kvon, candidate of physical and mathematical sciences, and T. N. Filatova, candidate of geographical sciences, Tiyrikoya Lake Station, Estonian Administration of Hydrometeorology and Environmental Monitoring, Institute of Hydrodynamics, Siberian Department, USSR Academy of Sciences, and State Hydrological Institute]

[Abstract] Soviet and foreign authors have now developed a number of mathematical models to be used in computations of wind currents in seas and internal water bodies. However, not one of these models has been evaluated using sufficiently reliable in situ data. This article describes a new mathematical model and gives the results of its use for computations of wind-driven currents in Chudskoye Lake. This water body was selected because unique experimental data on currents were available which have been generalized in the form of maps of currents characterizing a steady or near-steady process of transport of waters with winds of different directions. The modeling problem was solved numerically by the implicit difference schemes method. The model examined here was used in computing the vector fields of currents at different horizons and also computing elementary discharges of Chudskoye Lake. Particular attention was given to investigation of the spatial restructuring of the vector field with an increase in depth since the intermediate horizons are poorly supplied with in situ measurement data. A study was also made of stability of the vector fields of currents as a function of wind velocity, discharge of the Narva River and the Coriolis parameter. A comparison of computations made using this model and computations made using other models revealed that the model defined in this article gives superior results. In particular, there is more precise allowance for the coefficient of turbulent viscosity. The model is recommended for computations of wind-driven currents in other internal water bodies. Figures 2, tables 1; references 16: 15 Russian, 1 Western.

UDC 551.(54+55)(-062.4)

STRUCTURE OF ATMOSPHERIC PRESSURE AND WIND NEAR THE EQUATOR IN THE CENTRAL PART OF THE PACIFIC OCEAN

Moscow METEOROLOGIYA I GIDROLOGIYA in Russian No 7, Jul 81 (manuscript received 19 Sep 80) pp 102-105

[Article by N. A. Romanova, L. V. Kool' and Yu. A. Romanov, Institute of Oceanology]

[Abstract] During February-March 1980, on the 24th voyage of the scientific research ship "Dmitriy Mendeleyev," specialists carried out hydrological investigations in the central part of the Pacific Ocean, in an equatorial polygon bounded on the east and west by 163 and 167°W and 2° latitude on both sides of the equator. While working in the polygon the ship repeatedly crossed the equator. During the period 4-24 March hourly meteorological observations were made (total number of observations 504). These observational data were used in clarifying the real permanent features of the pressure and wind fields near the equator. It was found that at the equator the frequency of recurrence of the southerly, northerly and zero values of the meridional component was almost identical. To the north of the equator it was the southerly component which predominated, whereas to the south it was the northerly component. At a greater distance from the equator the v distribution was not so symmetric: in the northern hemisphere winds with northerly and southerly components were almost identical with respect to frequency of recurrence; in the southern hemisphere there is a predominance of winds with a northerly component. The frequency of recurrence of strictly easterly winds decreases with increasing distance from the equator to the north and south. Despite a minimum of atmospheric pressure at the equator, there is a divergence of air flows, not a convergence. The deviation of the easterly flow to the south in the northern hemisphere and to the north in the southern hemisphere near the equator is evidence of manifestation of Coriolis force. The asymmetry of deflection of the vectors on both sides of the equator is apparently evidence of the superposing of the macroscale circulation of both hemispheres on the easterly flow directed along the equator. The wind distribution near the equator determined from observations on this voyage agrees with the mean long-term wind field for March described by K. Wyrtki and G. Meyers (Hawaii Institute of Geophysics, 1975). Figures 2, tables 3; references 3: 2 Russian, 1 Western.

UDC 551.576.11:546.11

ROLE OF HYDROGEN PEROXIDE (H_2O_2) IN THE FORMATION OF MESOSPHERIC CLOUDS

Moscow METEOROLOGIYA I GIDROLOGIYA in Russian No 7, Jul 81 (manuscript received 1 Feb 80) pp 105-107

[Article by A. F. Kashtanov and B. M. Novikov, candidate of physical and mathematical sciences]

[Abstract] The role of atmospheric components other than water vapor in the formation of mesospheric clouds has been inadequately studied. Hydrogen peroxide (H_2O_2) warrants attention in this connection. Until now its role in mesospheric processes has been neglected because it is a relatively unstable compound and its atmospheric content has not been precisely known. However, studies show that H_2O_2 in its physicochemical properties is more active in the condensation process than water vapor. Computations show that the quantity of H_2O molecules for d = 0.3μm is $4.72 \cdot 10^8$ cm^{-3}, which is ensured with a corresponding supersaturation in the mesopause region. In the mesosphere there are regions where the H_2O_2 concentration is 10^7-10^8 cm^{-3}. This is adequate for the formation of mesospheric clouds with a mean diameter of the particles 0.1μm and a concentration 1 cm^{-3}. An appropriate supersaturation is ensured with a temperature less than 140°K. It is clear that hydrogen peroxide can play the role of primary condensation nuclei on which water droplets and ice crystals, constituting a mesospheric cloud, are subsequently formed. However, the lack of direct measurements of hydrogen peroxide concentration in the stratosphere and mesosphere make it possible to consider the conclusions drawn in this article to be only one of the possible mechanisms explaining condensation processes in the mesosphere. Figures 1, tables 2; references 10: 8 Russian, 2 Western.

UDC 551.5:633.16

INFLUENCE OF METEOROLOGICAL FACTORS ON THE YIELD OF SPRING WHEAT

Moscow METEOROLOGIYA I GIDROLOGIYA in Russian No 7, Jul 81 (manuscript received 13 Oct 80) pp 107-110

[Article by V. N. Garmashov, doctor of agricultural sciences, and A. N. Selivanov, candidate of biological sciences, All-Union Selection-Genetic Institute]

[Text]

Abstract: On the basis of many years of experiments it is demonstrated that for the formation of a high yield of spring barley the factors of the greatest importance are not autumn-winter precipitation and the reserves of productive moisture in the meter soil layer by the onset of the sowing period, but spring-summer precipitation, and most importantly, the precipitation falling during the tillering-leaf tube formation period, which occurs most frequently in May. At this time there are adequately good moisture reserves in the half-meter and especially in the cultivated soil layer where a considerable part of the spring barley root system is situated.

The cultivation of spring barley in the southern part of the Ukraine involves the negative influence of moisture shortage and increased temperatures. However, as noted by A. Shishkin [10], the reason for drought in the steppe zone must not be sought in the paucity of the total quantity of precipitation in the course of the year, but in its nonuniform distribution. According to the data of I. E. Buchinskiy [3], over a period of 97 years (1872-1968) in Odesskaya Oblast there were 41 years with a dry spring. Accordingly, it is assumed [2, 4, 6, 9] that under these conditions a guarantee of the yield of spring grains will be the moisture accumulated during the autumn-winter period.

However, other researchers [1, 5, 8] have come to the conclusion that the yield of spring barley to a considerable degree is dependent on the weather characteristics of the growing season.

In this connection it seems of interest to clarify how the moisture supply and temperature exert an influence on formation of the yield of spring barley under the conditions prevailing in the southern part of the Ukraine. Comparing the data on the yield of the varieties Chernomorets and Nutans 244 obtained in experiments

with the quantity of autumn-winter precipitation and the moisture reserves in the meter soil layer by the onset of the barley sowing period, we concluded that these indices cannot serve as a reliable measure determining the yield level (Table 1). More than 300 mm of precipitation fell during August-March in 1973, 1977 and 1978, but the yield was different -- from 12.5 to 42.5 centners/hectare; however, in 1974 only half as much precipitation fell (153 mm) but the yield was the highest in these years -- up to 49.0 centners/hectare.

A similar picture is also obtained when comparing the yield with the moisture reserves in the soil at the beginning of the barley sowing season. A high grain yield was obtained with both low moisture reserves (1974, 1976) and when there were high moisture reserves (1973, 1978), whereas the minimum yield in 1977 was with spring moisture reserves close to the best during this period. For the Chernomorets variety the correlation coefficient between these values was -0.30 and for the Nutans 244 variety it was -0.37.

The precipitation total during the growing season also did not constitute values determining the yield because the minimum yield corresponded to the maximum precipitation sum (1977). However, an analysis indicated that the greatest influence on the yield was from rains falling in May, as is indicated by the correlation coefficient, which for the Chernomorets variety was 0.84 and for the Nutans 244 variety was 0.91. In other months the correlation was not significant.

The high dependence of the yield of spring barley on May rains is attributable to the fact that in this month there is tillering, formation and growth of crown roots, on whose development is subsequently dependent the level of support of the above-ground mass with water and nutrients, as well as a differentiation of the apical cone into spikelets, which subsequently determine the size of the ear and its productivity. During this period it is not only moisture supply conditions which are of importance, but also the temperature factor. Precisely in May the higher air temperature has a negative effect on the future yield, whereas at the beginning of the growing season its positive influence is noted. The correlation coefficient is equal to -0.54 and 0.52 respectively (Nutans 244 variety).

It is well known that the prevailing weather conditions to a considerable degree can change the dates of onset of individual phases in growth and development and in the last analysis the length of the growing season for spring barley. It was therefore of interest to ascertain how changes in the levels of the studied factors exert an influence on the final result -- the grain yield -- not by calendar periods (months), but in individual corresponding segments of the growing season. For this purpose we made computations of the correlation between yield and the quantity of precipitation and the mean daily air temperature by interphase periods and obtained the following results (Table 2).

Between sowing and the tillering phase the increase in air temperature exerted a positive influence on the growth and development of barley plants, which was reflected thereafter in the yield. However, during the period when there was intensive tillering and formation of the secondary root system the lower temperatures were better, as is indicated by the negative correlation coefficient. The reduced temperatures during this period, when the apical cone is in the third-fourth stages of organogenesis, favor the formation of a great number of spikelets in the ear [7]. Later a negative correlation is also maintained between

Table 1

Role of Moisture Supply of Different Periods in Formation of Spring Barley Yield

Year	Sum of autumn-winter precipitation, mm	Reserves of productive moisture in meter soil layer by onset of sowing, mm	Sum of spring-summer precipitation, mm	Spring-summer precipitation by months, mm				Yield, Centners/hectare	
				April	May	June	July	Chernomorets	Nutans 244
1973	394	157	191	39	52	38	62	40.0	42.9
1974	153	118	235	33	52	37	113	40.9	49.0
1975	208	141	149	30	18	41	60	29.5	26.8
1976	239	118	212	23	52	57	80	41.9	44.5
1977	358	144	319	149	18	66	86	12.5	16.3
1978	312	154	209	60	57	48	44	36.1	39.6

yield and air temperature, but its closeness is reduced.

Table 2

Correlation Coefficient (r) Between Yield and Meteorological Factors by Growing Seasons (During 1973-1978). Chernomorets Variety

Sowing-sprouting	Sprouting-tillering	Tillering-leaf tube formation	Leaf tube formation-earing	Earing-total maturity
		Yield and mean daily air temperature		
0.27	0.63	-0.74	-0.45	-0.17
		Yield and quantity of precipitation		
0.02	0.39	0.68	0.49	-0.05

Table 3

Development of Tillering Sprouts and Crown Roots in Dependence on Weather

Indices	In "dry" years		In "moist" years	
	Chernomorets	Nutans 244	Chernomorets	Nutans 244
Bushiness	1.6	1.8	2.4	2.9
Number of nodes, roots	2.2	2.6	4.8	5.1
		Total maturity phase		
Productive bushiness	1.2	1.3	2.1	2.7
Number of grains in ear	17.5	18.5	17.2	18.2

There is also a small correlation between precipitation and the yield, as with air temperature, during the interphase tillering-stem growth stage, but in this case it is positive. It follows from this that the period from the onset of tillering to the onset of leaf tube formation is the most important in the fate of the future yield of spring barley. An adequate quantity of precipitation in the case of a low air temperature lays the basis for a high productivity of plants, which later can be realized in a high yield, and vice versa, unfavorable conditions lead to a decrease in high productivity factors (Table 3).

The cited data indicate not only a considerable decrease in the tillering coefficient and the number of nodal roots in barley plants in unfavorable years, but also a decrease in their relationship. In a dry year for each tillering sprout there are fewer roots than in the moist years. This leads to a worse supply of the sprouts with water and nutrients, as a result of which a considerable percentage of them die out. And since the yield is closely related to productive bushiness (correlation coefficient 0.84-0.91 in dependence on variety), it becomes possible to understand the main reason for reduction in barley yield

in years when there is hot and dry weather in the tillering phase.

The size of the ear and its productivity, it was found, cannot serve as a reliable indicator of the yield level because these quantities are influenced, on the one hand, by weather conditions, and on the other hand by the tillering stage. In the case of great tillering there are fewer ears formed than when there is slight tillering. In addition, soil fertility and the variety of barley are of importance. With the application of fertilizers the ears increase in size even in the case of strong tillering. Among the biological peculiarities of the variety the factor exerting the greatest influence on ear size is the sprout-forming capacity. For example, in our experiments with Nutans 244 the number of grains in the ear was less for the plants which thickened out well than for the Chernomorets variety.

The determination of the relationship between yield and moisture content of different soil layers during the growing season indicated that the closest correlation was observed in the interphase period tillering-leaf tube formation with layers 0-10 and 0-20 cm ($r = 0.69$ and 0.60 respectively). A less close correlation was observed for the half-meter layer and especially with the content of productive moisture in the meter layer. This can serve as an indirect indication of the shallow positioning of the main mass of roots for spring barley.

Thus, our investigations indicated that the most important factors in the formation of a high yield of spring barley are not autumn-winter precipitation and the reserves of productive moisture by the beginning of the sowing period in the meter soil layer, but instead, the spring-summer precipitation and especially the precipitation falling during the tillering-leaf tube formation period, as occurs most commonly in May. Good moisture reserves in the half-meter layer and especially in the cultivated layer, where a considerable part of the root system of spring barley is situated, are adequate for these purposes.

BIBLIOGRAPHY

1. Alpat'yev, A. M., "Rational Use of Precipitation -- the Basis for Overcoming Droughts," AGROKLIMATICHESKIYE USLOVIYA STEPI UKRAINSKOY SSR I PUTI IKH ULUSHENIYA (Agroclimatic Conditions of the Steppe in the Ukrainian SSR and Ways to Improve Them), Kiev, Izd-vo AN UkSSR, 1950.

2. Borisonik, Z. B., YACHMEN' YAROVOY (Spring Barley), Moscow, Kolos, 1974.

3. Buchinskiy, I. Ye., ZASUKHI, SUKHOVEI, PYL'NYYE BURI NA UKRAINE I BOR'BA S NIMI (Droughts, Drying Winds, Dust Storms in the Ukraine and Contending With Them), Kiev, Urozhay, 1970.

4. Verbin, A. A., ZASUKHA I BOR'BA S NEY V STEPI UKRAINY (Drought and Contending With It in the Ukrainian Steppe), Odessa, Odesskoye Obl. Izd-vo, 1948.

5. Kudinov, M., "Influence of the Density of Sowing in Relation to Variety on the Yield of Spring Wheat and Barley," STEPOVIY DOSVIDNIK (Steppe Reporter), No 3, 1928.

6. Kulik, M. S., OSOBENNOSTI ZASUKH V STEPNYKH RAYONAKH UkSSR I UCHET KLIMATICHESKIKH FAKTOROV PRI RAZRABOTKE SISTEMY ZEMLEDELIYA (Characteristics of Droughts in the Steppe Regions of the UkSSR and Allowance for Climatic Factors in Developing an Agricultural System), Moscow, Izd-vo MSKh, 1958.

7. Mordvinova, M. N., "Influence of Cooling of a Root System on Formation of a Barley Ear," ISSLEDOVANIYE POCHVENNYKH, RASTITEL'NYKH I FAUNISTICHESKIKH RESURSOV YAKUTII (Investigation of the Soil, Plant and Faunistic Resources of Yakutia), Yakutsk, 1964.

8. Podgornyy, P., "Increasing Grain Yields," STEPOVIY DOSVIDNIK, No 3, 1928.

9. Rotmistrov, V. G., SUSHCHNOST' ZASUKHI PO DANNYM ODESSKOGO OPYTNOGO POLYA (The Essence of Drought According to Data of the Odessa Experimental Field), Odessa, 1911.

10. Shishkin, A., K VOPROSU OB UMEN'SHENII VREDNOGO DEYSTVIYA ZASUKH NA RASTITEL'NOST' (Problem of Reducing the Harmful Effect of Drought on Vegetation), St. Peterburg, 1876.

UDC 551.521.17

EXPERIMENTAL INVESTIGATIONS OF ULTRAVIOLET RADIATION IN THE LOWER ATMOSPHERE

Moscow METEOROLOGIYA I GIDROLOGIYA in Russian No 7, Jul 81 (manuscript received 4 Oct 80) pp 111-116

[Article by N. F. Yelanskiy and Yu. L. Truttse, candidates of physical and mathematical Sciences, and O. A. Matveyeva, Institute of Atmospheric Physics]

[Text]

Abstract: This article gives the results of measurements of the total fluxes of direct, scattered and total radiation in the spectral region 300-400 nm made from aboard an aircraft. The results agree satisfactorily with the results of numerical modeling.

Introduction. The numerical model of radiation transfer in the atmosphere presented in [4] includes such factors and dependences which cannot be rigorously described mathematically. But the introduction of simplifying assumptions and representations of different quantities in approximations with few parameters are inevitably reflected in the accuracy of the results of numerical computations. Their experimental checking is required. However, the making of observations in the spectral range 290-340 nm meets with a number of difficulties which are caused by an abrupt change in the intensity of the solar radiation reaching the earth's surface and the complexity of precise calibration of instruments in this spectral region. Accordingly, the number of such observations is rather limited. Nevertheless, the principal regularities in the geographical distribution of the total fluxes of UV radiation at the earth's surface during different seasons have been described and studied in [1, 4]. During recent years a number of measurements have also been made to ascertain the spectral composition of the fluxes of UV radiation in the ozone absorption region [7, 8]. These observations make it possible to refine individual details of the numerical model, but they are inadequate for its total certification. Additional information is needed on the vertical structure of the fluxes of UV radiation and their dependence on rapidly changing observation conditions. For this purpose in this article we give the results of measurements of the total fluxes of direct, scattered and total radiation in the spectral region 300-340 nm from an aircraft.

Instrumentation and Measurement Method

The measurements were made using specially fabricated UV photometers in which the radiation detectors are F-7 photocells. The maximum response of the F-7 corresponds to a wavelength of approximately 225 nm. With an increase in wavelength the detector response decreases and when $\lambda \simeq 320$ nm does not exceed 4% of the maximum value.

The F-7 phoelement is intended for the registry of the radiation arriving from a hemisphere. Its angular characteristic is close to cosinal. Since individual samples have their own particular characteristics, radiation detectors with a spectral response dropping off most steeply in the sector 290-340 nm were selected for installation in the instrument; for these detectors the angular characteristics come closest to a cosinal dependence (the discrepancies must not exceed 3-4% within a range of angles 75-80° from the normal).

The precise absolute calibration of the UV photometers is a complex problem. And although in the measurement of the vertical structure of the radiation fluxes and albedo of the reflecting surface an analysis is made of the relative changes in parameters, the relationship between model computations and experimental data expressed in absolute energy units must be known quite precisely for a proper interpretation. The calibration of instruments was accomplished by two methods: using an SI-8 standard lamp and on the basis of direct solar radiation. Recent measurements were made at the High-Mountain Scientific Station, Institute of Atmospheric Physics, USSR Academy of Sciences (near Kislovodsk, at an elevation of 2,070 m above sea level) over the course of several months before and between aircraft flights. At the same time measurements were made of the total ozone content and the aerosol attenuation of radiation was evaluated. A knowledge of these parameters made the calibration on the basis of solar radiation adequately correct.

The aircraft carried two photometers with coinciding spectral characteristics in the upper and lower parts of the fuselage. The lower photometer measured the radiation reflected from the underlying surface and scattered in the lower layer F_{refl}; the upper photometer measured the total radiation F_{tot} and direct F_{dir} radiation incident on the horizontal surface from above. For this purpose the sensor of the upper instrument is mounted in such a way that it can move relative to the entry aperture by a distance up to 1 m. In this case the instrument field of view is not greater than 8°. The angle within which the sun illuminates the entire cathode is from 4 to 6°, depending on the position of the sun relative to the time of the measurements.

The flux of scattered radiation was found from the difference $F_{tot} - F_{dir}$. The error in determining this parameter, as a result of excluding the contribution of radiation scattered at small angles, does not exceed 3-4%, and as a result of deviation of the angular dependence from cosinal is not more than 3% for zenith distances $\theta_0 \leqslant 60°$. The total error in determining the F_{scat}/F_{dir} ratio for these same θ_0 is about 10-15%.

The total measurements of radiation fluxes using photometers in the region 300-340 nm have one substantial shortcoming. With a change in ozone content the nature of the spectrum in this region changes. As a result, the effective wavelength of instrument response (Forbes effect) shifts. This usually makes very difficult the interpretation of data from measurements carried out under conditions differing greatly with respect to solar altitude, ozone content and optical characteristics of atmospheric aerosol. However, in investigations of the relative changes in UV radiation at different altitude levels in a particular place during the short time of aircraft descent θ_0 and X change insignificantly and the influence of the Forbes effect is small (Fig. 1). With a further decrease of its influence the comparison of experimental data was always made with those computed values which were obtained with the substitution of the true θ_0 and X values at each comparison point into the numerical model. It is only important that the optical

characteristics of both instruments be kept so during the flight time. The instrument parameters were monitored under terrestrial and flight conditions (change in position of the instruments) by comparison of their readings during a 24-hour period (different θ and X). As a rule, the selected photoelements retain their characteristics over a long period of time.

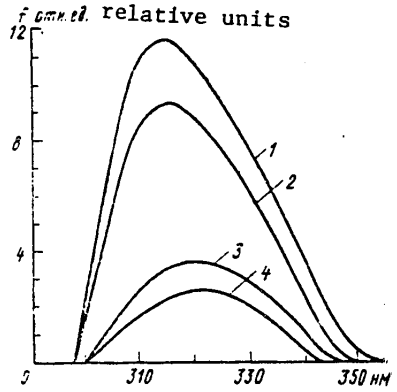

Fig. 1. Photometer transmission functions computed for solar zenith angle $\theta = 0^{\circ}$ and altitude levels z = 4 and 0 km (curves 1 and 2 respectively) for zenith angle $\theta = 60^{\circ}$ and z = 4 and 0 km (curves 3 and 4). Ozone content 0.200 cm; aerosol distribution M1.

Measurements of UV radiation in the thickness of the atmosphere were made under cloudless conditions during rapid linear descent (rarely ascent) of an Il-14 aircraft from an altitude of 5-5.5 km to the earth's surface or altitudes 100-200 m. Measurements of direct solar radiation were made each 250 or 500 m vertically. The radiation reflected from the underlying surface was measured at altitudes up to 100 m.

The flights were made in Central Asia and to a lesser extent over the European USSR. The observations were continued with interruptions from May 1978 through May 1980 and took in all seasons.

As has already been noted, for the proper interpretation of the observations of variability of UV radiation in the thickness of the atmosphere it is necessary to have data on ozone content. Accordingly, the aircraft carried two spectrophotometers for measuring total ozone content continuously during the entire flight, including in the descent segment. The measurement and computation method was described in [3]. Some differences are related only to improvement in the system for tracking the sun.

Analysis of Results

A total of about 90 vertical sections were obtained. The resulting profiles of the fluxes of UV radiation F were characterized by a great variability. The maximum F variations with equal θ_0 were caused by fluctuations of the aerosol component in the lower atmosphere, as is in agreement with the conclusions drawn from model investigations if it is taken into account that the λ_{eff} of the instrument falls in the range 317-322 nm with a change in θ_0 from 25 to 60°. During the flights there

were no direct measurements of the aerosol characteristics. Therefore, an analysis of the dependence of radiation fluxes in the region 300-400 nm on ozone content cannot be entirely correct and is not given in this study.

The vertical profiles of radiation fluxes, supplemented by data on ozone content, carry information on the processes of scattering of radiation in the thickness of the atmosphere containing aerosol and in comparison with the results of computations make it possible to evaluate the reliability and limits of effective use of the concepts of aerosol attenuation of radiation and reflection from the underlying surface serving as the basis of the numerical model in [4].

a) Total radiation. The vertical profiles of total radiation reflect that great diversity of observation conditions which were encountered in the process of implementing the work. In order in the comparison of these profiles with the computed values that individual characteristics be taken into account as completely as possible, a comparison of data was made for the individual levels 0, 1,..., 5 km with the corresponding values θ_0 and X. Such an operation made it possible to discriminate four groups of data corresponding to the following regions and observation times: Central Asia (May-September), European USSR (May-September) and these same regions during December-March. The ratios of the mean values of the relative increase in F_{tot} with a change in altitude by 1 km $(F_{i+1} - F_i/F_i)$ to the $(F_{i+1} - F_i/F_i)_{theor}$ values computed for mean global aerosol conditions for these groups are given in Table 1.

The greatest differences between the computed and measured increase in F_{tot} with altitude are observed in the warm season of the year in Central Asia; the minimum values are observed in winter over the European USSR. In general, however, the influence of aerosol is more important than that which it must be as a global mean. (Detailed tables of F_{tot} values at different levels in the lower atmosphere are given in [4]. The nature of the change in the F_{tot} parameter with altitude change for a special case is illustrated in Table 2). Even in winter over the European USSR aerosol attenuation predominates in the layer 0-2 km over the means for the earth.

During the warm period of the year the changes in F_{tot} with altitude to a considerable degree and everywhere differ from the computed value for a pure atmosphere up to a level 4 km. In Central Asia the nature of the altitudinal dependence of F_{tot} even on the average corresponds to a dust-filled atmosphere rather than a pure atmosphere. In individually considered situations (relating, as a rule, to the Samarkand region) the attenuation of radiation by aerosol is greater than follows from computations for a highly dust-filled atmosphere (M2), which was regarded as an extremal case. An example of such a situation is shown in Fig. 2. Above the level 4 km the change in F_{tot} with altitude virtually coincides with that computed for the pure atmosphere and these variations are small. This means that local factors exert no significant influence on the distribution of aerosol in the middle troposphere.

Thus, on the basis of a mean model of aerosol distribution M1 it is possible to compute the vertical structure of the fluxes of total radiation in the entire investigated thickness of the atmosphere during winter, and at other seasons of the year -- in the region above 3-4 km. Below this level during the summer in order to determine the vertical structure of UV radiation it is necessary to change the M1

distribution introduced into the computation program in accordance with Table 1, or, without changing the initial parameters, use the values present in it as correction coefficients.

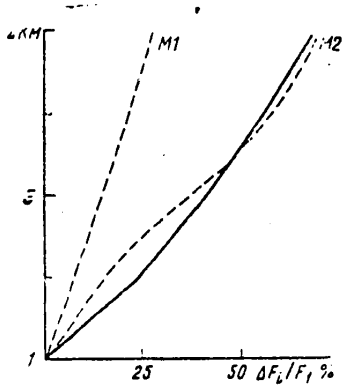

Fig. 2. Vertical change in F_{tot} in percent relative to the values at the level z = 1 km over Samarkand on 24 August 1979. Dashed curve -- computed $\Delta F_i/F_1$ profiles for pure and dust-filled atmosphere (θ_0 = 42°, X = 0.360 cm, A = 0.11.

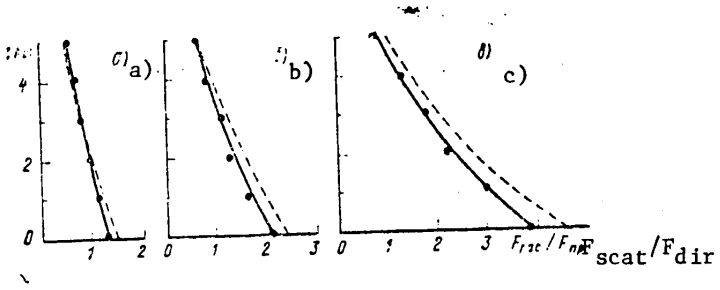

Fig. 3. Mean vertical profiles F_{scat}/F_{dir} by intervals of zenith angles 25-35° (a), 40-50° (b), 55-65° (c), obtained from observations. (Dashed curve -- vertical profiles computed for pure atmosphere and mean X and A values.

b) Direct and scattered radiation. During aircraft descent the direct radiation decreases and to a greater degree the greater the solar zenith angle and atmospheric turbidity. Since the latter factor varies in a wide range, a change in F_{scat} with altitude also experiences a strong scatter from one situation to the next. Taking into account that the experimental data are rather limited and that in the turbid atmosphere the errors in determining F_{dir} increase, it makes no sense no carry out a comparative analysis for F_{dir} similar to that which was

carried out for F_{tot}. From the point of view of comparison with model computations it is most convenient and indicative to examine the behavior of the F_{scat}/F_{dir} ratio with altitude.

Table 1

Mean Values of Ratios $(F_{i+1} - F_i/F_i)_{exp}:(F_{i+1} - F_i/F_i)_{theor\ M\ 1}$ for Total Radiation ($i = 0, 1, \ldots 4$)

Region and time of observation	Number of sections	Levels, km 0:1	1:2	2:3	3:4	4:5
Central Asia, May-September	41	1.5	1.8	1.6	1.2	1.05
European USSR. May-September	15	1.6	1.6	1.4	1.1	1.0
Central Asia, December-March	21	1.25	1.2	1.2	1.1	1.0
European USSR, December-March	12	1.1	1.1	1.0	0.95	0.95

Table 2

Increase in F_{tot} (%) With Ascent by 1 km in Pure (M1) and Dust-Filled (M2) Models of Atmosphere for θ_0 = 30 and 60° (Results of Computations, X = 0.320 cm, A = 0.1)

θ_0, degrees	Aerosol	Levels, km 0:1	1:2	2:3	3:4	4:5
30	M1	7.9	6.4	5.4	5.1	5.2
	M2	15.9	13.3	19.8	11.4	5.4
60	M1	11.2	10.1	9.2	7.6	7.8
	M2	19.0	18.0	27.8	20.2	7.7

Figure 3 shows the mean F_{scat}/F_{dir} profiles characterizing the peculiarities of the altitudinal dependence of the ratio under the conditions of a pure atmosphere. For this we selected such sections for which the change in the altitudinal dependence of total radiation approximately coincided with the dependence computed using the M1 model.

The profiles shown in the figure represent the results of observations of fluxes of UV radiation in Central Asia and the European USSR averaged by intervals of solar zenith angles 25-35, 40-50 and 55-65° over a snowless surface. Using the mean θ_0 values from these intervals and other parameters it was possible to construct

theoretical altitudinal dependences F_{scat}/F_{dir}. Both curves on each graph have virtually identical shapes -- F_{scat}/F_{dir} decrease monotonically with increasing distance from the earth's surface. The absence of appreciable stratification in the layer from 0 to 5 km is attributable primarily to the character of the choice of experimental data and their subsequent averaging in time and place.

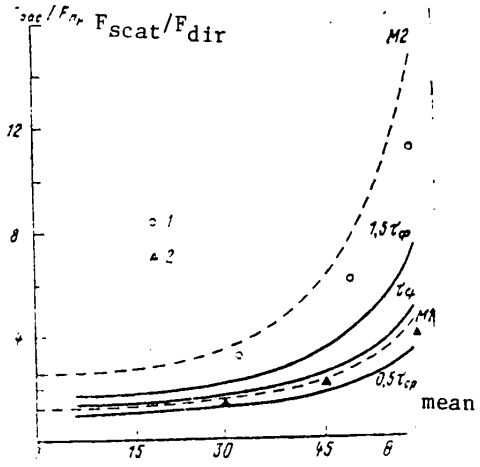

Fig. 4. Angular dependence of F_{scat}/F_{dir} at sea level for different aerosol conditions according to Shettle and Green model (see [9]) with allowance for photometer transmission function (τ_{mean} corresponds to mean aerosol attenuation) and on the basis of the model considered in this study (dashed curve). Separately plotted are the F_{scat}/F_{dir} values measured on 21 August 1979 at Samarkand (1) and the mean value of the ratio for three θ_0 intervals (2) (see Fig. 3).

At the same time the figure clearly reproduces the discrepancies between experimental and theoretical values F_{scat}/F_{dir}. These discrepancies have a regular characteristic: the measured values are always less than those obtained by computations (the only exception is the layer 3-5 km with small θ_0). The discrepancies increase with a decrease in altitude and an increase in θ_0. In order to explain this effect it is necessary to return to the measurement method. As already mentioned, in F_{dir} observations the photometer registers the radiation arriving from an angle greatly exceeding the angular dimensions of the sun, that is, the instrument registers $F_{dir}+F_{aur}$ (F_{aur} is the contribution from the aureole). Subtracting the flux of direct radiation from the flux of total radiation, for the scattered radiation we obtain a value not less than the computed value. The brighter the aureole, the greater the discrepancy must be between the experimental and theoretical F_{comp}/F_{dir} values. Qualitatively this is confirmed well by the curves in Fig. 3.

We will estimate the contribution of the aureole quantitatively at the level of the earth's surface from measurements. For $\theta_0 = 30°$ $F_{scat} - F_{aur}/F_{dir} + F_{aur} = 1.35$, $F_{scat}/F_{dir} = 1.5$. Hence it is easy to find that F_{aur} will be 6.4% of

the flux of direct radiation and 4.2% of the scattered radiation. For $\theta_0 = 45°$ 8.6 and 3.8% respectively, for $\theta_0 = 60°$ -- 14 and 3.1% respectively. Similarly it is possible to estimate the contribution of the aureole for other levels in the atmosphere.

The cited figures coincide well with those values of the errors in determining F_{scat} and F_{dir} which were obtained when carrying out calibration measurements. Accordingly, within the framework of instrumental and methodological errors it can be assumed that the model describes well the real F_{scat}/F_{dir} profiles for the atmosphere with aerosol characteristics close to the mean global values. In a turbid atmosphere it is considerably more difficult to discriminate definite patterns which could be compared with the results of numerical modeling. However, despite the great fluctuations in the experimental data, in general they do not exceed the limits which are the results of computations for a dust-filled atmosphere M2 (Fig. 4), although to a considerable degree they exceed the corresponding values obtained using other models of radiation transfer in an inhomogeneous atmosphere (corrections for these were made with allowance for instrument transmission).

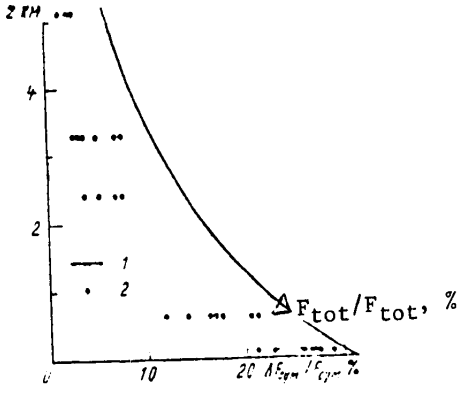

Fig. 5. Increase in F_{tot} (in %) at different levels in the atmosphere with transition from the underlying surface with an albedo of 0.1 to a surface with an albedo of 0.7. 1) computed dependence for pure atmosphere, 2) measurement data for 26-29 February 1979 with $\theta_0 = 45$-$55°$.

In general the limiting cases (pure and highly dust-filled atmosphere) considered in [4] actually take in the entire range of actually encountered situations. And the fact that the F_{scat}/F_{dir} experimental data agree with the computed data (with allowance for corrections for the aureole influence) additionally confirms the correctness of the model description of aerosol attenuation of radiation, that is, there is experimental confirmation of the conclusion which was drawn from a comparison of different published models.

c) Reflected radiation. As follows from computations, reflection from the underlying surface with a great albedo A should be reflected appreciably in the fluxes of total and scattered radiation in the spectral region 300-340 nm. Observations confirm this conclusion.

An aircraft was used in measuring the albedo of different types of underlying surfaces and study of the character of its change with aircraft ascent to considerable altitudes. An analysis of the dependence of albedo A on altitude indicated that the influence of the atmospheric layer situated below the aircraft becomes significant already beginning with an altitude of 100-150 m. On the other hand, measurements of A from altitudes less than 100 m are also infeasible due to the difficulties arising in identification of the nature of the underlying surface and those distortions which the entry of the aircraft shadow into the region of instrument sighting introduces. Accordingly, the flights were made at an altitude of 100 m. The errors in measuring albedo were from 1 to 3%, depending on turbidity of the air surface layer.

The principal results of measurements of the albedo parameter for solar zenith angles 30-40°, and with the presence of snow -- for angles 45-55°, are given below (in %):

Water surface (calm or with low waves)	2-4
Green plantings and rice paddies	2-4
Desert with sparse vegetation	3-5
Sand	4-7
Forest (snow on ground)	7-17
Snow-covered field	60-85
Dense cloud field	65-80

Flight altitude over the clouds was not constant but varied in the range 50-250 m, but the influence of the scattered radiation in this thin layer was substantially less than near the earth.

The albedo of the snowless surface adopted in the computations, equal to 0.1, somewhat exceeds the values cited above, but A = 0.7 for snow agrees well with the actual values.

It was possible to check the contribution of radiation reflected from the earth's surface to the flux F_{tot} at different levels only in the case of transition from a surface covered with snow to a snowless or snowy plain to a forested area. Under real conditions it was impossible to find adequately extensive uniform sharply delimited surfaces. Therefore, the effect of modification of reflected radiation on F_{scat} and F_{tot} is blurred and to a greater extent the greater the altitude. This is attributable to a lesser increase in F_{tot} in comparison with the computed values (Fig. 5) at all altitudes. However, near the earth's surface the jump F_{tot} with transition from a snow-covered plain to a forested area in most cases is 23-28% and is close to the computed value.

Summary

The mean characteristics of the vertical structure of fluxes of UV radiation in the lower atmosphere cited in this article coincide satisfactorily with the redults obtained using numerical modeling [4]. Such a coincidence leads to the

conclusion that the proposed model can be used effectively in practical work. However, in order for the results of the computations to characterize the specific situation reliably, it is necessary to know the aerosol characteristics, the albedo of the underlying surface and total ozone content. The latter two parameters can be determined rather simply and with good accuracy [5, 6]. With respect to aerosol attenuation, it can be evaluated using the same materials from ozonometric observations [2, 6], which are being carried out in the USSR in a broad network of stations. For most problems it is sufficient to know the mean values of all these parameters for certain conditions.

BIBLIOGRAPHY

1. Belinskiy, V. A., Garadzha, M. P., Mezhennaya, L. M. and Nezval', Ye. I., UL'TRAFIOLETOVAYA RADIATSIYA SOLNTSA I NEBA (Solar Ultraviolet Radiation and the Sky), Moscow, Izd-vo MGU, 1968.

2. Gushchin, G. P., OZON I AEROSINOPTICHESKIYE USLOVIYA V ATMOSFERE (Ozone and Aerosynoptic Conditions in the Atmosphere), Leningrad, Gidrometeoizdat, 1964.

3. Yelanskiy, N. F. and Truttse, Yu. L., "Some Characteristics of the Distribution of the Total Content of Ozone and Nitrogen Dioxide in the Atmosphere According to Observations From an Aircraft," IZV. AN SSSR: FIZIKA ATMOSFERY I OKEANA (News of the USSR Academy of Sciences: Physics of the Atmosphere and Ocean), Vol 15, No 1, 1979.

4. Yelanskiy, N. F., Truttse, Yu. L. and Ustinov, Ye. A., "Fluxes of UV Radiation in the Lower Atmosphere," Deposited at the All-Union Institute of Scientific and Technical Information, No 5168-80, deposited, 1980.

5. RADIATSIONNYYE KHARAKTERISTIKI ATMOSFERY I ZEMNOY POVERKHNOSTI (Radiation Characteristics of the Atmosphere and the Earth's Surface), edited by K. Ya. Kondrat'yev, Leningrad, Gidrometeoizdat, 1969.

6. Khrgian, A. Kh., FIZIKA ATMOSFERNOGO OZONA (Physics of Atmospheric Ozone), Leningrad, Gidrometeoizdat, 1973.

7. Chou, A. T. and Green, A. E. S., "Ratio Measurement of Diffuse to Direct Solar Irradiances in the Middle Ultraviolet," APPL. OPT., Vol 15, No 5, 1976.

8. Coulson, K. L., SOLAR AND TERRESTRIAL RADIATION, Acad. Pr., 1975.

9. Garrison, L. M., Murray, L. E., Doda, D. D. and Green, A. E. S., "Diffuse-Direct Ultraviolet Ratios With a Compact Double Monochromator," APPL. OPT., Vol 17, No 5, 1977.

METEOROLOGICAL WORK OF I. N. UL'YANOV (150TH ANNIVERSARY OF HIS BIRTH)

Moscow METEOROLOGIYA I GIDROLOGIYA in Russian No 7, Jul 81 (manuscript received 29 Apr 81) pp 117-118

[Article by V. V. Rakhmanov, doctor of geographical sciences, USSR Hydrometeorological Scientific Research Center]

[Abstract] July 1981 marked the 150th anniversary of the birth of Il'ya Nikolayevich Ul'yanov, remembered by the Soviet people as the father and first teacher of V. I. Lenin, founder of the Communist Party in the Soviet Union. However, meteorologists also recall that for more than eight years (from 1855 through 1863), while an instructor of mathematics and physics at the Penza Nobiliary Institute, he carried out regular meteorological observations. Il'ya Nikolayevich arrived in Penza in June 1855 and continued his meteorological tasks until his transfer to Nizhniy Novgorod in 1863. The scientific community at Penza regarded these observations as being highly important. The observational data which he collected were sent to the observatory at Kazan' University and to the Agricultural Society of Southeast Russia. His work was not confined to observations alone; during this period he wrote a paper on thunderstorms and lightning rods. It provides evidence that he was very familiar with investigations in the field of atmospheric physics both in his land and abroad. After departure from Penza I. N. Ul'yanov became an educational administrator who accomplished much beneficial work in Simbirskaya Province. Soviet meteorologists, however, will remember him for his early, pioneering, effective meteorological observations.

REVIEW OF COLLECTION OF ARTICLES ON ATMOSPHERIC PHYSICS AND CLIMATE

Moscow METEOROLOGIYA I GIDROLOGIYA in Russian No 7, Jul 81 pp 119-120

[Review by I. L. Karol', doctor of physical and mathematical sciences, and V. A. Frol'kis, of collection of articles "Fizika Atmosfery i Problema Klimata" [Atmospheric Physics and the Climate Problem], edited by G. S. Golitsyn, corresponding member USSR Academy of Sciences, and A. M. Yaglom, Nauka, Moscow, 1980]

[Text] The breadth and diversity of the problems now brought together in the theory of climate make it possible (and as will be demonstrated below -- useful) to make available collections of articles such as the one reviewed here. It includes nine large (more extensive than those appearing in journals) articles on extremely different branches of atmospheric physics which have been studied at the Institute of Atmospheric Physics USSR Academy of Sciences.

Three articles in the collection are devoted to "abstract" problems of a theoretical and sometimes an experimental character in laboratory models, investigations of simplified models of so-called hydrodynamic systems (HDS) (articles by F. V. Dolzhanskiy and L. A. Pleshanova and A. M. Obukhov, et al.) and a stochastic model (article by M. I. Fortus). The objective of such investigations is the important, and for practical purposes almost fundamental problem of prediction of changes in the climatic system and its unambiguous realization with one and the same ambient conditions. The HDS introduced by A. M. Obukhov and in some foreign investigations make it possible by relatively simple mathematical and graphic laboratory procedures to obtain and analyze the "changeover" phenomenon -- occurrences of different current regimes (in particular, in ellipsoidal regions) in an ideal fluid under identical ambient conditions.

These articles develop HDS investigations at the Institute of Atmospheric Physics and examine a model of convective currents (with few parameters) in a rotating fluid described by equations similar to the equations of motion of a heavy gyroscope with additional terms linear with respect to velocity and temperature (article by Dolzhanskiy and Pleshanova) and the phenomenon of a changeover between quasistationary regimes in HDS with the inclusion in the equation of the model of random noise, which has an analogy in processes of general circulation of the atmosphere.

In an article by M. I. Fortus, for some class of random processes with sharp and frequency-spaced spectral peaks with an increasing intensity for the lesser frequencies (such are the spectra of many climatic elements), the author has

determined the most precisely predictable characteristics (functionals) of random parameters and the corresponding mean square forecasting errors.

An article by A. S. Ginzburg and Ye. N. Feygel'son is devoted to the implementation of radiation computations. They formulated the fundamental principles which must be taken into account in formulating the radiation blocks of models of climate and general circulation. As a result of detailed analysis of radiation transfer processes, the authors give quite simple expressions making it possible to compute the fluxes in the ultraviolet, visible, solar infrared and thermal ranges, taking into account the scattering and absorption by water vapor, carbon dioxide, ozone and aerosol in the case of a rough vertical resolution and minimum information on the optical parameters of the atmosphere. Estimates are given for the integral albedo of the system and the integral transmission of the atmosphere in the solar and thermal ranges. An effective scheme is proposed for computing the fluxes of thermal radiation for a "piecewise-isothermic" cloudy atmosphere containing aerosol. Further means are given for simplifying the parameterizations used, these being different for weather forecasting models and models of climate and making it possible to include these parameterizations in models of different complexity.

A zonal climatic model of the atmosphere and surface layer of the ocean is presented in an article by V. K. Petukhov. He proposed simple and original parameterizations for the dependences of the longitudinally averaged meridional macroturbulent transfers of the moment of momentum, heat and moisture, as well as the vertical gradient of temperature and humidity on the field of mean zonal temperature of the atmosphere and also for heat transfer in the ocean.

The article gives two variants of the model. In the first the employed parameterizations are based on the use of empirical data and coefficients. In the second the parameterizations were obtained from simplified equations of dynamics and thermodynamics of the atmosphere and the introduction of the characteristic scales of macroturbulent transfer, which makes it possible to dispense with the use of empirical coefficients tied in to modern climate. In the article use is made of the first of these variants and it is shown that in principle there is a possibility of the development of an autooscillatory regime when using parameters close to those of modern climate.

M. B. Galin, in an article entitled "Investigation of General Circulation of the Atmosphere on the Basis a 12-Component Model," gives a two-level quasisolenoidal model for a hemisphere, making it possible to describe the joint effect of the barotropic and baroclinic mechanisms, the "inputs" and "outputs" of energy, such as radiation heating in conformity to Newton's law, and vertical turbulent friction. A solution is obtained which describes a stationary zonal circulation, which coincides with the solution obtained earlier in a similar 6-component model. A study was made of the reaction of the model to different values of the external excitation parameter. It is demonstrated that with its increase the zonal circulation undergoes transition into a solution of the travelling wave type with a constant amplitude, which also substantially transforms the temperature field, resulting in a decrease in the thermal gradient from the pole to the equator. In addition to a wave regime with a constant amplitude there are regimes with a periodically changing amplitude, which undergoes transition into more complex regimes with additional frequencies. With a sufficiently great value of the external

excitation parameter the system returns to a wave regime with a constant amplitude. An investigation of the interactions of waves with zonal flows and their evolution indicated that the energy cycle of these interactions is close to the cycle of energy transformations in the real atmosphere.

An article by V. P. Kukharts, L. R. Tsvang and A. M. Yaglom, entitled "Relationship of Turbulence Characteristics in the Surface and Boundary Layers of the Atmosphere," gives a review of the results of measurement of turbulence characteristics in the surface and atmospheric boundary layers. It is noted that the discrepancies among the numerous measurement results are attributable not only to the inaccuracy in methods and instrument errors, but also to the existence of some factors creating these differences which are not taken into account in similarity theory. In the surface layer such factors are the vertical variability of the turbulent flux of heat, the macroscale disturbances (of the ordered longitudinal eddies type) penetrating from above into the surface layer, and in the atmospheric boundary layer -- the radiational nonuniformity of the underlying surface. There is a discussion of the measurement method and the results of determination of the universal functions for the gradients of mean wind velocity and temperature, turbulent fluxes, thickness of the atmospheric boundary layer, rates of dissipation of turbulent energies and the structural characteristics of temperature fluctuations.

The tables in an article by A. S. Aliyev, A. S. Zubkovskiy and L. R. Tsvang give the results of measurements of the characteristics of turbulence in the near-water layer of the atmosphere in 107 series of experiments. On their basis it was possible to determine a number of universal functions in dependence on the stratification parameter. It is shown that the universal functions for the near-water layer coincide with the similar dependences for the surface layer within the limits of their scatters known from data in the literature.

An article by G. V. Rozenberg, et al., entitled "Optical Parameters of Atmospheric Aerosol," generalizes extensive data from his own investigations and the literature. The analysis and generalization enabled the authors to propose a physical model of aerosol in different layers of the atmosphere and provide a broad set of parameters of its optical characteristics in dependence on atmospheric humidity for tropospheric aerosol. Such a model makes it possible to compute the fluxes of radiation in the atmosphere under the operating conditions for optical systems. The extensive tables in the article provide valuable material for this.

Despite all the above-mentioned value of the articles in the collection, it is impossible not to note that there is some excessive diversity of subject matter. In the future, probably, it would be better to issue collections of articles of a lesser volume (and price) on individual significant aspects of the considered range of important problems.

SEVENTIETH-FIFTH BIRTHDAY OF IDA ARTUROVNA GOL'TSBERG

Moscow METEOROLOGIYA I GIDROLOGIYA in Russian No 7, Jul 81 p 121

[Article by the climatologists of the Main Geophysical Observatory]

[Abstract] April 1981 marked the 75th birthday and 50th anniversary of the scientific activity of the well-known Soviet climatologist Professor Ida Arturovna Gol'tsberg. All her activity has been closely associated with the meteorological support of practical needs, especially in agriculture. Between 1929 and 1942 she worked at the All-Union Institute of Plant Cultivation and from 1942 through 1979 at the Main Geophysical Observatory. At the latter for many years she headed the Agroclimatology Section, later transformed into the Microclimate Laboratory. I. A. Gol'tsberg made a considerable contribution to climatology, taking an active part in the solution of timely problems in Soviet meteorological science. During the prewar years she carried out a series of climatological studies, among which there was a series of investigations devoted to world agroclimatic analogues of the USSR subtropics. During the Great Fatherland War she worked at Leningrad. During 1954-1955 I. A. Gol'tsberg actively participated in an evaluation of the agroclimatic resources of the virgin and idle lands. In her subsequent studies she examined problems relating to allowance for microclimatic characteristics in agriculture and construction. In 1961 Ida Arturovna published the monograph AGROKLIMATICHESKAYA KHARAKTERISTIKA ZAMOROZKOV V SSSR I METODY BOR'BY S NIMI (Agroclimatic Characteristics of Frosts in the USSR and Methods for Contending With Them), which still remains the most complete work on this phenomenon. Later, in collaboration with her colleagues, she produced such original works as MIKROKLIMAT SSSR (USSR Microclimate) and AGROKLIMATICHESKIY ATLAS MIRA (Agroclimatic Atlas of the World), having great scientific and practical importance. I. A. Gol'tsberg has published more than 130 studies. During recent years, under the editorship of I. A. Gol'tsberg, the Main Geophysical Observatory has produced a series of climatic maps of the zone of exploitation of the Baykal-Amur Railroad. I. A. Gol'tsberg has actively participated in the cooperation among the meteorologists of the socialist countries, representing the Hydrometeorological Service in work on the theme "Agroclimatic Resources of the Socialist Countries of Europe."

GOVERNMENT AWARDS TO SOVIET HYDROMETEOROLOGISTS

Moscow METEOROLOGIYA I GIDROLOGIYA in Russian No 7, Jul 81 pp 121-124

[Unsigned article]

[Abstract] The following specialists of the State Committee on Hydrometeorology and Environmental Monitoring have been presented government awards for active participation in the organization and implementation of Soviet Antarctic expeditions and contributions to study of Antarctica: Order of Lenin -- Nikolay Nikolayevich Ovchinnikov, senior engineer of the laboratory of the AANII (Arctic and Antarctic Scientific Research Institute); Vladimir Aleksandrovich Shamont'yev, head of the 26th Soviet Antarctic Expedition (SAE) of the AANII; Order of the October Revolution -- Nartsiss Irinarkhovich Barkov, senior scientific specialist of the AANII; Arnol'd Bogdanovich Budretskiy, head of Vostok station, 25th SAE; Order of the Red Banner of Labor -- Il'dus Khaybullovich Abdrakhmanov, aerological engineer, 26th SAE; Gennadiy Ivanovich Bardin, head of the Pevek Administration of the Hydrometeorological Service; Sergey Grigor'yevich Kovtanyuk, head of the personnel division, AANII; Aleksandr L'vovich Matusov, laboratory supervisor, AANII; Vladimir Nikolayevich Petrov, section head, AANII; Oleg Nikolayevich Struin, section head, AANII; Nikolay Gavrilovich Taranov, senior work leader, 26th SAE; Yuriy Andreyevich Khabarov, participant on the 9th SAE, now head of administration at the State Committee on Hydrometeorology and Environmental Monitoring; Artur Nikolayevich Chilingarov, former head of Bellinsgauzen station, 17th SAE, now head of administration at the State Committee on Hydrometeorology and Environmental Monitoring; Vladimir Yevgen'yevich Shirshov, deputy head of the SAE, AANII. In addition, the "Emblem of Honor" was presented to 35 persons, the Order of Work Valor (Third Degree) -- to 10 persons, the medal "For Illustrious Work" -- to 26 persons, and the medal "For Distinction in Work" -- to 35 persons.

NEW INTERNATIONAL HYDROMETEOROLOGICAL CODE

Moscow METEOROLOGIYA I GIDROLOGIYA in Russian No 7, Jul 81 pp 125-126

[Article by N. P. Fakhrutdinova]

[Abstract] A new international unified code for the transmission of hydrometeorological data from stations of all types (manned and automated, on land and at sea, on buoys and platforms) is being introduced by a resolution of the WMO dated 1 January 1982. The international designation of the new code is FM 12-VII SYNOP (for land stations) and FM 13-VII SHIP (for sea stations). It will replace six presently used codes. The new international unified code consists of six sections which are intended for the transmission of data at different exchange levels: global, regional and national. The content of these six sections is outlined. The new code will ensure the possibility of a more detailed transmission of hydrometeorological data: air temperature and dew point are transmitted with an accuracy to tenths of a degree; in coding of the state of the land surface provision is made for use of 20 digits (10 for the state of the soil without snow and 10 for the state of the snow cover) instead of the 10 digits employed in existing codes; instead of using one digit for the state of the weather between observations, there will be two, making possible a more complete characterization of weather during this period. At the present time much work is being done in the USSR for ensuring the introduction (beginning on 1 January 1982) of the new unified code for all land and sea stations of the State Committee on Hydrometeorology and Environmental Monitoring.

NOTES FROM ABROAD

Moscow METEOROLOGIYA I GIDROLOGIYA in Russian No 7, Jul 81 pp 126-127

[Article by B. I. Silkin]

[Abstract] A group of specialists at the Max Planck Institute of Aeronomy, Lindau, West Germany, over a three-year period collected atmospheric samples from altitudes between 10 and 35 km. Samples were also taken during aircraft flights between Zurich and Stockholm. Unexpected results were obtained. It had been assumed earlier that fuel combustion results in the rapid penetration of its product CO_2 into the stratosphere. New data refute this. It was found that the consequences of an increased discharge of CO_2 into the atmosphere over Northern Europe begin to be reflected at an altitude of about 25 km only about five or six years later. It was possible to construct a map of the vertical distribution of CO_2 over Northern and Central Europe. Maps of the seasonally varying maxima of CO_2 content in the region of the upper troposphere, which evidently supplies CO_2 to the lower stratosphere through a slowly operating "filter" (the boundary of the tropopause), were also constructed.

***

The ship of the arctic explorer William Barents spent the winter of 1596-1597 locked in the ice near Novaya Zemlya. To the surprise of the crew, the polar night ended two weeks earlier than anticipated. At the time of sunrise the sun should have been 5° below the horizon. This phenomenon, later known as the "Novaya Zemlya effect," was subsequently repeatedly observed. This has been most frequently attributed to refraction, but it was later found that atmospheric refraction cannot account for more than one-tenth of the "Novaya Zemlya" effect. Specialists of the University of Manitoba have now described the specific meteorological conditions responsible for this phenomenon. It is necessary that the atmosphere over a great extent be clearly stratified, that there be layers differing sharply from one another with respect to temperature, humidity and pressure. When there is such a stratification the atmosphere serves as a sort of light conductor, conveying images of distant features (in this case the sun) far above the earth's surface. Eric the Red probably set forth in his quest for Greenland after hearing reports of distant shores from others who were misled as to distance due to the "Novaya Zemlya" effect.

***

American specialists have estimated that the total quantity of fresh water on the earth is 37 million km^3. However, 75% is locked in mountain and continental glaciers and cannot now be used. Ground water accounts for 24% of the water supply and less than 1% is in rivers, lakes and in the atmosphere. Evaporation from the seas is about 430,000 km^3 annually, and from the land is about 70,000 km^3. Precipitation falling over the land amounts to 110,000 km^3 of water annually. Only about 14,000 km^3 is available for human consumption, primarily surface runoff of rivers and underground runoff. More than a third of the total water is carried in rivers which traverse inaccessible or sparsely populated areas. With the present level of consumption the available water will meet the needs of five or six times more people than now live on the earth. In many parts of the world water is used without proper allowance for hydrogeological conditions. The result is an inadmissible rise in ground water, with the soils becoming swampy or saline. By the year 2000 fresh water will be in short supply in almost 30 countries.

OBITUARY OF NIKOLAY SERGEYEVICH SHISHKIN (1912-1981)

Moscow METEOROLOGIYA I GIDROLOGIYA in Russian No 7, Jul 81 p 128

[Article by a group of comrades]

[Abstract] Professor Nikolay Sergeyevich Shishkin, doctor of physical and mathematical sciences, head of the Cloud Physics and Artificial Modification Division of the Main Geophysical Observatory, an outstanding Soviet scientist in the field of cloud physics and artificial modification, died prematurely on 17 February 1981. He defended his doctoral dissertation in 1952. His monograph OBLAKA, OSADKI I GROZOVOYE ELEKTRICHESTVO (Clouds, Precipitation and Thunderstorm Electricity), written on the basis of the dissertation, became a reference manual for several generations of specialists in these fields. The Division of Cloud Physics and Artificial Modification was organized on his initiative in 1958 and he headed this division to the end of his life. Under his supervision and with his direct participation the division carried out extensive investigations of natural and artificial formation of precipitation and the dynamics of convective clouds. Studies were made of apparatus and methods for the modification of clouds for the purpose of forming precipitation. A method was developed for extinguishing forest fires by artificially induced precipitation which helped to save millions of hectares of forest. A special method for the short-range forecasting of convective cloud cover was widely introduced into work for the regulation of precipitation. His work on investigation of the electrification of cloud elements made a major contribution to the formulation of a theory of thunderstorm phenomena and the methods for the regulation of thunderstorms. N. S. Shishkin published more than 150 scientific studies, including two monographs. He was the editor of more than 30 numbers of the TRUDY GGO (Transactions of the Main Geophysical Observatory) on cloud physics and artificial modification. Shishkin represented Soviet science at many international conferences and symposia.

5303 - END -
CSO: 1864/1